June 2009

Master's Thesis

Polymer Solar Cells

Steps Towards Improving the Power Conversion Efficiency

Lasse Bo Lumholdt Riisager

AALBORG UNIVERSITY
Department of Biotechnology, Chemistry and Environmental Engineering

AALBORG UNIVERSITY

Department of Biotechnology, Chemistry and Environmental Engineering
Section of Chemistry

Title

Polymer Solar Cells –
Steps Towards Improving the Power
Conversion Efficiency

Theme

Polymer Science

Master Student

Lasse Bo Lumholdt Riisager

Supervisor

Donghong Yu

Semester

K9K-K10K

Project period

September 1st 2008 to June 10th 2009

_____

Lasse Bo Lumholdt Riisager

Number of copies	5
Number of pages	76
Number of appendices	3

Abstract

The intent of this master thesis is to improve the power conversion efficiency of polymer solar cells by controlling the morphology of the active layer. By employing block copolymers, which are well known for their ability to phase separate in a nanometer scale, it should be possible to control the morphology. Polymers with electron donating and accepting properties were chosen on the basis of the size of their band gaps as well as the relative positions of their LUMO levels in order to maximize the solar cells performance.

Poly(5,7-bis(2-thienyl)-2,3-bis(3,5-bis(2-ethylhexyloxy) phenyl)thieno[3,4-b]pyrazine) and poly(3-cyano-4-hexylthiophene) were chosen as donor and acceptor polymers respectively. None of the polymers could be synthesized due to problems with the synthesis and purification of the monomers.

Grignard Metathesis was attempted for polymerization, but an inactive catalyst offered no polymers. Instead, three copolymers were synthesized by Suzuki coupling. Their properties were tested with UV/vis spectroscopy, gel permeation chromatography and in polymer solar cells with [6,6]-phenyl-C$_{61}$-butyric acid methyl ester as electron acceptor. Of the three polymers the novel polymer of 9,9-dioctylfluorene-2,7-diboronic acid bis(1,3-propanediol) ester and 5,5''-dibromo-3',4'-dinitroterthiophene resulted in the highest efficiency of 0.011 %.

AALBORG UNIVERSITET

Institut for Kemi, Miljø og Bioteknologi
Sektion for Kemi

Titel
Polymersolceller –
skridt mod forbedring af effektiviteten

Tema
Polymervidenskab

Kandidatstuderende
Lasse Bo Lumholdt Riisager

Vejleder
Donghong Yu

Semester
K9K-K10K

Projektperiode
1. september 2008 til 10. juni 2009

_____

Lasse Bo Lumholdt Riisager

Oplagstal	5
Sideantal	76
Bilagsantal	3

Synopsis

Hensigten med denne kandidatafhandling er at forbedre effektiviteten af polymersolceller ved at kontrollere morfologien af det aktive lag. Ved at benytte blokcopolymere, som er kendt for at faseseparere i nanometerskala, burde det være mulig er kontrollere morfologien. Polymere med elektrondonerende og elektronaccepterende egenskaber blev valg på basis af størrelsen af deres båndgap såvel som den relative position af deres LUMO niveauer for at maksimere solcellens ydelse.

Poly(5,7-bis(2-thienyl)-2,3-bis(3,5-bis(2-ethylhexyloxy)phenyl)thieno[3,4-b]pyrazin) og poly(3-cyano-4-hexyl-thiophen) blev valgt som henholdsvis donor og acceptor polymer. Ingen af polymererne kunne syntetiseres pga. problemer med syntese og oprensning af monomererne.

Grignard Metathesis blev forsøgt anvendt til polymerisation, men resulterede ikke i nogle polymere pga. en inaktiv katalysator. Tre copolymere blev i stedet syntetiseret ved hjælp af Suzuki kobling. Deres egenskaber blev testet ved hjælp af UV/vis spektroskopi, gelpermeationskromatografi og i polymersolceller med [6,6]-phenyl-C_{61}-butansyre-methylester som elektronacceptor. Af de tre polymere havde den nye polymer syntetiseret af 9,9-dioctylfluoren-2,7-diborsyre-bis(1,3-propandiol)ester og 5,5''-dibromo-3',4'-dinitroterthiphen den højeste effektivitet på 0,011 %.

Preface

This thesis is written on the basis of work done at the Faculty of Engineering, Science and Medicine at Aalborg University in the period from September 2008 to June 2009 under the guidance of associate professor Donghong Yu. Additionally some experimental work was carried out at the National Laboratory for Sustainable Energy, Risø DTU, under the supervision of senior scientist Mikkel Jørgensen and scientist Kristian O. Sylvester-Hvid.

The thesis is divided into five chapters. Chapter 1 offers a short introduction to the motivation for renewable energy and the use of solar energy in particular. The chapter is followed by a detailed exposition of the principles of polymer solar cells in chapter 2. Chapters 3, 4 and 5 cover experimental work, results and discussion and conclusion of the synthesis and purification of conjugated polymers and their characterization.

The thesis is addressed mainly to people with a similar or higher educational level in chemistry or chemical engineering.

Table of Contents

1 Introduction

Today's political considerations to move the world's energy consumption away from fossil fuels such as oil, coal and gas has increased the focus on renewable energy[1]. Renewable energy is perceived as a sustainable solution to ensure future energy supply as well as being carbon dioxide emissions free or neutral.

Solar energy is by far the renewable energy source with the greatest potential (cf. table 1). It has the ability to cover the world's energy demand several thousand times over and, unlike fossil fuels, solar energy is readily available world-wide.

Table 1. Energy available for harvesting from different sources compared to the global energy demand [25][15]

Global consumption	Hydro	Gerthermal	Wind	Solar
15 TW	7.2 TW	32 TW	870 TW	86,000 TW

Unfortunately, utilization of solar energy is very expensive, something that particular goes for the conversion into electricity. Solar cells are therefore not widely used for commercial electricity production since they cannot compete with fossil fuels or other renewable energy sources as seen in figure 1.
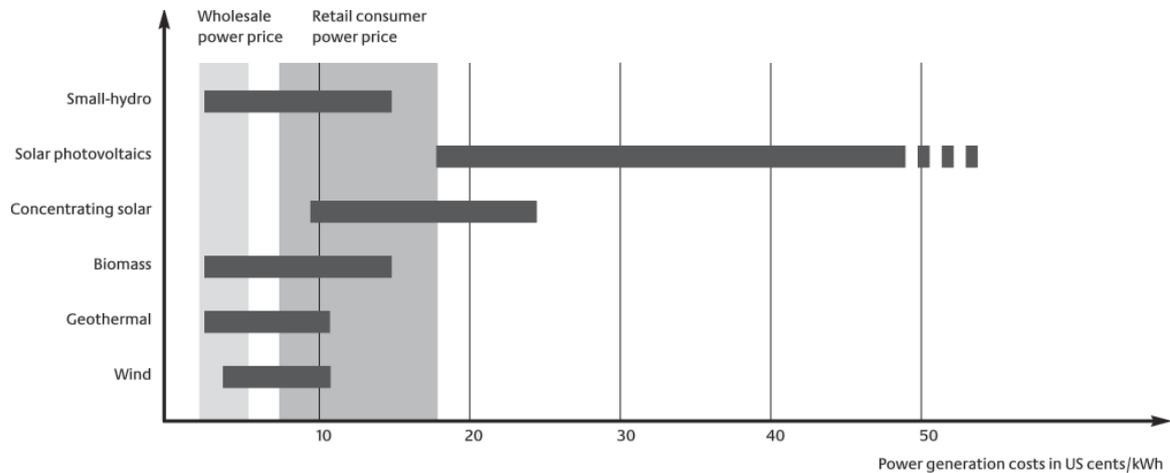
Figure 1. Prices of electricity produced from different renewable energy sources [31]

For this reason, solar cells are commonly used in remote regions with no access to the power grid or in private homes as a green alternative to fossil fuels. As a result a mere 0.04 % of the world's energy supply came from solar photovoltaics in 2006.[49]

To understand why electricity from solar cells is so expensive one needs to look closer at the solar cells used to produce it. A typical solar cell is made out of silicon wafers similar to those used in the production of micro chips.[60] The production of these wafers is outlined in figure 2.

---

[1] This should be seen in relation to the environmental concerns, e.g. cutting carbon dioxide emissions and supply concerns, which can have a large economic and political influence

The process is long and very energy intensive due to the elevated temperatures needed in most steps.[60] Solar cells are as a result relatively expensive.[60]
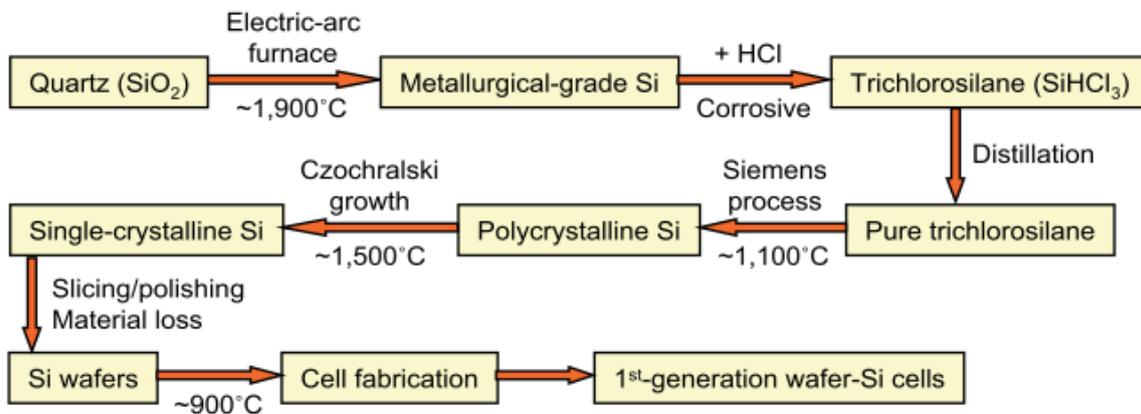
In order to earn back the production cost within a reasonable timeframe the electricity needs to be more expensive than other types of electricity.[60]

The introduction of polymer solar cells is a promising candidate to lower the manufacturing price of solar energy.[19] Polymer solar cells are based on semiconducting polymers. Their solubility means that they are easy to process.[8] However, unlike silicon solar cells the efficiency and the lifetime of polymer solar cell are still quite low as illustrated in figure 3.
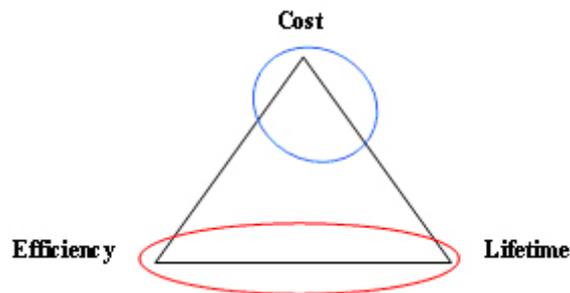
Figure 3. Problem areas associated with inorganic solar cells (blue) and polymer solar cells (red) [7]

1.1 The aim of the thesis

The aim of this project will be to address the efficiency problems of polymer solar cells. A detailed description of how polymer solar cells work and which parameters are important will be outlined. On the basis of this description a possible solution will be suggested. A model system will be created and tested. The lifetime issues will not be addressed in this project.

2 Polymer Solar Cells

Polymer solar cells are typically comprised of a photon absorbing active layer sandwiched between two electrodes and placed on a substrate of glass or clear plastic foil.[14][54] One of the electrodes is transparent in order to allow photons to penetrate into the absorbing layer. Indium tin oxide (ITO) is commonly used as transparent electrode and metals like aluminum, calcium or magnesium as the other electrode [54] (cf. figure 4). The absorbed photons excite electrons in the active layer and thereby promoting them from the highest occupied molecular orbital (HOMO) to the lowest unoccupied molecular orbital (LUMO) within the polymer.[54] The excitation of an electron leaves behind an empty electron space in the HOMO level called "a hole".[14] The hole and the excited electron are not totally independent but associated to one another in a form called an exciton.[19] In most organic molecules excitation is followed shortly by relaxation, typically in the form of recombination when the excited electron falls back into the hole.[12] This releases the absorbed energy as either radiative or non-radiative energy which cannot be utilized for electricity. In polymer solar cells recombination still occurs but not right away.[38] Instead the exciton is separated into a free hole and a free electron which are then transported to different electrodes due to differences in the electrodes' ionization energy.[54] The electron is then forced to travel from one electrode through an external circuit to the other electrode in order to recombine with the hole.[52] The absorbed energy can then be utilized in the external circuit.[8]
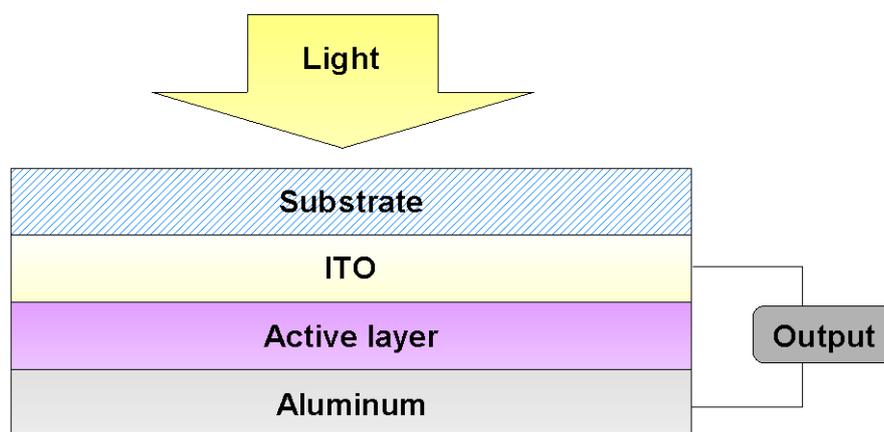
Figure 4. Schematic presentation of a polymer solar cell. The active layer is sandwiched between two electrodes, aluminum and indium tin oxide (ITO) which is transparent. The sandwich structure is placed on a substrate of glass or clear plastic

The separation of the electron from the hole in polymer solar cells is achieved by utilizing an electron accepting material along with the electron donating polymer.[12][14][19][58] The electron donor and acceptor are mixed to form a heterogeneous active layer.[19] This type of device is known as a bulk heterojunction solar cell.[19] The charge separation occurs when an exciton has diffused to the donor/acceptor interface.[12][14][38] Here a difference in potential of the two phases pulls the electron into the electron accepting phase leaving behind the hole in the electron donating phase. The electron and the hole are then free to move through their respective phases to the electrodes [19] (cf. figure 5).
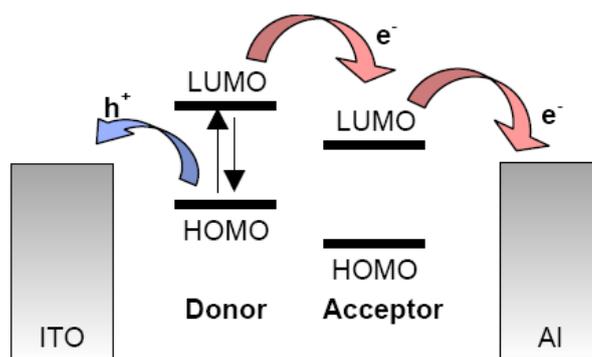
Figure 5. Charge separation within the active layer. Upon excitation the electron is transferred into the electron accepting phase due to an offset in the LUMO levels of the donor and acceptor materials. Charges are then transported to their respective electrodes [54]

In order for a material to act as an electron acceptor it has been found empirically that the potential of the LUMO level has to be at least 0.3 eV lower than the potential of the LUMO level of the electron donor.[6][21] Buckminsterfullerene derivatives like [6,6]-phenyl-C_{61}-butyric acid methyl ester (PCBM) shown in figure 6 are currently used as the electron acceptor in most applications but the use of other materials such as small organic molecules, inorganic crystals as well as another polymer is possible.[10][12][42][54][58]
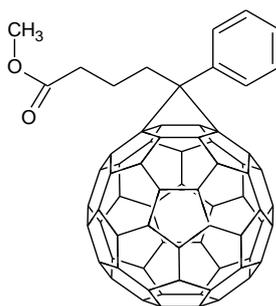
Figure 6. The commonly used electron accepting material
[6,6]-phenyl-C_{61}-butyric acid methyl ester (PCBM)

In order for an electron to get excited it needs to overcome the band gap of the polymer.[54] The band gap is the difference in energy between the HOMO and the LUMO and thereby the minimum amount of energy required for an excitation. Different wavelengths of light have different amounts of energy corresponding to the equation:

$$E_\lambda = h \cdot v = \frac{h \cdot c}{\lambda}$$

energy (*E*), wavelength (*λ*), Planck's constant (*h*), frequency (*v*), speed of light in vacuum (*c*) [22]

From the equation it can by deduced that a decrease in band gap allows light with longer wavelengths, and thus less energy, to be absorbed. The size of the band gap is therefore of great importance in solar cells as it limits the maximum amount of light that can theoretically be absorbed and thereby the maximum electric current that can be achieved.[8] The sunlight that reaches the earth's surface is comprised of light with a wide span of wavelengths, although the majority is found in the visible and near infrared regions as seen in figure 7.
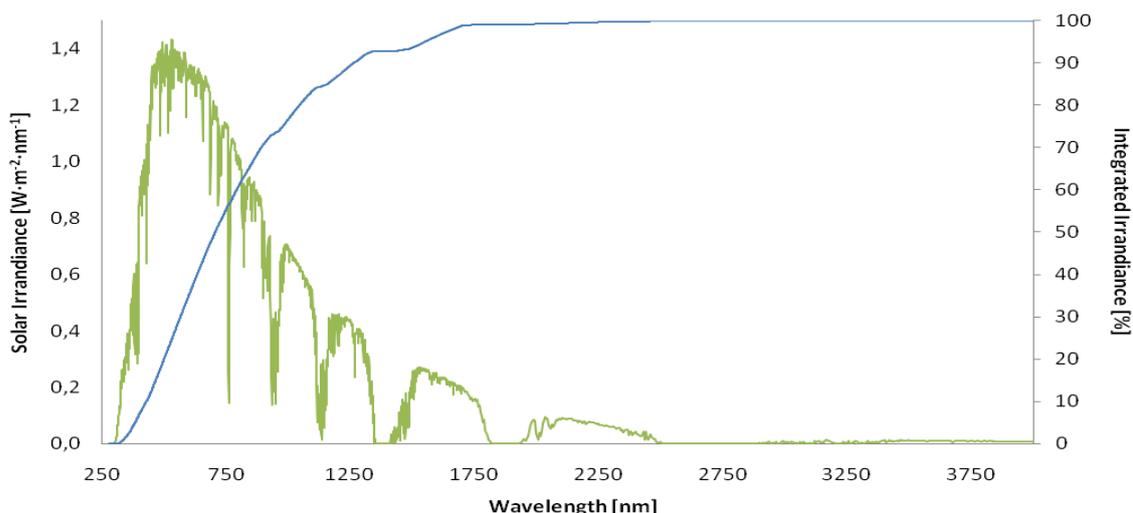
Figure 7. Solar irradiance as function of wavelength (green). Integrated solar irradiance (blue) [1]

If, for example, a polymer has a band gap of 2.07 eV it is able to absorb light with wavelengths up to 600 nm.[7] This, however, only corresponds to 17 % of the incoming photons corresponding to a current of 11.1 mA·cm^{-2}.[7] Lowering the band gap to 1.24 eV would make it able to absorb light with wavelengths up to 1000 nm and in theory up to 53 % of the incoming photons corresponding to a current of 43.9 mA·cm^{-2}.[7] In practice, however, a polymer is seldom able to absorb efficiently over the entire spectral range.[7]

Finding the ideal size of the band gap can be tricky due to many factors. Simply making the band gap as small as possible will not make a good solar cell. Although it might result in great photon absorption, the power the device would be able to produce would be little to none.[7] This is due to the physics of the assembled solar cells. One of the factors that influence the power output is the voltage produced by the solar cell.[7] The maximum theoretical voltage a polymer solar cell can produce is given by the difference in potential between the HOMO of the donor and the LUMO of the acceptor.[7] For this reason it is of great importance that the offset of the LUMO levels of the donor and acceptor is tuned to allow efficient charge separation without wasting possible voltage as illustrated in figure 8.
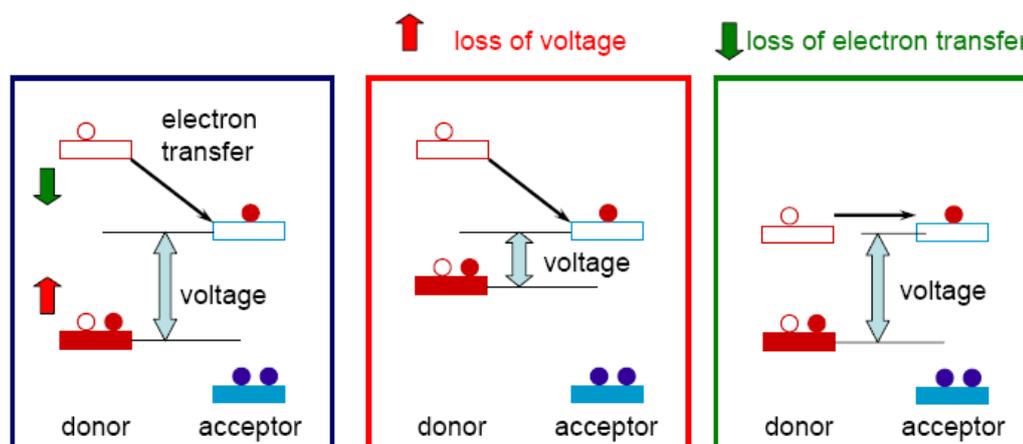
Figure 8. Schematic representation of the influences of incorrect energy level alignment. Assuming a constant acceptor raising the donor HOMO will reduced the voltage of the solar cell (red box) and lowering the donor LUMO will reduce charge separation (green box) [33]

An offset of around 0.3-0.5 eV has been found emperially to be optimal.[6][21] Along with the loss in voltage due to this offset a loss at each of the electrodes is commonly observed. The loss at the electrodes is a result of non ohmic contact between the active layer and the electrodes.[40] A small insulating layer is observed at the metal electrode which is believed to be the product of electrode material diffusing into the active layer and reacting with the vinyl groups, hence disrupting the conjugation.[54] Counter measures such as depositing a thin layer of LiF, MgO or Sm between the active layer and the electrode are usually taken to reduce electrode losses.[20][29][40] The widely used transparent electrode of indium tin oxide also causes problems.[53] Reaction between oxygen and polymer has been observed and diffusion of indium into the polymer acts as trapping sites for charge carriers.[53] As a counter measure a layer of poly(3,4-ethylenedioxythiophene) doped with poly(styrenesulfonate) (PEDOT:PPS) is widely used.[14][19] Still losses of around 0.2 eV is commonly observed at each electrode due to band bending.[40] The combined losses in voltage from the electrodes and the LUMO offset of 0.7-0.9 V are relatively constant regardless of the size of the band gap. That also means that the percent-wise loss in voltage increases as the band gap is made smaller. The ideal band gap is therefore a compromise between absorbing as many photons as possible and decreasing the loss in voltage, in percentage terms.[8][68] According to Kroon *et al.* (2008) the optimal band gap should be around 1.3 to 1.5 eV.

The size of the band gap can be engineered to some extend by the modification of six different parameters: molecular weight, bond length alternation, torsion angle, aromatic resonance energy, substituents and intermolecular interactions.[35][50] Most modifications aim at narrowing the band gap. Currently the most applied modifications are based on the bond length alternation. Minimizing the bond length alternation through increased double bond character between the repeating units has been shown to narrow the band gap.[64] Two different approaches are currently used.[64] One is the use of fused rings.[64] Fused rings have a quinoid resonance structure which increases the double bond character between the repeating units.[64] An example is poly(isothianaphthene) (PITN) as seen in figure 9.
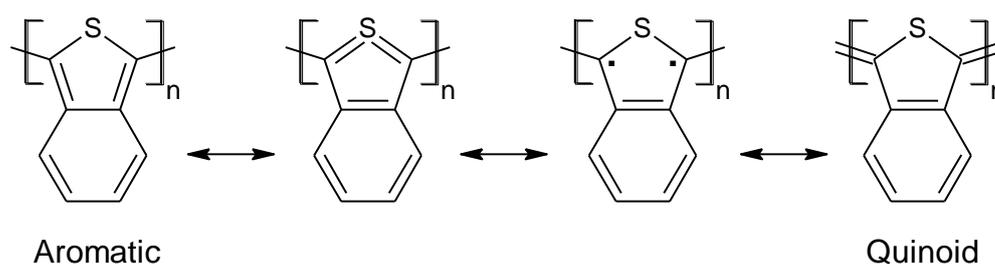
<div align="center">Aromatic   Quinoid</div>

Figure 9. Resonance structures of the fused ring system poly(isothianaphthene) (PITN)

The driving force towards the quinoid structure is the gain in aromaticity of the fused benzene ring.[64]

The second method for minimizing the bond length alternation is the donor-acceptor approach which is based on the incorporation of alternating donor and acceptor units in the polymer backbone.[64] This alternation also helps stabilize the quinoid form since they can accommodate the charges that are associated with such a resonance structure (D-A $\leftrightarrow$ D$^+$=A$^-$).[64] The band gap

is further narrowed by the donor-acceptor approach due to the fact that it is determined by the HOMO of the donor and the LUMO of the acceptor as seen in figure 10.
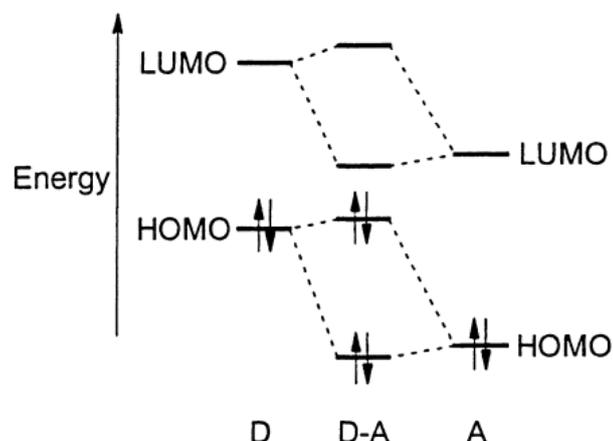
Figure 10. The band gap of a copolymer (D-A) based on donor (D) and acceptor (A) moieties is narrower then the band gap of either the donor or acceptor [64]

In addition to the size of the band gap other factors influence the absorption of photons such as the thickness of the active layer.[12] Depending on the density of the chromophores within the active layer a certain thickness is needed to absorb all photons. The density of the chromophores is dependent on which polymer and the amount of acceptor that is used.[19] Conductive polymers are very rigid by nature due to the conjugated double bonds and the extensive presence of aromatic rings in the backbone.[38] Without any aliphatic side chains they would be practically impossible to dissolve and therefore process.[38] For this reason, many or all of the aromatic hydrogen are often substituted with long chains. This increases the solubility by adding more degrees of free rotation but also dilutes the chromophores.[19] The absorption of the buckminsterfullerenes commonly used as the acceptor is limited and when used in large amounts the chromophore density is further diluted.[52]

Making the active layer thicker to the point where all incoming photons with energies exceeding the band gap are absorbed would intuitively make a device more efficient. This, however, is not necessarily the case, which is partly due to the low charge carrier mobility as well as the morphology of the active layer.[56] In inorganic solar cells the active layer is comprised of a crystalline lattice where the HOMOs and LUMOs form a valence and conductive band respectively resulting in good charge carrier mobility.[54] In polymer solar cell no crystalline lattice is present and the charge carriers are forced to travel via a hopping mechanism between localized states rather than in a band.[54] In inorganic solar cells the donor and acceptor phases are placed on top of each other forming a bi-layer called a p-n-junction. The high mobility of the charges enables them to be transported easily to the junction where charge separation occurs. An exciton formed in polymer solar cells, however, is able to diffuse only 5-20 nm before relaxation occurs.[19][23] Excitons created more than 5-20 nm from a donor/acceptor interface are therefore lost resulting in a lower efficiency. For this reason the donor/acceptor bi-layer configuration is a poor solution in polymer solar cells. Although the structure of the bulk heterojunction solar cell solves this problem quite effectively,[28] another problem arises. The physical mixing of the donor and acceptor components introduces the risk of creating isolated region.[63] This is when a region is in contact with the wrong electrode or none at all (cf. figure

11). This renders the region useless for creating electricity. The random distribution of phases also results in inefficient charge transport since a charge carrier's path to an electrode might be long and complicated, increasing the risk of decay.
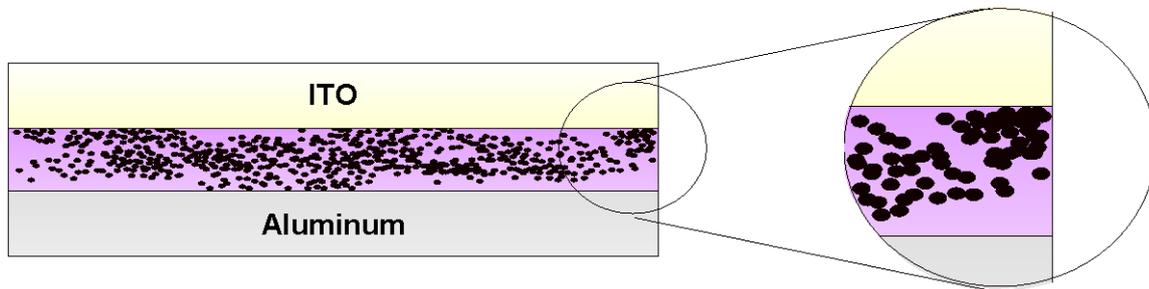
Figure 11. Example of an isolated region within a bulk heterojunction solar cell. Black areas represent the electron acceptor and purple the electron donor. Here are areas that are in contact with either the wrong electrode or none at all. Electrons collected in the isolated regions have no way of getting to the aluminum electrode

In order to achieve an effective charge transport the morphology of the active layer is therefore critical.[12] It is widely believed within the polymer solar cell community that the optimal morphology would by a distribution of phases as seen in figure 12.[12][42][48][55]
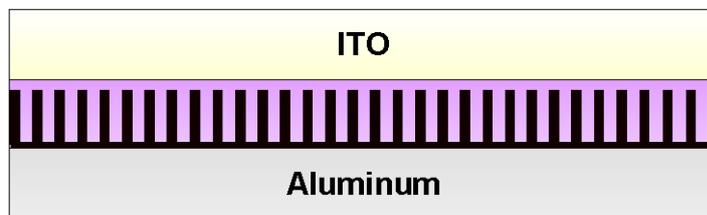
Figure 12. Optimized phase separation. No isolated regions are present and the electron donor phase is in contact with the ITO electrode and the electron acceptor phase is in contact with the aluminum electrode

Controlling the morphology, however, is not simple. Most often thermal annealing is used on constructed devices in order to change the morphology to achieve better efficiency.[8][14][19][62] Several different attempts have been made to control the morphology, most notable the use of CdSe nanocrystals and the use of a mesoporous skeleton of titania.[12][30] The use of donor-acceptor block copolymers has also been theorized as a possible solution.[56][62] Where the nanocrystals and the skeleton aims at controlling the morphology by introducing a fixed structural element and surrounding it with polymer, the block copolymers works by forming a self-assembled supramolecular phase separation in a nanometer scale.[5]

The block copolymer solution seems to have several advantages over the other methods. Compared to the CdSe nanocrystals block copolymers are less toxic [24] and, contrasting mesoporous skeletons, block copolymer solar cells can be produced with roll-to-roll printing techniques for fast and cheap production.

In addition to controlling the morphology, block copolymers potentially have another advantage over conventional bulk heterojunction solar cells. By substituting the expensive and poor photon

absorbing buckminsterfullerenes as electron acceptors with an absorbing polymer, an increase in absorption would be expected along with a further cost reduction. Furthermore, by making the band gap of the acceptor different from that of the donor, the spectral range covered efficiently by the active layer would be widen.[11]

Block copolymers phase separate due to incompatibility between the different blocks.[62] Due to the covalent bonds between the blocks a macroscopic phase separation cannot take place.[5] Depending on the relative volume fractions of the blocks, however, several different morphologies can be obtained as illustrated in figure 13.
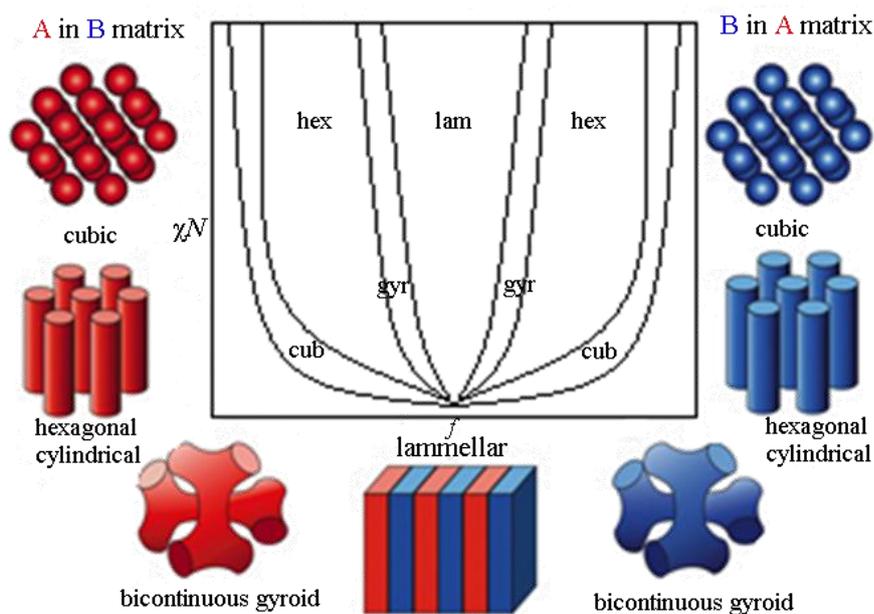
Figure 13. Phase separation of block copolymers.[47] Flory-Huggins interaction parameter (χ), degree of polymerization (N), compositional parameter (f)

Block copolymers with blocks of comparable volume fractions results in a lamellae architecture.[5] When moving towards blocks with increasing differences in volume fractions one first obtains a gyroid phase separation then hexagonally closely packed cylinders and lastly a phase of spheres in a bulk matrix. In order to achieve these phases a low polydispersity is vital.[9] At some point the smallest block will be small enough to become miscible in the large block matrix and no phase separation is observed.[5]

The phase separations shown figure 13 have been found in poly(styrene-b-isoprene) block copolymers where both blocks are comparatively flexible. The conjugated polymers used in polymer solar cells are very rigid and are not likely to behave exactly in the same way as poly(styrene-b-isoprene).[5] Bockstaller & Thomas (2002) has carried out experiments with so-called rod-coil block copolymers comprised of a rigid rod block and a flexible coil block and found that new morphologies are obtained. Block copolymers of conjugated polymers cannot be described as neither coil-coil nor rod-coil copolymers, but rather as rod-rod copolymers. How the phase separation in these rod-rod copolymers will be is difficult to predict. Sun (2003) has proposed the usage of flexible non-conjugated bridge units in order for the rigid donor and acceptor blocks to phase separate more easily and prevent conjugation distortion. A non-

conjugated bridge would furthermore prevent electron-hole recombination within the polymer chains due to its insulating properties.[56]

According to Scharber *et al.* (2006), a power conversion efficiency exceeding 10 % should be possible by controlling the morphology along with the size of the band gap and the LUMO offset. The power conversion efficiency (η_e) is a measure of the degree of incident sunlight being converted into electricity [19] and is calculated from the equation:

$$\eta_e = \frac{V_{oc} \cdot I_{sc} \cdot FF}{P_{in}}$$

The open circuit voltage (V_{OC}) is the potential when the current is zero and the short circuit current (I_{SC}) is the maximum current that can run through the device.[54] Both are essentially depending on the size of the band gap. The fill factor (FF) is a proportionality coefficient and is depended, amongst other things, on the internal charge transport abilities and the morphology.[19][42] The fill factor is the ratio of the actual maximum obtainable power to the maximum theoretical power [7] and is determined from an I-V curve such as the one seen in figure 14 and calculated from the equation:

$$FF = \frac{I_{max} \cdot V_{max}}{I_{sc} \cdot V_{oc}}$$
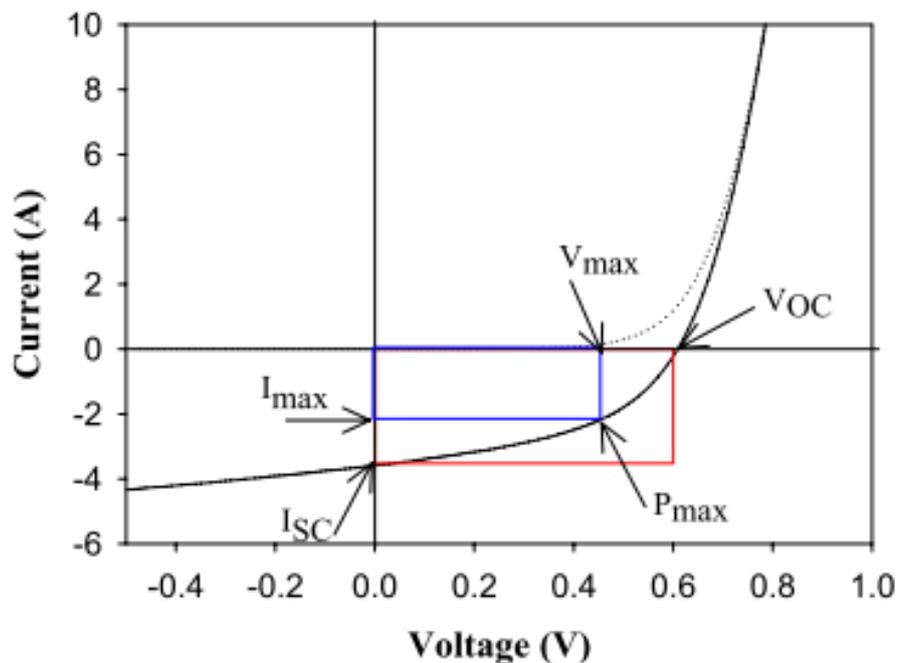
Figure 14. I-V curve. The intersection with the x- and y-axis is called the open circuit voltage (V_{OC}) and the short circuit current (I_{SC}) respectively. The point where the product of I·V is of greatest magnitude is called the maximum power point (P_{max}) [7]

The incident light power density (P_{in}) used for determining the I-V curve is standardized according to the Air Mass (AM) 1.5 standard resembling the sunlight from a solar zenith angle of 48.19° at sea level. This is similar to the sun light in northern Europe and northern America.[1]

18

2.1 Project plan

The project aims at producing donor-acceptor block copolymers and investigating their properties in polymer solar cells. In order to do so a suitable acceptor polymer has to be found. Several acceptor units such as benzothiadiazole, benzo-bis(thiadiazole) and thienopyrazines are well described, albeit mostly only in copolymers with donor units. The HOMO and LUMO of the homopolymers, therefore, are often unknown. Furthermore homopolymers of benzothiadiazole and benzo-bis(thiadiazole) lack aliphatic side chains and would therefore be difficult to dissolve. Chochos et al. (2007) reported the use of poly(3-cyano-4-hexylthiophene) (P3CN4HT) (cf. figure 15) as an acceptor polymer.
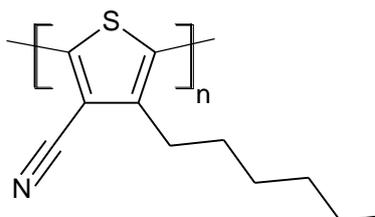
Figure 15. Poly(3-cyano-4-hexylthiophene)

P3CN4HT is a derivative of the widely used P3HT polymer where the electron subtracting cyano group alters the electron donating properties of P3HT into an electron accepting polymer. HOMO and LUMO of P3CN4HT was reported to be -6.1 and -3.6 eV versus vacuum respectively.[11]

In order to achieve good charge separation a donor polymer with a LUMO of around -3.3 eV versus vacuum is therefore needed. At the same time a band gap of 1.3 to 1.5 eV would be preferable. Poly(5,7-bis(2-thienyl)-2,3-bis(3,5-bis(2-ethylhexyloxy)phenyl)thieno[3,4-b]pyrazine) (PTBEHT) (cf. figure 16) is with a LUMO of -3.33 eV and a band gap of 1.46 eV [68] a promising candidate and therefore chosen.
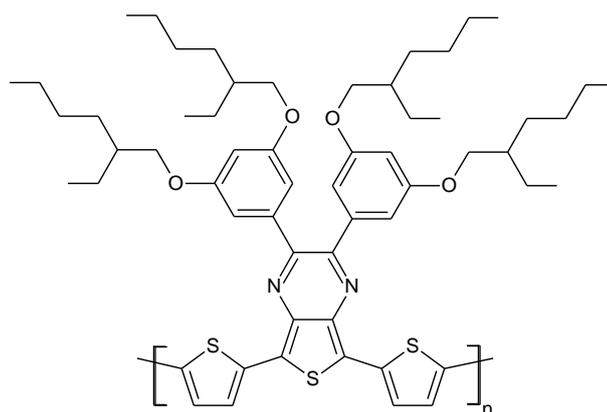
Figure 16. Poly(5,7-bis(2-thienyl)-2,3-bis(3,5-bis(2-ethylhexyloxy)phenyl)thieno[3,4-b]pyrazine)

The project will be focused on the synthesis and purification of the chosen donor and acceptor monomers along with the polymerization into conductive polymers in different configurations and ultimately into block copolymers. The optical and electrical properties of the obtained polymers are then to be tested.

3 Experimental

Chemicals were purchased from a range of chemical suppliers of which a detailed list is to be found in Appendix A (cf. page 57). DMF and toluene were dried with 4 Å molecular sieves that had been activated through an hour's heating to 600 °C. THF was dried with sodium lumps and distillated before use. *N*-bromosuccinimide (NBS) was recrystallized from water before use. As for the rest of the chemicals, these were used as received.

Characterization of synthesis products were carried out using either NMR or FTIR. NMR spectra are to be found in Appendix C (cf. page 63).

^{1}H and ^{13}C NMR was performed on a Bruker DRX600 NMR spectrometer operating at a field strength of 14.1 T, equipped with a triple-axis gradient TXI (H/C/N) probe. TopSpin 2.0 was used for acquisition and data processing.

FTIR measurements were performed on a Varian 660-IR equipped with a diamond ATR crystal.

3.1 Donor monomer synthesis

The donor monomer was synthesized in 8 main steps as shown in figure 17. Each step is explained and described in the following sections.
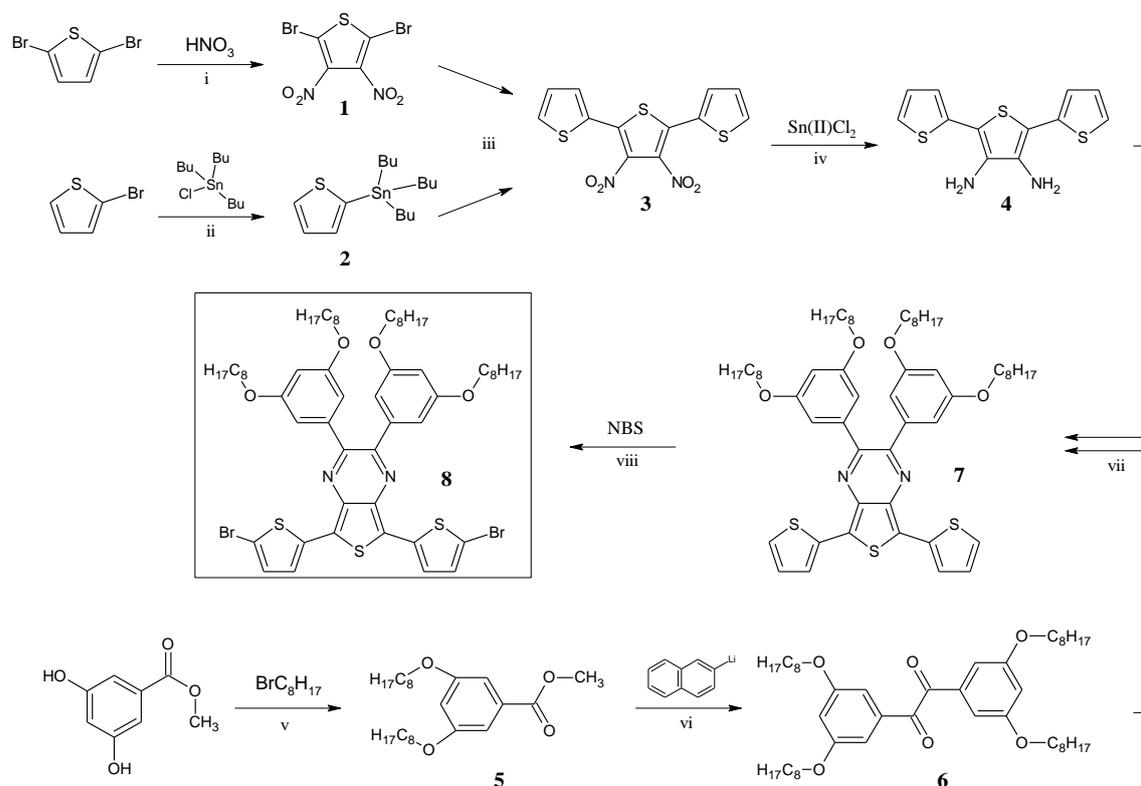
Figure 17. Synthesis of the donor monomer. 2,3-bis(3,5-bis(2-ethylhexyloxy)phenyl)-5,7-bis(5-bromothiophen-2-yl)thieno[3,4-b]pyrazine

3.1.1 Synthesis of 2,5-dibromo-3,4-dinitrothiophene (1)

Reaction mechanism

2,5-dibromo-3,4-dinitrothiophene was obtained by nitration of 2,5-dibromothiophene. Nitration is in principal a two step reaction [17] (cf. figure 18). First the reaction of nitric acid with sulfuric acid creates the positively charges nitronium ion which is then attacked by the nucleophilic aromatic ring of thiophene. A hydrogen atom is then replaced by a nitro group and the sulfuric acid is regenerated. Thus sulfuric acid acts as a catalyst. The function of the sulfuric acid is not only to facilitate the creating of the nitronium ion, but also to shift the equilibrium towards the nitrated compound by binding the reaction byproduct, water.

Nitro groups draw electrons from the aromatic ring and thus act deactivating. The use of fuming sulfuric acid has therefore been shown necessary by Mozingo *et al.* (1945) to facilitate the attachment of the second nitro group in acceptable yields.
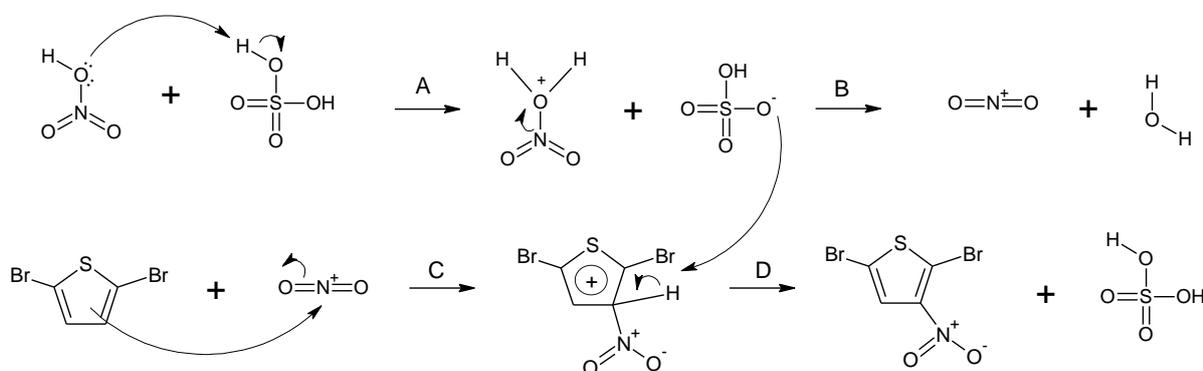
Figure 18. Nitration of 2,5-dibromothiophene. Reaction between nitric acid and sulfuric acid (A) yields a nitronium ion upon dehydration (B). The aromatic ring then attacks the nitronium ion to form an arenium ion intermediate (C) which upon reaction with HSO_4^- yields the nitro compound and regenerates the sulfuric acid (D)

Procedure

2,5-dibromothiophene (26.00 g, 107.5 mmol), sulfuric acid (96 %, 150 ml) and fuming sulfuric acid (20 % SO_3, 150 ml) were mixed and cooled by using an ice bad. Nitric acid (69 %, 125 ml) was then added slowly keeping the temperature below 20 °C. Precipitate was quickly formed. After completed addition the suspension was stirred for 2 hours and then poured over ice (500 g) and filtered. The off-white crude product was washed with large amount of water to neutralize it, dried at 105 °C and then recrystallized from methanol. Light yellow crystals were collected by filtration, washed with water and dried at 105 °C. Yield: 32.04 g, 96.5 mmol, 89.8 %.

^{13}C NMR (CDCl$_3$): 113.59, 140.89 ppm. IR: 1538, 1498, 1455, 1405, 1389, 1363, 1345, 1316, 1084, 938, 900, 802, 749, 736 cm^{-1} (IR data is in accordance with Wen & Rasmussen, 2007).

3.1.2 Synthesis of 2-(tributylstannyl)thiophene (2)

Reaction mechanism

2-(tributylstannyl)thiophene was obtained by transmetalation of 2-lithiothiophene with tributyltin chloride. 2-lithiothiophene was prepared by halogen-lithium exchange of 2-bromothiophene with n-butyllithium. Two predominant theories of the mechanism of lithium-halogen exchange are currently discussed, namely single electron transfer and anionic atom transfer. It appears that the mechanism is dependent on substrate structure, solvent and temperature.[67] The reaction is for that reason not sketched in detail in figure 19. The mechanism of the second step, the transmetalation, on the other hand is well known. The partial negative charge on the α-carbon of 2-lithiothiophene attacks the partial positively charged tin atom of tributyltin chloride resulting in a S_N2 reaction with the chloride ion as leaving group.
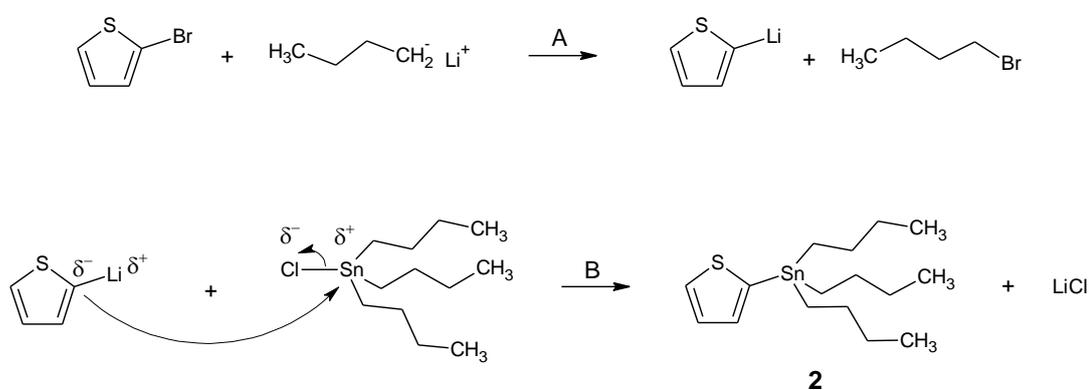
Figure 19: Synthesis of 2-(tributylstannyl)thiophene. First halogen-lithium exchange of 2-bromothiophene with n-butyllithium results in 2-lithiothiophene (A) which is then reacted with tributyltin chloride to yield 2-(tributylstannyl)thiophene (B)

Procedure

2-bromothiophene (25.09 g, 153.9 mmol) was dissolved in dry THF (75 ml) under nitrogen. The mixture was cooled to -60 °C and n-butyllithium (1.6 M in hexanes, 100 ml, 160 mmol) was added with a deoxygenized syringe keeping the temperature below -40 °C. The mixture was stirred for 1.5 hours and then tributyltin chloride (48.77 g, 149.8 mmol) was added dropwise keeping the temperature below -35 °C. The reaction was kept below -35 °C for 1 hour and then allowed to rise to room temperature while stirred overnight. Saturated sodium bicarbonate solution (100 ml) was added and the organic phase was collected. The organic phase was washed with saturated sodium bicarbonate solution (2 x 100 ml) and brine (2 x 50 ml), and dried with anhydrous magnesium sulfate. The colorless crude product was purified by column chromatography (neutral alumina, petroleum ether 60-80 °C fraction). Yield: 25.16 g, 67.4 mmol, 45.0 %.

^{1}H NMR (CDCl$_3$): δ = 1.05 (t, 9H), 1.26 (m, 6H), 1.49 (m, 6H), 1.73 (m, 6H), 7.34 (t, 1H), 7.38 (d, 1H), 7.75 (d, 1H) ppm. ^{13}C NMR (CDCl$_3$): δ = 11.02, 13.87, 27.49, 29.20, 127.98, 130.74, 135.34, 136.20 ppm.

3.1.3   Synthesis of 3',4'-dinitro-[2,2';5',2"]-terthiophene (3)

Reaction mechanism

3',4'-dinitro-[2,2';5',2"]-terthiophene was prepared by Stille coupling of 2-(tributylstannyl)-thiophenes and 2,5-dibromo-3,4-dinitrothiophene in the presence of a palladium catalyst. The reaction mechanism [61] is illustrated in figure 20 and the overall reaction in figure 21.
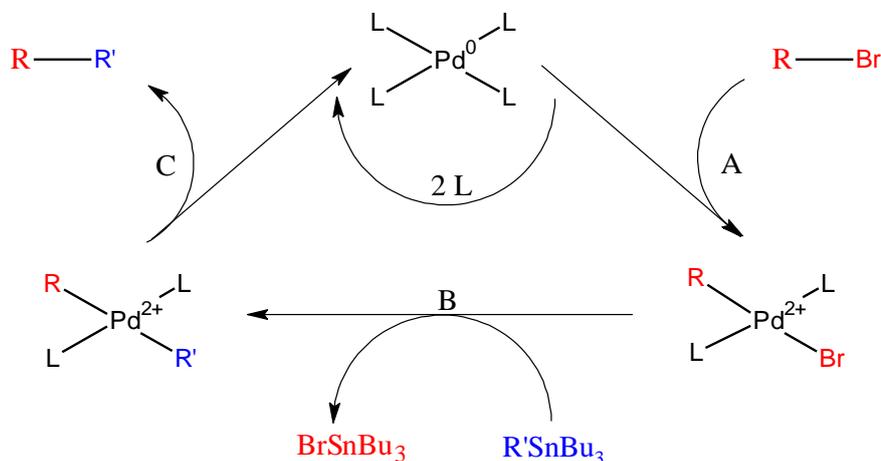
Figure 20. Stille coupling mechanism

Firstly oxidative addition of the 2,5-dibromo-3,4-dinitrothiophene (R-Br) to the active palladium(0)-complex forms a palladium(II)-ligand$_2$-Br-R-complex **(A)**. Secondly 2-(tributylstannyl)thiophene (R'SnBu$_3$) attacks the complex causing transmetalation of the complex forming palladium(II)-ligand$_2$-R-R' and tributyltin bromide **(B)**. Finally reductive elimination of the complex results in the R-R' product and regenerating of the active palladium(0) complex **(C)**.
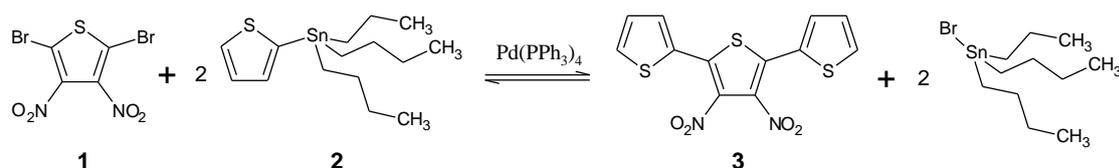
Figure 21. Synthesis of 3',4'-dinitro-[2,2';5',2'']terthiophene by Stille coupling

Procedure

2,5-dibromo-3,4-dinitrothiophene (**1**) (20.03 g, 60.3 mmol) and 2-(tributylstannyl)thiophene (**2**) (45.85 g, 122.9 mmol) were dissolved in dry toluene (200 ml) and Pd(PPh$_3$)$_4$ (1500 mg) was added. The mixture was refluxed for 10 hours under a nitrogen atmosphere. The solvent was removed from the mixture and the brown residue was dissolved in chloroform (250 ml) and filtered through a layer of silica. The silica was eluated with chloroform (350 ml) until washings turned clear. The chloroform was removed and the remaining solid was filtered, washed with heptane and dried at 105 °C resulting in light brown crystals. Yield: 18.15 g, 53.6 mmol, 88.9%.

^{1}H NMR (CDCl$_3$): δ = 7.19 (t, 2H), 7.56 (d, 2H), 7.62 (d, 2H) ppm. ^{13}C NMR (CDCl$_3$): 128.28, 128.65, 131.39, 131.50, 134.08, 136.19 ppm.

3.1.4 Synthesis of [2,2';5',2'']-terthiophene-3',4'-diamine dihydrochloride (4)

Reaction mechanism

[2,2';5',2'']-terthiophene-3'4'-diamine dihydrochloride was obtained by reduction of 3'4'-dinitro-[2,2';5',2'']-terthiophene by using a common reduction method for aromatic nitro groups, namely stannous chloride in ethanol/hydrochloric acid solution.[4] The nitrogen atom is reduced from an oxidation state of +V to –III and the tin atom is oxidized from +II to +IV hence four equivalents of tin is needed per nitro group. Due to 3',4'-dinitroterthiophene's low solubility in ethanol, THF was also added.
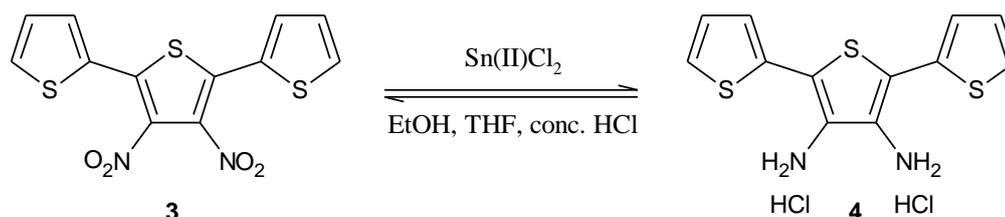
Figure 22. Reduction of aromatic nitro groups into amino groups with stannous chloride in acidic media

Procedure

3',4'-dinitroterthiophene (**3**) (12.02 g, 35.5 mmol) and stannous chloride (40.23 g, 212.2 mmol) was dissolved in a mixture of ethanol (99.9 %, 150 ml), THF (90 ml) and conc. hydrochloric acid (60 ml). The reaction was stirred at room temperature for 24 hours and then ethanol and THF were removed by rotary evaporation. The resultant dark green suspension was basified with NaOH to a pH above 8 and then continuously extracted with ethyl acetate for 46 hours. The mixture was concentrated and conc. hydrochloric acid (60 ml) was added. A dark green precipitate was filtered of, washed with petroleum ether (80-100 °C fraction) and dried in vacuum. Yield: 5.25 g, 16.7 mmol, 46.9%.

^{1}H NMR (DMSO-d$_6$): δ = 7.11 (t, 2H), 7.27 (d, 2H), 7.51 (d, 2H) ppm.

3.1.5 Synthesis of methyl 3,5-bis(2-ethylhexyloxy)benzoate (5)

Reaction mechanism

Methyl 3,5-bis(2-ethylhexyloxy)benzoate was prepared by combining methyl 3,5-dihydroxybenzoate with 1-bromo-2-ethylhexane via the Williamson ether synthesis [2] (cf. figure 23). The Williamson ether synthesis [39] utilizes a base to convert an alcohol into an alcoxide. The alcoxide then reacts with an alkyl halide via an S$_N$2 mechanism. Aprotic polar solvents promote the reaction so *N,N*-dimethylformamide (DMF) was chosen.
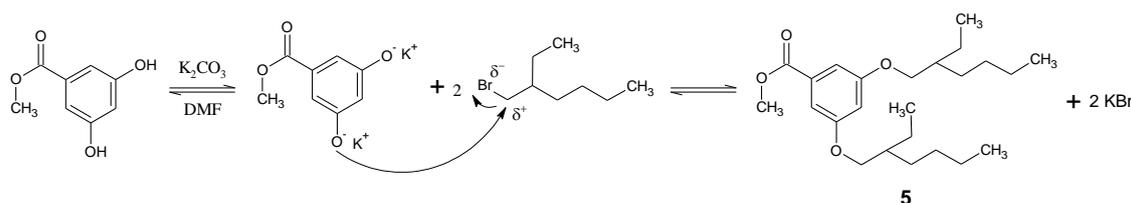
Figure 23. Synthesis of methyl 3,5-bis(2-ethylhexyloxy)benzoate by Williamson ether synthesis

Methyl 3,5-dihydroxybenzoate (25.76 g, 153.2 mmol) and dried K_2CO_3 (150.02 g, 1.09 mol) was dissolved in dry DMF (1300 ml). The mixture was stirred for 1 hour under nitrogen atmosphere before 1-bromo-2-ethylhexane (116.96 g, 605.6 mmol) was added. The mixture was stirred under nitrogen for 17 hours before being poured into water (2.6 L) and extracted with ethyl acetate (5 x 400 ml) to give a golden solution of crude product. The solution was washed with brine solution (4 x 500 ml) and subsequently dried with anhydrous magnesium sulfate. The solvent and the remaining 1-bromo-2-ethylhexane were removed by vacuum distillation at 125 °C to yield a golden liquid. Yield: 50.77 g, 129.3 mmol, 84.4 %.

^{1}H NMR (CDCl$_3$): δ = 0.91 (m, 12H), 1.40 (m, 16H), 1.72 (m, 2H), 3.86 (m, 4H), 3.90 (s, 3H), 6.65 (t, 1H) 7.18 (d, 2H) ppm.

3.1.6 Synthesis of 1,2-bis(3,5-bis(2-ethylhexyloxy)phenyl)ethane-1,2-dione (6)

Reaction mechanism

1,2-bis(3,5-bis(2-ethylhexyloxy)phenyl)ethane-1,2-dione was obtained by bimolecular reductive coupling of methyl 3,5-bis(2-ethylhexyloxy)benzoates using a super strong base. The reaction mechanism (cf. figure 24) resembles that of an acyloin condensation reaction.[43] By using less equivalents of base, however, a mixture of acyloin and α-diketone with the latter as the major component is acquired.[3][13] The acyloin by-product can subsequently be oxidized to α-diketone.[3]

The reaction is usually carried out using metallic sodium as the base. Lithium naphthalenide, however, has been used by Corey *et al.* (1995) and Bayardon & Sinou (2005). It reacts more mildly and makes the reaction easier to control which might result in a higher yield. Rühlmann (1971) has shown that the addition of trimethylsilyl chloride completely prevents base-catalyzed side reactions such as ß-eliminations and Claisen- or Dieckmann-condensations which also improves the yield. The reaction has to be carried out in an aprotic solvent otherwise it will result in a Bouveault-Blanc reduction into primary alcohols.[43] For this reason dry THF is used.
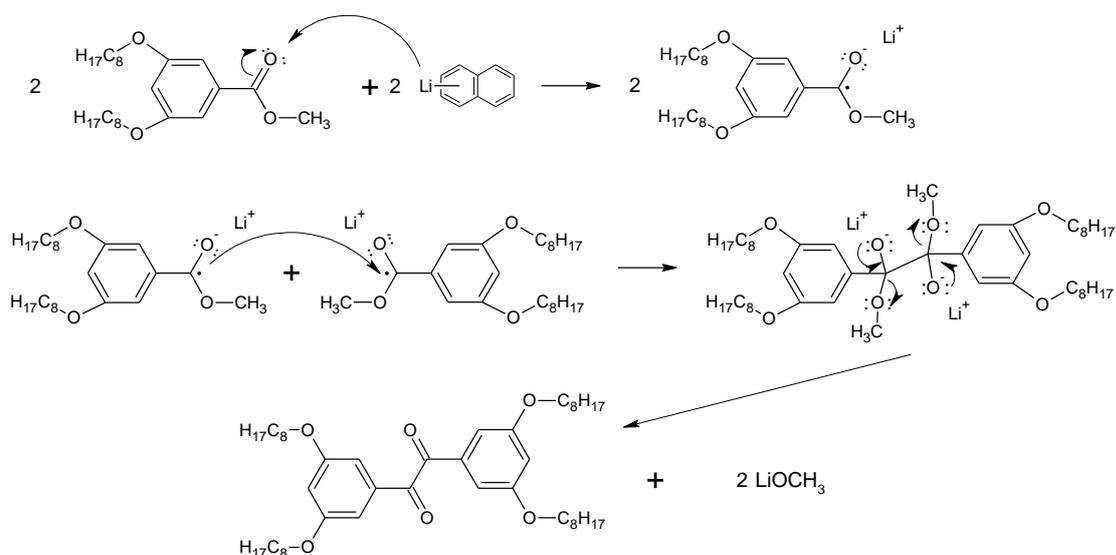
Figure 24. Synthesis of 1,2-bis(3,5-bis(2-ethylhexyloxy)phenyl)ethane-1,2-dione by reductive coupling of methyl 3,5-bis(2-ethylhexyloxy)benzoates

Procedure

Naphthalene (51.74 g, 403.7 mmol) was dissolved in dry THF (500 ml) under a nitrogen atmosphere. The solution was cooled to -10 °C and lithium (2.65 g, 381.8 mmol) was added. The mixture was stirred at room temperature for 12 hours and cooled to -78 °C. A solution of methyl 3,5-bis(2-ethylhexyloxy)benzoate (**5**) (50 g, 127.4 mmol) dissolved in dry THF (50 ml) was added drop wise maintaining a temperature of -78 °C. After addition the solution was allowed slowly to heat to room temperature. The solution was stirred for 1 hour at room temperature and quenched with trimethylsilyl chloride (30 ml). The reaction was then stirred for 30 minutes, cooled to 0 °C and poured into water (200 ml). The aqueous phase was extracted with diethyl ether and discarded. The ether phase was mixed with the THF phase and the solvent was evaporated to give a red residue. This was suspended in 80 % acetic acid (100 ml) along with $Cu(OAc)_2 \cdot H_2O$ (0.48 g, 2.4 mmol) and NH_4NO_3 (5.64 g, 70.5 mmol) and refluxed for 1.5 hours. The suspension was mixed with ethyl acetate and washed several times with water until washings stopped turning green. The ethyl acetate was removed by evaporation and this resulted in a dark red sticky residue. This was heated to 80 °C for 2 hours in order to remove the naphthalene by sublimation. The product was a dark red viscous oil. Yield: 38.54 g, 53.3 mmol, 83.7%.

^{1}H NMR (CDCl3): δ = 0.90 (m, 24H), 1.03-1.54 (m, 32H), 1.69 (m, 4H), 3.69-3.93 (m, 8H), 6.31-7.23 (m, 6H) ppm. ^{13}C NMR (CDCl3): δ = 11.08, 14.06, 23.01, 23.79, 29.05, 30.45, 39.33, 70.53, 106.03, 107.83, 140.90, 161.00, 194.4 ppm.

3.1.7 Synthesis of 2,3-bis(3,5-bis(2-ethylhexyloxy)phenyl)-5,7-bis(thiophene-2-yl)thieno-[3,4-b]pyrazine (7)

Reaction mechanism

2,3-bis(3,5-bis(2-ethylhexyloxy)phenyl)-5,7-bis(thiophene-2-yl)thieno[3,4-b]pyrazine was obtained by condensation of 1,2-bis(3,5-bis(2-ethylhexyloxy))ethane-1,2-dione and [2,2';5',2'']-terthiophene-3'4'-diamine. The basic mechanism [69] is illustrated in figure 25.
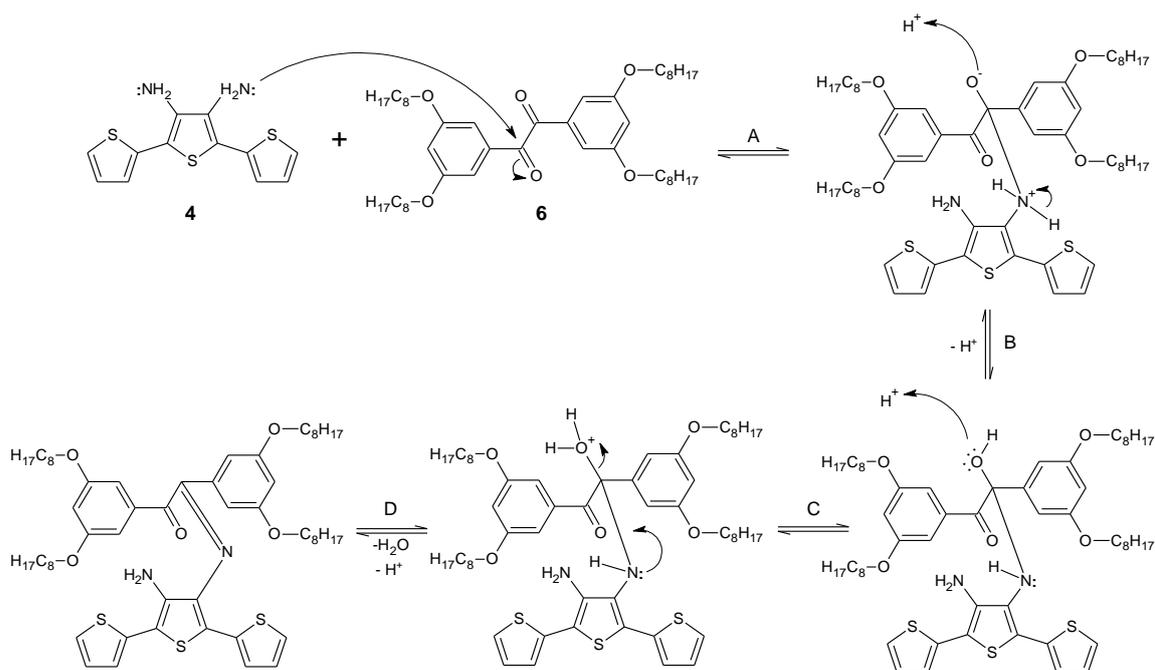
Figure 25. Synthesis of 2,3-bis(3,5-bis(2-ethylhexyloxy)phenyl)-5,7-bis(thiophene-2-yl)thieno[3,4-b]pyrazine

Initially the lone pair electrons of a nitrogen atom on [2,2';5',2'']-terthiophene-3'4'-diamine attacks a carbonyl carbon of 1,2-bis(3,5-bis(2-ethylhexyloxy))ethane-1,2-dione **(A)**. Then protonation and deprotonation of the alcoxide and quaternary nitrogen respectively occurs **(B)**. Formation of a carbon-nitrogen double bond induced by the nitrogen lone pair then forces deprotonation of the nitrogen along with the departure of the hydroxyl group **(C)** which by protonation forms water as a leaving group **(D)**. This procedure is then repeated to complete the pyrazine ring.

Procedure

1,2-bis(3,5-bis(2-ethylhexyloxy))ethane-1,2-dione (**6**) (11.57 g, 16 mmol) was dissolved in 99.9 % ethanol (200 ml) along with [2,2';5',2'']-terthiophene-3'4'-diamine dihydrochloride (**4**) (5.62 g, 16 mmol) and triethylamine (2.48 g, 24 mmol). The reaction was refluxed for 70 hours resulting in a purple precipitate. The solvent was evaporated and a purple oil was obtained. This was dissolved in chloroform (300 ml) and mixed with silica gel (50 ml). The chloroform was evaporated and the solid mixture was applied to column chromatography using 70-230 mesh silica (60 Å pore size) and heptane as eluent. The fractions were mixed and the solvent was evaporated to yield a viscous purple oil. Yield: 6.31 g, 6.5 mmol, 40.6 %.

^{1}H NMR (DMSO-d_6): δ = 0.90 (m, 24H), 1.20-1.77 (m, 36H), 3.63-3.89 (m, 8H), 6.47 (t, 2H), 6.75 (d, 4H), 7.12 (t, 2H), 7.37 (d, 2H), 7.70 (d, 2H) ppm.

3.1.8 Synthesis of 2,3-bis(3,5-bis(2-ethylhexyloxy)phenyl)-5,7-bis(5-bromothiophen-2-yl)thieno[3,4-b]pyrazine (8)

Reaction mechanism

2,3-bis(3,5-bis(2-ethylhexyloxy)phenyl)-5,7-bis(5-bromothiophen-2-yl)thieno[3,4-b]pyrazine was synthesized by free radical bromination with NBS. The mechanism is subject to some discussion.[59] Two of the suggested mechanisms are illustrated in figure 26.
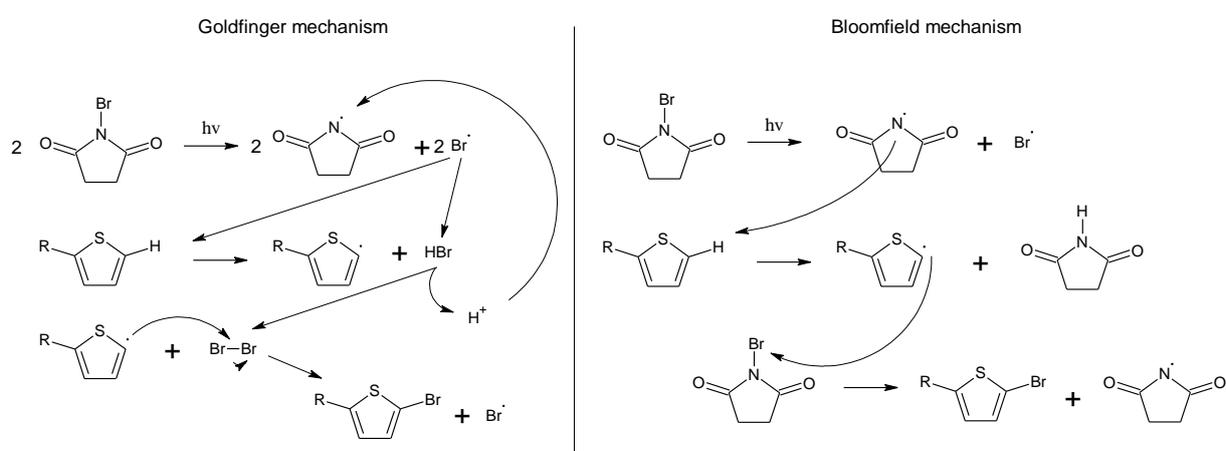
Figure 26. Suggested bromination mechanism of *N*-bromosuccinimide

Procedure

2,3-bis(3,5-bis(2-ethylhexyloxy)phenyl)-5,7-bis(thiophene-2-yl)thieno[3,4-b]pyrazine (**7**) (6.00 g, 6.2 mmol) was dissolved in dry THF (600 ml) under argon atmosphere and shielded from light with aluminum foil. *N*-bromosuccinimide (1.62 g, 9.1 mmol) was dissolved in dry THF (100 ml) in a dripping funnel also shielded from light. *N*-bromosuccinimide solution was added dropwise until the desired disubstituted product was obtained as the major product. Progress was followed with TLC using silica plates and heptane/toluene (4:1) as eluent. Silica gel (25 ml) was added and the solvent was removed in vacuum. The solid mixture was applied to column chromatography using 70-230 mesh silica (60 Å pore size) and heptane/toluene (4:1) as eluent. This purification did not yield a pure disubstituted product but rather a mixture of mono-, di- and trisubstituted products according to TLC and NMR (cf. figure 27).
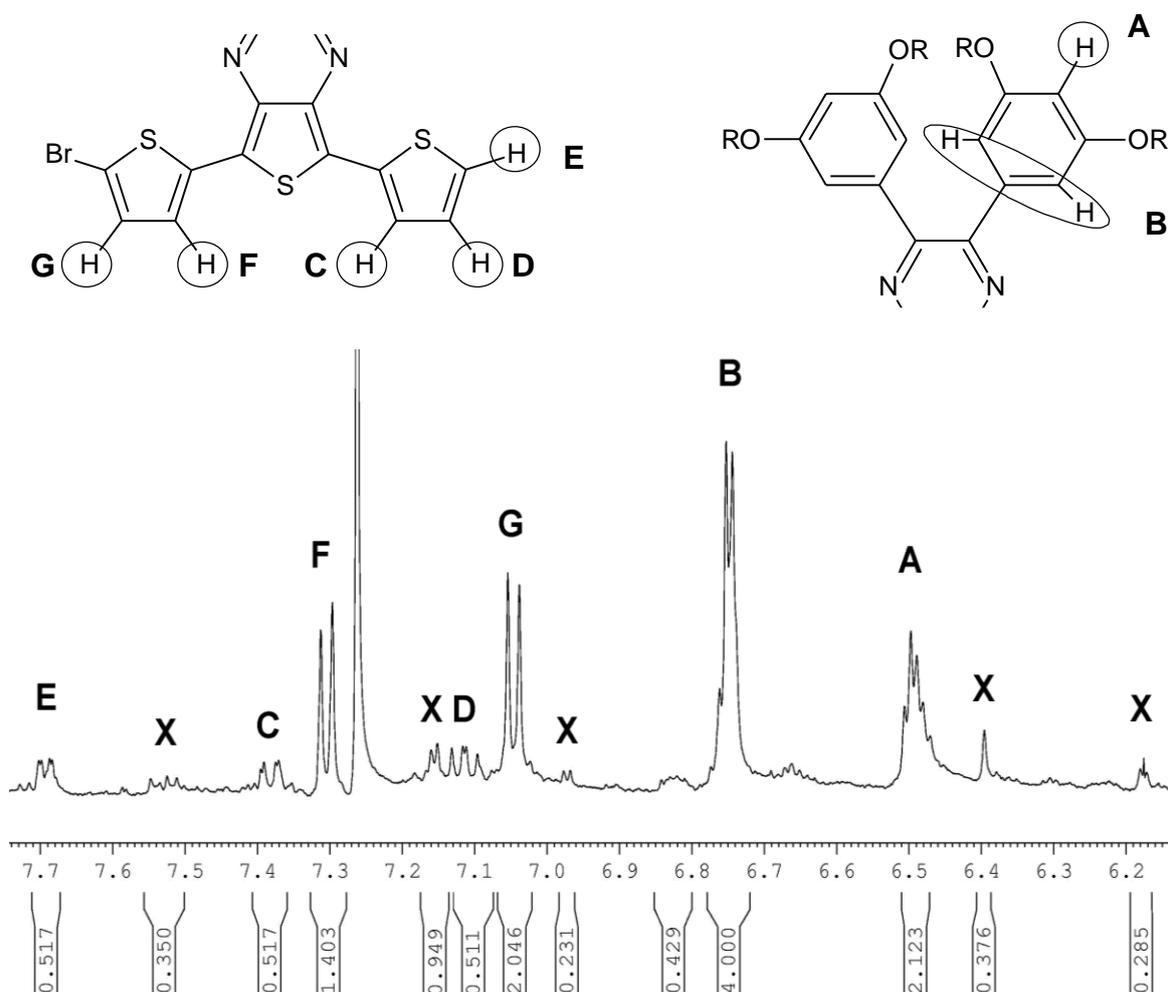
Figure 27. Assignment of NMR signals from the product mixture obtained by bromination. Peaks labeled X are inconsistent with the un-, mono- and dibrominated monomer

In order to polymerize without the risk of crosslinking or premature termination to occur it is essential that only the dibrominated product is present. It seems like the four 2-ethylhexyloxy chains are too dominant to allow compounds with different amounts of bromine attached to be separated in practice. A different synthesis strategy was needed. Maybe by attaching the bromine before the 2-ethylhexyloxy chains are introduced would make for an easier purification. A second strategy for the donor monomer synthesis was therefore carried out.

3.2 Donor monomer synthesis II

The second attempt to synthesis the donor monomer was done according to the scheme below. Steps denoted *i*, *ii*, *iii*, *v* and *vi* are identical to the first synthesis strategy (cf. section 3.1). New steps are number *ix*, *x* and *xi* seen in figure 28. The main idea is to attach bromine to the terthiophene early in the synthesis in order to avoid multibromination and thereby obtain the pure dibrominated monomer.
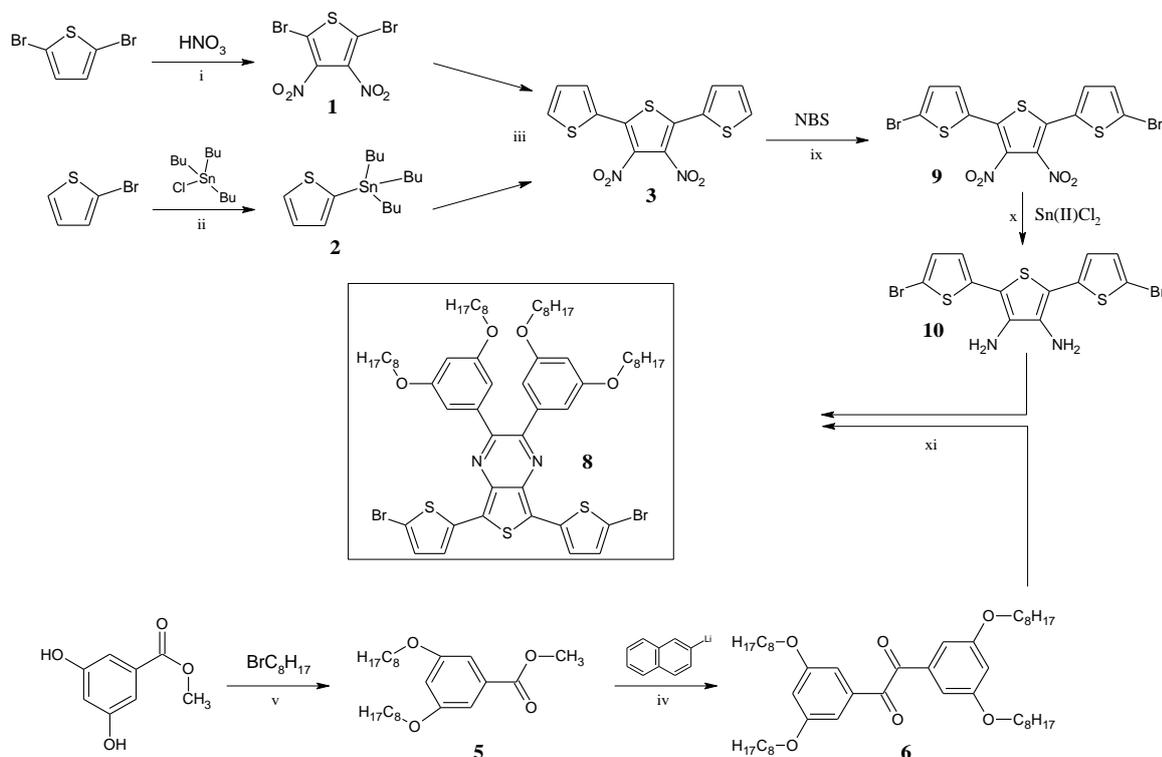
Figure 28. Second synthesis strategy for the donor monomer

3.2.1 Synthesis of 5,5''-dibromo-3',4'-dinitroterthiophene (9)

Reaction mechanism

5,5''-dibromo-3',4'-dinitroterthiophene was obtained by free radical bromination of 3',4'-dinitroterthiophene similar to that described in section 3.1.8. 3',4'-dinitroterthiophene was obtained as described in section 3.1.1 to 3.1.3.

Procedure

3',4'-dinitroterthiophene (**3**) (8.00 g, 23.7 mmol) was dissolved in dry DMF (100 ml) under nitrogen and shielded from light with aluminum foil. *N*-bromosuccinimide (16.88 g, 94.8 mmol) was then added in small portions over a period of one hour. After stirring for 18 hours the mixture was cooled to 5 °C and filtered to collect a bright orange precipitate. This was washed with methanol (100 ml) and dried at 105 °C before being recrystallized from 150 °C *N*-methyl-2-pyrrolidone under nitrogen. Crystals were filtered, washed with methanol and water and finally dried at 105 °C to yield orange needle-like crystals. Yield: 9.30 g, 18.7 mmol, 63.3 %

^{1}H NMR (CDCl$_3$): δ = 7.16 (d, 2H), 7.31 (d, 2H) ppm. ^{1}H NMR (Pyridine-d$_5$): δ = 7.26 (d, 2H), 7.43 (d, 2H) ppm. ^{13}C NMR (Pyridine-d$_5$): δ = 120.56, 128.10, 129.83, 132.40(q), 133.38(d), 134.32 ppm

3.2.2 Synthesis of 5,5''-dibromoterthiophene-3',4'-diamine dihydrochloride (10)

Reaction mechanism

5,5''-dibromoterthiophene-3',4'-diamine was synthesized with a number of different reducing agents, solvent mixtures, temperatures and reaction times. A detailed list of the experiments is to be found in Appendix B (cf. page 59). An overview of the results is outlined in table 2 below.

Table 2. Overview of the attempts made to produce 5,5''-dibromoterthiophene-3',4'diamine dihydrochloride

Attempt #	Solvent mixture	Reductant per nitro group	Time Temperature	Reduction obtained	Purification
Sn1	EtOH, THF & HCl (4:1:1) 30 ml/g	$Sn(II)Cl_2$, 0.5 eqv.	28 Hours RT °C	Yes	No
Sn2	EtOH, NMP & HCl (4:7:2) 60 ml/g	$Sn(II)Cl_2$, 3 eqv.	95 Hours RT	Yes	No
Sn3	EtOH, NMP & HCl (2:4:1) 70 ml/g	$Sn(II)Cl_2$, 3 eqv.	70 Hours RT	Yes	No
Sn4	EtOH, THF & HCl (8:6:3) 43 ml/g	$Sn(II)Cl_2$, 3 eqv.	28 Hours RT	Yes	No
Sn5	EtOH, THF & HCl (2:2:1) 40 ml/g	$Sn(II)Cl_2$, 3 eqv.	22 Hours 35 °C	Yes	No
Sn6	EtOH, THF & HCl (6:4:3) 26 ml/g	$Sn(II)Cl_2$, 3 eqv.	20 Hours RT	Yes	No
Sn7	EtOH, THF & HCl (2:2:1) 50 ml/g	$Sn(II)Cl_2$, 3 eqv.	95 Hours RT	Yes	No
Sn8	EtOH, THF & HCl (5:3:3) 92 ml/g	$Sn(II)Cl_2$, 10 eqv.	40 Hours RT	Yes	No
Fe1	EtOH, THF & HCl (4:4:1) 23 ml/g	Fe 15.7 eqv.	0.5 Hour RT	Yes	No
Fe2	EtOH, THF & HCl (1:1:1) 38 ml/g	Fe 10 eqv.	9.5 Hours RT	Yes	No
Fe3	EtOH, THF & HCl (7:7:1) 22 ml/g	Fe 6.7 eqv.	2.5 Hours RT	Yes	No
Zn1	MeOH, THF (3:1) 300 ml/g	Zinc + NH_4HCOOH 1.2/12 eqv.	2 Hours 40 °C	No	-
Zn2	MeOH 50 ml/g	Zinc + NH_4HCOOH 1.2/20 eqv.	1 Hour RT	No	-
Zn3	MeOH & $NH_2NH_2.HCOOH$ (10:1) 22 ml/g	Zinc 2 eqv.	1 Hour RT	No	-
Zn4	MeOH, THF & $NH_2NH_2.HCOOH$ (5:5:1) 22ml/g	Zinc 2 eqv.	1 Hour RT	No	-

As indicated in table 2, reductions with stannous chloride and iron were successful, whereas those done with zinc were not. The reduction was monitored with TLF (THF/Heptane 2:3 on silica plates) and confirmed with NMR which showed an upfield shift compared with the nitro compound: ^{1}H NMR ($CDCl_3$): δ = 6.84 (d, 2H), 7.04 (d, 2H) ppm.

However no method was found that could isolate the title compound from the byproducts of the reductions. These were probably either $SnCl_6^{2-}$ or $FeCl_3 \cdot xH_2O$ as well as excess reducing agent.

3.2.3 Synthesis of 2,3-bis(3,5-bis(2-ethylhexyloxy)phenyl)-5,7-bis(5-bromothio-phen-2-yl)thieno[3,4-b]pyrazine (8)

Reaction mechanism

2,3-bis(3,5-bis(2-ethylhexyloxy)phenyl)-5,7-bis(5-bromothiophen-2-yl)thieno[3,4-b]pyrazine was synthesized using the condensation reaction described in section 3.1.7. Since no pure compound **10** was obtained the crude product from reduction Sn8 (cf. table 2) was used.

Procedure

1,2-bis(3,5-bis(2-ethylhexyloxy))ethane-1,2-dione (**6**) (5.00 g, 6.9 mmol) was dissolved in 99.9 % ethanol (100 ml) along with crude 5,5''-dibromoterthiophene-3',4'-diamine dihydrochloride (**10** from reduction Sn8) (5.00 g) and triethylamine (2.50 g, 24.7 mmol). The reaction was refluxed for 24 hours resulting in a purple oil indicating the formation of **8**. A small amount of the purple oil was dissolved in chloroform and subjected to TLC (THF/Heptane 2:3 on silica plates). TLC showed the presence of compound **8** but also two other purple compounds in much larger quantities. These were determined to be compound **7** and monobrominated **7** by comparing TLC results from reaction **viii**. This indicates that the stannous chloride contaminants had causes dehalogenation at elevated temperatures. Pure compound **8** could therefore not be obtained by synthesis strategy II either.

Due to time constraints no further work was done on the synthesis of the donor monomer.

3.3 Acceptor monomer synthesis

The structure and the synthesis of the acceptor monomer (**15**) is show in figure 29 below. Each step is explained and described in the following sections.
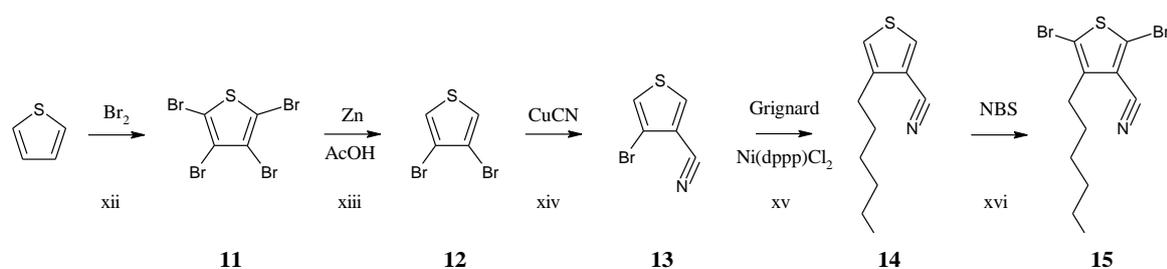
Figure 29. Synthesis of the acceptor monomer. 2,5-dibromo-4-hexylthiophene-3-carbonitrile

3.3.1 Synthesis of tetrabromothiophene (11)

Reaction mechanism

Tetrabromothiophene was obtained by complete brominating of thiophene. The reaction is an electrophilic aromatic substitution reaction [39] (cf. figure 30). First the electron rich thiophene attacks an electrophile bromonium cation resulting in a carbon-bromine bond along with a nonaromatic carbocation intermediate called and arenium ion. The arenium ion is a resonance structure which helps to stabilize the carbocation. The aromatic structure is then recovered by the departure of the excess proton by reaction with bromide.
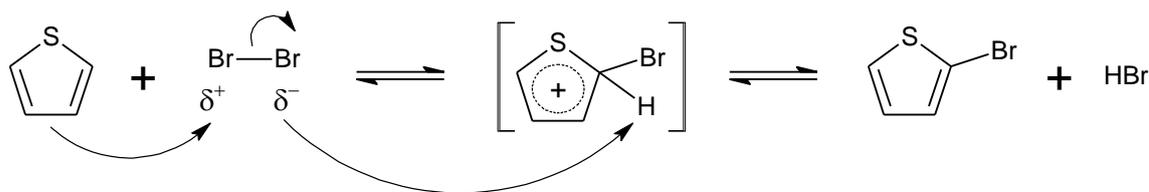
Figure 30. Basic principle of the bromination of thiophene

Procedure

Thiophene (40.07 g, 476.2 mmol) was dissolved in chloroform (15 ml) and cooled to 0 °C. Bromine (305 g, 3.82 mol) was added dropwise during a time span of 3.5 hours. The mixture was then refluxed for 20 hours. NaOH (1.5 M, 150 ml) was then added slowly and the reaction was stirred for 30 minutes at 50 °C. The suspension was filtered and the brown sticky residue was washed with water (2.5 L). The brown residue (55.58 g) was assumed to consist of a mixture of thiophenes with different degrees of bromination. The residue was used without further purification.

3.3.2   Synthesis of 3,4-dibromothiophene (12)

Reaction mechanism

3,4-dibromothiophene was obtained by selective dehalogenation of tetrabromothiophene with zinc in acetic acid.[18] The reaction is similar to the Grignard reaction but with magnesium substituted with zinc. Zinc reacts with the tetrabromothiophene creating an organozinc halide. This only occurs at the α-positions when zinc is used.[18] The organozinc bond is highly polarized resulting in a carbon with a partial negative charge that upon reaction with a proton e.g. from water yields the dehalogenated compound.
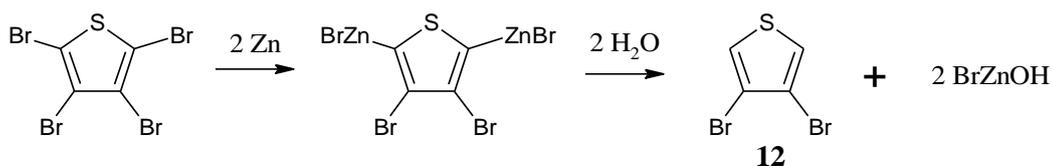
Figure 31. Selective dehalogenation of tetrabromothiophene into 3,4-dibromothiophene

Procedure

Brown residue obtained in reaction **11** (52.0 g) and zinc dust (52.0 g) was suspended in a mixture of acetic acid (99 %, 65 ml) and water (200 ml). Shortly after addition a violent exothermic reaction took place, consuming the brown residue and yielding a clear liquid with zinc residues. The mixture was stirring for five minutes and then rapidly distilled as described by Gronowitz (1959). The distillate consisted of a lower yellow organic phase and an upper aqueous phase. The organic phase was collected and fraction distilled in vacuum to yield a clear oil. Yield: 20.09 g, 83.0 mmol, 17.4 % (reaction A+B combined)

3.3.3 Synthesis of 4-bromothiophene-3-carbonitrile (13)

Reaction mechanism

4-bromothiophene-3-carbonitrile was obtained via a Rosenmund-von Braun reaction [37] (cf. figure 32). Copper(I)cyanide in a polar high-boiling solvent is used to substitute a bromine with a carbonitrile group. The precise mechanism is not known but it probably involves the formation of a Cu(III) species through oxidative addition of the aryl halide.[44] Subsequent reductive elimination then leads to the product.
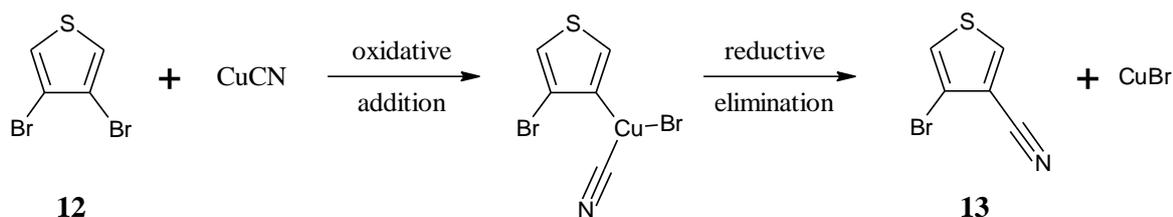
Figure 32. Synthesis of 4-bromothiophene-3-carbonitrile

Procedure

3,4-dibromothiophene (**12**) (10.00 g, 41.3 mmol) and copper(I)cyanide (3.71 g, 41.3 mmol) was suspended in NMP (100 ml) and heated to 180 °C under nitrogen for 200 hours. TLC (THF/Heptane 2:3 on silica plates) showed the emergence of two new compounds along with traces of the starting material. After cooling to room temperature hydrochloric acid (1 M, 100 ml) was added and the mixture was stirred for 1 hour. Ethyl acetate (100 ml) was added and the organic phase was collected, washed twice with saturated sodium bicarbonate and brine solutions and dried with magnesium sulfate. The mixture was filtered and the solvent was evaporated to yield a mixture of three compounds as a beige solid. This was separated by column chromatography using 70-230 mesh silica (60 Å pore size) and heptane/THF (3:2) as eluent. The title compound was eluted after a fraction containing 3,4-dibromothiophene and followed by a fraction containing thiophene-3,4-dicarbonitrile. Evaporation of the solvent resulted in a beige solid. Yield: 4.32 g, 23.0 mmol, 55.7 %

^{1}H NMR (CDCl$_3$): δ = 7.93 (d, 1H), 7.34 (d, 1H) ppm. ^{13}C NMR (CDCl$_3$): δ = 112.20, 113.50, 114.56, 124.90, 136.32 ppm.

3.3.4 Synthesis of 4-hexylthiophene-3-carbonitrile (14)

Reaction mechanism

The synthesis of 4-hexylthiophene-3-carbonitrile was attempted by Kumada coupling of 4-bromothiophene-3-carbonitrile and hexylmagnesium bromide using a nickel catalyst.[57] The basic catalytic cycle is similar to the one described in section 3.1.3 for the Stille coupling.
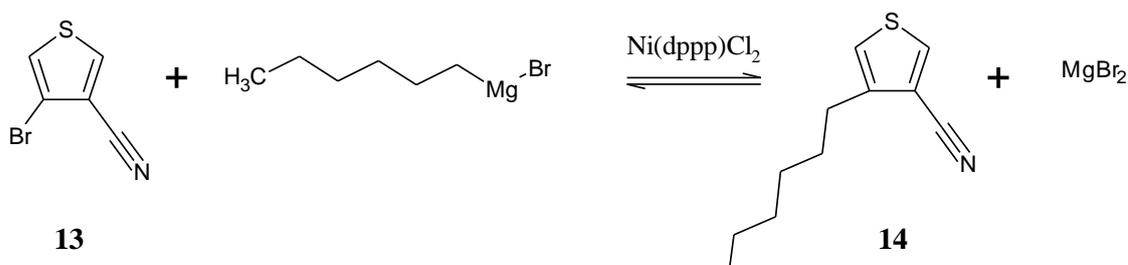
Figure 33. Synthesis of 4-hexylthiophene-3-carbonitrile by Kumada coupling

Procedure

1-bromohexane (10.00 g, 60.6 mmol) and magnesium (1.50 g, 61.7 mmol) were suspended in THF (35 ml) under nitrogen and stirred for one hour at room temperature to yield a hexylmagnesium bromide solution (1.4 M).

In another flask was placed 4-bromothiophene-3-carbonitrile (**13**) (4.04 g, 21.5 mmol), [1,3-Bis(diphenylphosphino)propane]dichloronickel(II) (100 mg) and THF (100 ml) under nitrogen and in an ice bath. Hexylmagnesium bromide solution (1.4 M, 23 ml, 32.2 mmol) was added dropwise. The reaction was stirred at 0 °C for 1.5 hours and then heated to reflux for 18 hours. The reaction was monitored with TLC (THF/Heptane 2:3 on silica plates) and after 18 hours apparently none of the starting material had been converted and no new compounds had formed. The mixture was hydrolyzed with hydrochloric acid solution (10 %, 20 ml) and extracted with ethyl acetate without obtaining the title compound.

Due to time constraints no further work was done on the synthesis of the acceptor monomer.

3.4 Polymerization

Due to the failed donor and acceptor synthesis substitutes were purchased. 2,5-dibromo-3-hexylthiophene (97 %) and 4,7-dibromobenzo[*c*]-2,1,3-thiadiazole (95 %) were purchased as donor and acceptor molecules respectively.
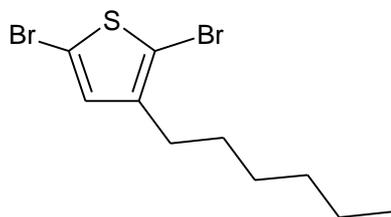
Figure 34. 2,5-dibromo-3-hexylthiophene Electron donor
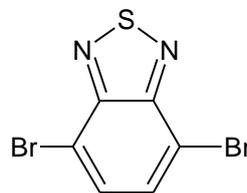
Figure 35. 4,7-dibromobenzo[c]-2,1,3-thiadiazole Electron acceptor

Polymerization of block copolymers was attempted by Grignard Metathesis (GRIM) polymerization. GRIM is in principle a poly-Kumada coupling using Ni(dppp)Cl$_2$ as catalyst.[32] Unlike other polymerization methods for conjugated polymers such as Stille and Suzuki couplings which proceed in a step-growth manner, GRIM has been shown to proceed in a chain-growth manner.[32] As a result GRIM should yield high and predictable molecular weights in a

short period of time as well as low polydispersity which is essential in block copolymers in order to control the morphology.[9][32] Furthermore GRIM has shown to exhibit a quasi-living nature making it ideal for producing block copolymers by sequential addition of monomers.[32]

3.4.1 GRIM polymerization 1 – homopolymer (P3HT)

GRIM polymerization is a two step procedure.[32] First a Grignard intermediate is made by mixing the monomer with a stoichiometric amount of Grignard reagent, typically methylmagnesium halide, isopropylmagnesium halide or tertbutylmagnesium halide.[32] This result in a magnesium-halogen exchange reaction also referred to as Grignard Metathesis. The second step is the actual polymerization initiated by the addition of Ni(dppp)Cl$_2$. The polymerization is believed to proceed by the catalytic cycle shown in figure 36.
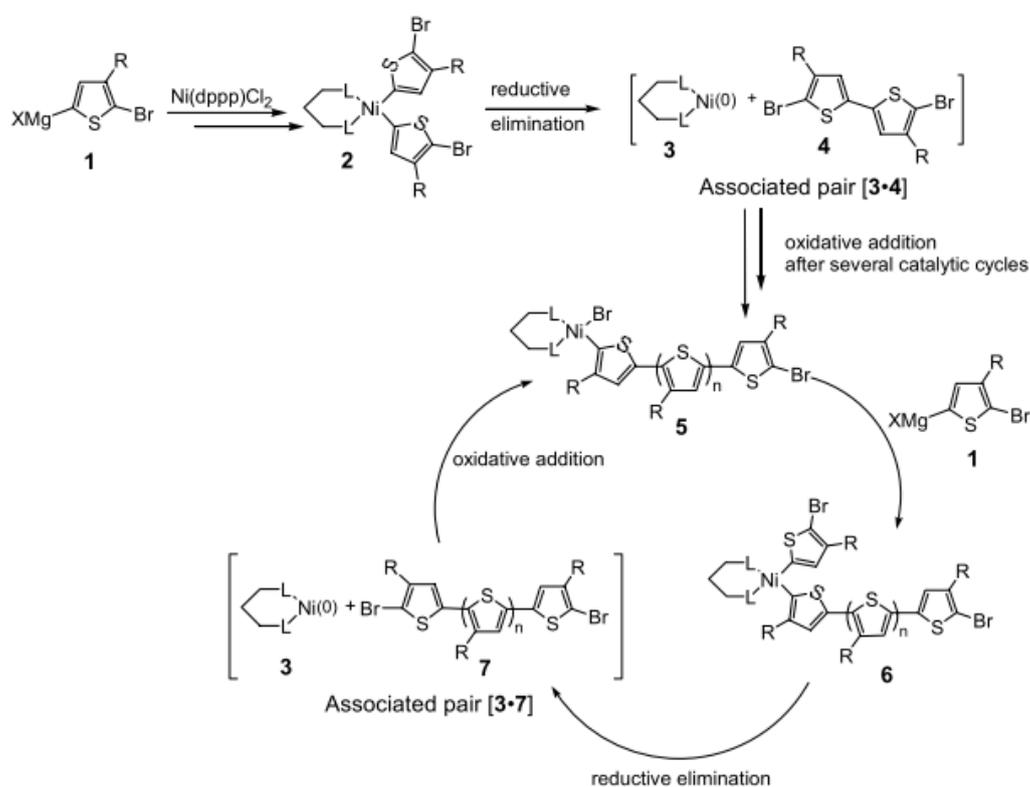
Figure 36. Catalytic cycle of GRIM polymerization shown with 2,5-dibromo-3-hexylthiophene [32]

Procedure

A dry nitrogen flushed flask was charged THF (100 ml) and 2,5-dibromo-3-hexylthiophene (0.502 g, 1.53 mmol). Methylmagnesium bromide (3.0 M in Et$_2$O, 0.51 ml, 1.53 mmol) was added via a deoxygenized syringe and the mixture was gently refluxed for 2 hours. The mixture was cooled to room temperature and Ni(dppp)Cl$_2$ (7.2 mg, 13.3 µmol) was added as a suspension in THF (1 ml). After 4 hours the polymerization was quenched with methanol and the solvent was evaporated. No polymer was obtained.

The polymerization was tried once more using the same procedure but with 24 hours of polymerization time but no polymer was obtained here either.

3.4.2 GRIM polymerization 2 – homopolymer (PFO)

The GRIM polymerization was tried with 9,9-dioctyl-2,7-dibromofluorene, another donor monomer, to test if the monomer might be the problem.
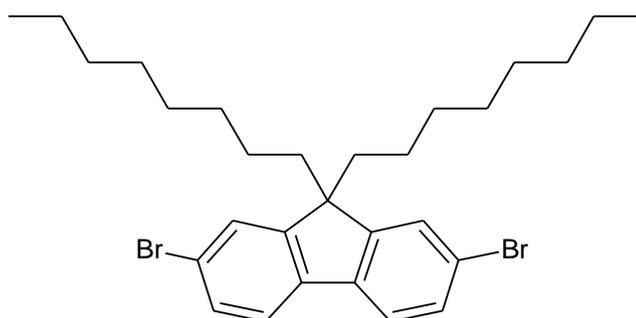
Figure 37. 9,9-dioctyl-2,7-dibromofluorene

Procedure

9,9-dioctyl-2,7-dibromofluorene (0.82 g, 1.5 mmol) and THF (100 ml) was charged into a dry nitrogen flushed flask. Methylmagnesium bromide (3.0 M in Et$_2$O, 0.50 ml, 1.5 mmol) was added via a deoxygenized syringe and the mixture was gently refluxed for 1.5 hours. The mixture was cooled to room temperature and Ni(dppp)Cl$_2$ (3.0 mg, 5.5 µmol) was added as a suspension in THF (1 ml). The polymerization was quenched with methanol after 24 hours and the solvent was evaporated. No polymer was obtained. This could indicate that the Ni(dppp)Cl$_2$ was inactive.

3.4.3 Suzuki polymerization 1 – Homopolymer (PFO) #1

Since no polymers could be achieved with the Ni(dppp)Cl$_2$ catalyst, a Pd(PPh$_3$)$_4$ catalyst was tested using the same 9,9-dioctyl-2,7-dibromofluorene monomer as in the second GRIM polymerization. The Pd(PPh$_3$)$_4$ catalyst does not lead to a GRIM polymerization, but can be used for a Suzuki polymerization. A Suzuki coupling is the coupling between a halogen substituted molecule and a boronic acid substituted molecule in the presence of a base.[45] The catalytic cycle is illustrated in figure 38 and the overall polymerization reaction in figure 39.
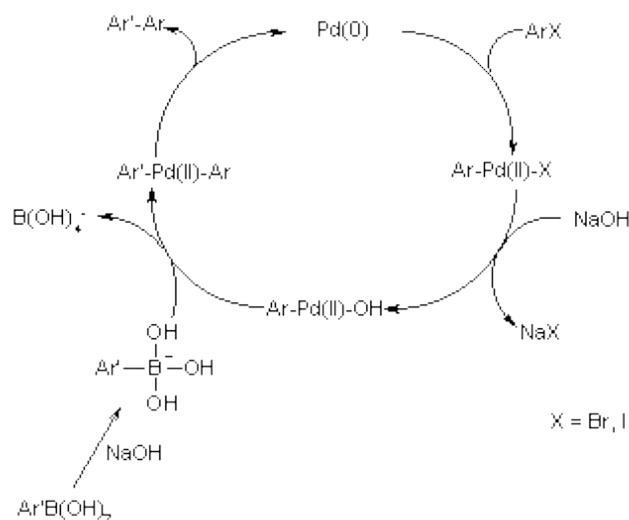
Figure 38. Catalytic cycle of the Suzuki coupling. In this example sodium hydroxide is used as the base but other bases can readily be used [45]

Figure 39. Polymerization of PFO by Suzuki coupling

Procedure

9,9-dioctylfluorene-2,7-diboronic acid bis(1,3-propanediol) ester (1.00 g, 1.79 mmol) and potassium carbonate solution (2 M, 25 ml) were mixed and stirred under nitrogen for one hour. 9,9-dioctyl-2,7-dibromofluorene (0.98 g, 1.79 mmol) dissolved in THF (100 ml) was added followed shortly by catalytic amounts of Pd(PPh$_3$)$_4$. The reaction was refluxed for 5 hours and hydrochloric acid solution was added (2 M, 50 ml) after which the mixture was stirred for 30 minutes. The THF was removed by rotary evaporation and the resultant suspension was filtered to yield a yellow solid. The solid was purified by soxhlet extracted with methanol to remove catalyst and monomer impurities as well as small oligomers. The polymer was following extracted with chloroform and obtained by removing the chloroform. Yield: 1.13 g, 57.1 %.

By obtaining a polymer with the Pd(PPh$_3$)$_4$ catalyst from the same monomer, which the Ni(dppp)Cl$_2$ catalyst could not polymerize indicates that the Ni(dppp)Cl$_2$ catalyst in some ways had become inactive. Due to time constraints no new Ni(dppp)Cl$_2$ could be obtained, and hence the creation of block copolymers therefore could not be achieved through the use of GRIM. Instead a series of donor polymers were created and characterized in the same way block copolymers would have been characterized.

3.4.4   Suzuki polymerization 2 – Homopolymer (PFO) #2

The Suzuki polymerization 1 was only reacted for 5 hours which is a quite short when dealing with step-growth polymerizations. For this reason the polymerization was repeated with a longer reaction time.

Procedure

Except for a reaction time of 24 hours the procedure is the exact same as in section 3.4.3. Yield: 1.12 g, 56.6 %, green solid.

3.4.5   Suzuki polymerization 3 – Alternating copolymer (P8BT)

An alternating copolymer of 9,9-dioctylfluorene and benzo[c]-2,1,3-thiadiazole was obtained by Suzuki coupling as described in section 3.4.3. The polymer is denoted P8BT.
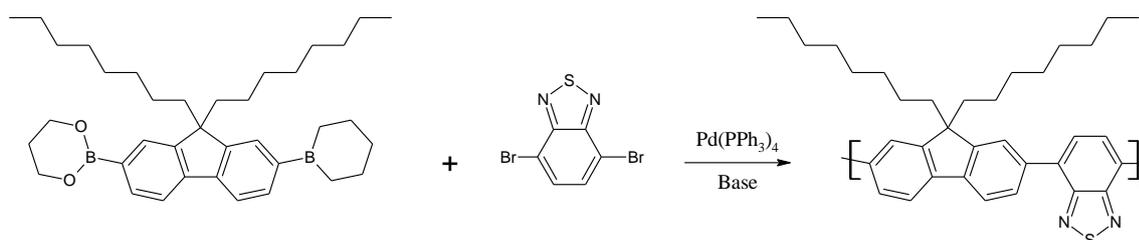
Figure 40. Polymerization of P8BT by Suzuki coupling

Procedure

9,9-dioctylfluorene-2,7-diboronic acid bis(1,3-propanediol) ester (1.00 g, 1.79 mmol) and potassium carbonate solution (2 M, 25 ml) was mixed and stirred under nitrogen for one hour. 4,7-dibromobenzo[*c*]-1,2,5-thiadiazole (0.53 g, 1.79 mmol) dissolved in THF (100 ml) was added followed shortly by catalytic amounts of Pd(PPh$_3$)$_4$. The reaction was refluxed for 24 hours and quenched with hydrochloric acid (4 M, 50 ml). The THF was evaporated and the resultant suspension was filtered to yield an orange solid. The solid was purified by soxhlet extracted with methanol to remove catalyst and monomer impurities as well as small oligomers. Subsequently the polymer was extracted with chloroform and obtained as a dark red solid by removing the chloroform. Yield: 0.91 g = 59.5 %

3.4.6 Suzuki polymerization 4 – Alternating copolymer (P8FDNT)

An alternating copolymer of 9,9-dioctylfluorene and 3',4'-dinitroterthiophene (**9**) was obtained by Suzuki coupling as described in section 3.4.3. The polymer is denoted P8FDNT.
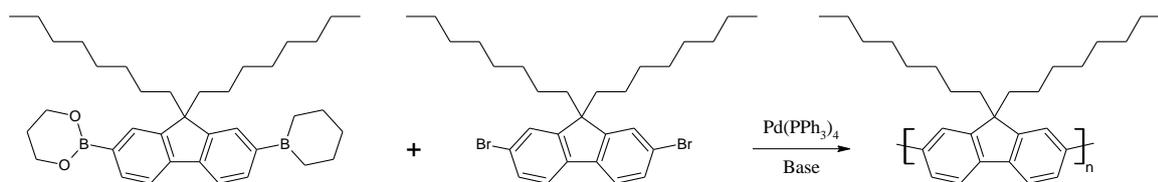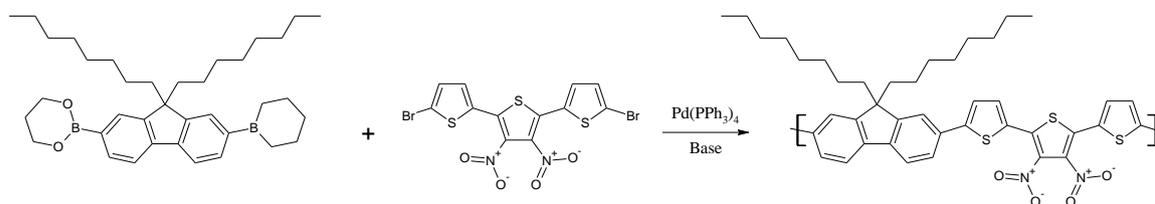

Figure 41. Polymerization of P8FDNT by Suzuki coupling

Procedure

9,9-dioctylfluorene-2,7-diboronic acid bis(1,3-propanediol) ester (0.50 g, 0.90 mmol) and potassium carbonate solution (2 M, 25 ml) were mixed and stirred under nitrogen for one hour. 5,5''-dibromo-3',4'-dinitroterthiophene (**9**) (0.45 g, 0.90 mmol) suspended in THF (100 ml) was added followed shortly by catalytic amounts of Pd(PPh$_3$)$_4$. The reaction was refluxed for 24 hours and quenched with hydrochloric acid (4 M, 50 ml). The THF was evaporated and the resultant suspension was filtered to yield a deep red semisolid. The solid was purified by soxhlet extracted with methanol to remove catalyst and monomer impurities as well as small oligomers. Then the polymer was following extracted with chloroform and isolated as a black solid by removing the chloroform. Yield: 0.36 g = 37.9 %

3.5 Polymer characterization

3.5.1 Gel Permeation Chromatography (GPC)

The molecular weights of the polymers and the polydisperities were determined by gel permeability chromatography (GPC) using polystyrene standards and a Waters Styralgel ® HR 4 THF (4.6 x 300 mm) column. Dionex pump (P680), autosampler (ASI-100) and UV detector (UVD170U) were used. The detection wavelength was set to 250 nm.

3.5.2 Ultraviolet/visible light spectroscopy (UV/vis)

Absorption spectra of polymer solutions and of spin casted films were obtained on a Varian Cary 50 Bio Spectrophotometer. 25 µg/ml chloroform solutions were used along with 10 mm quartz curvettes. Films were casted on glass slides using 1,2-dichlorobenzene. Wavelength scans were performed from 280 nm to 900 nm at 300 nm/min.

3.6 Solar cell manufacturing

PEDOT:PPS (1.3 wt % dispersion in H_2O, conductive grade) and aluminum evaporation slugs (99.999 %) from Aldrich and PCBM (99 %) from Solenne were used along with the synthesized polymers.

Solar cells were prepared on ITO coated glass substrates. These were first thoroughly cleaned, rinsed with water and spin coated with a layer of PEDOT:PPS at 2800 rpm. The coated substrates were heated to 150 °C for one minute and left to cool. After cooling the substrates were cleaned with pressurized air to remove any dust particles and then transferred into a glove box (<1 ppm O_2 and <1 ppm H_2O). Here the substrates were heated to 150 °C for five minutes to ensure that they were completely dry. After the substrates had cooled they were cleaned with chlorobenzene and an active layer was spin coated on top of the PEDOT:PPS layer using the following solutions:

Table 3. Active layers were spin casted from the listed solutions

#	Donor	Acceptor	Solvent
1	PFO #1 (20 mg/ml) *	PCBM (20 mg/ml)	1,2-dichlorobenzene
2	P8BT (20 mg/ml)	PCBM (20 mg/ml)	1,2-dichlorobenzene
3	P8FDNT (20 mg/ml)	PCBM (20 mg/ml)	1,2-dichlorobenzene

* PFO #1 did not fully dissolve and the precise concentration is therefore unknown.

The solutions had been stirred over night and filtered through a 1 µm filter before use. PFO #2 was only very slightly soluble in 1,2-dichlorobenzene and was therefore not used.

The active layer was casted at a spin rate of 800 rpm. The solar cells were completed by depositing a layer of aluminum on top of the active layer.

3.7 Solar cell characterization

The photovoltaic response under simulated sunlight (AM 1.5, 1000 W/m^2) was measured by using a Solar Constant 575 from Steuernagel Lichttechnik GmBH, Germany and a Keithley 2400 sourcemeter. All measurements were carried out in air immediately after completed assembly.

4 Results and discussion

4.1 Monomer synthesis

4.1.1 Donor monomer

The donor monomer was not obtained in its pure form. Instead a mixture of the compounds in figure 42 was obtained. Two different approaches were carried out. The first described in section 3.1 had the bromination as the final step in the synthesis strategy. In this approach problems with the attachment of more than two bromines were found.
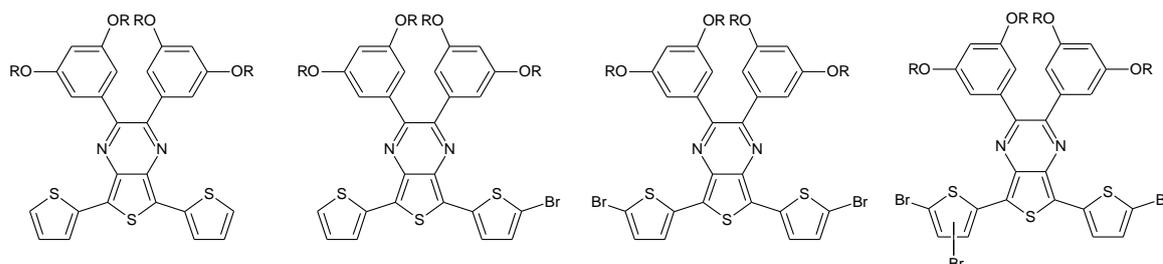
Figure 42. Monomer units with different amounts of bromine attached

Brominations of thiophene usually have very high α-position selectivity.[27][34] Hoffmann & Carlsen (1999) e.g. reported the bromination of 2,2'-dithienylmethane (cf. figure 43) with NBS with excellent α-position selectivity.
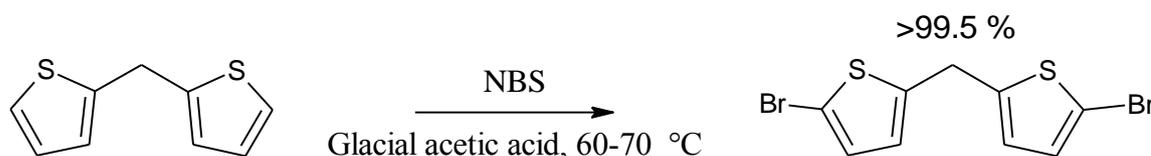
Figure 43. Bromination of 2,2'-dithienylmethane with NBS reported by Hoffmann & Carlsen (1999)

For some reason the β-positions are more prone to bromination in the thiophene-thienopyrazine-thiophene system. This has also been reported by Petersen et al. (2007). The four 2-ethylhexyloxy side chains were found to have a large influence on the physical properties compared to the number of bromine making the purification inefficient. It was therefore found impractical to isolate reasonable amount for polymerization using this approach.

The second approach described in section 3.2 had the bromination as an early step in the monomer synthesis. Using this strategy only the α-positions were brominated hence no problems with multibrominated compounds were found. Furthermore the mono- and unsubstituted species could easily be removed by recrystallization and thereby solving the problems encountered in the first synthesis strategy. Instead problems with the next synthesis step, the reduction of the nitro groups, were encountered. Dehalogenation is a common side reaction in reduction reaction but it was found not to occur with either stannous chloride or elemental iron in acid media at room temperature. However a method for the following purification could not be found. Liquid/liquid extraction with ethyl acetate as performed in the

first strategy was unsuccessful as the amino compound was insoluble in ethyl acetate. Column chromatography could not be performed since no suitable eluent mixture could be found.

The use of the impure product mixture in the following condensation reaction with the α-diketone found that the elevated temperatures used caused dehalogenation to occur. This emphasizes the need for purification in this strategy. A third strategy might be more successful. A suggestion could be to brominate after the reduction of the nitro groups. In this case care must be taken to protect the amino groups from oxidation.

Most reaction steps were completed with satisfactory yields of 80 to 90 %. The synthesis of terthiophene-3',4'-diamine, however, only yield 47 %. The lower yield is ascribed to the liquid/liquid extraction which was very slow. It was terminated after 48 hours at which time visible amounts of compound were still present in the extraction vessel. A higher yield could therefore be achieved by performing the liquid/liquid extraction for a longer period of time. Petersen *et al.* (2007) reported that the product obtained using this purification procedure was contaminated with tin in the form of hexachloro stannate salt. This was not a problem in the condensation between the α-diketone and the diamine, but the effects on bromination as suggested in synthesis strategy III is unknown. Another aspect is that the reduction agent still needs to be removed before the condensation in synthesis strategy III. The reduction is therefore somewhat problematic and another method would be preferable. Petersen *et al.* (2007) tried catalytic hydrogenation with palladium on carbon but concluded that it was not practically applicable due to poisoning of the catalyst. It is believed that using this reduction method, a simple filtration to remove the carbon particles would be sufficient purification. The question is whether or not the ease of purification outweighs the cost of catalyst or if the catalyst could be regenerated. This needs to be investigated.

4.1.2 Acceptor monomer

The Kumada coupling reaction to attach a hexyl chain to the acceptor unit was unsuccessful and hence the acceptor monomer was not obtained. The Kumada coupling was attempted using the Ni(dppp)Cl$_2$ catalyst which also failed to yield any product in the GRIM polymerizations. It therefore seems reasonable to assume that the Ni(dppp)Cl$_2$ was inactive.

The first three steps in the synthesis resulted in low yields. Too fast addition of bromine in the first reaction causing it to evaporate before it could react as well as difficulties with the distillation in the second step due to poor vacuum control were the main contributors to the low yields. Both problems are easy to overcome and higher yields should be expected in an industrial production. The third step, the cyanation, is more difficult to improve. The cyanation with copper cyanide is slow even at temperatures of about 200 °C and results in product mixtures with different degrees of cyanation. Wagner *et al.* (2006) reported a method using tosyl cyanide (cf. figure 44). This method is safer, faster and results in higher yields but is also more expensive. The method involves forming a Grignard intermediate and then adding the tosyl cyanide. The method was attempted without any yield indicating that it might be more difficult than reported.
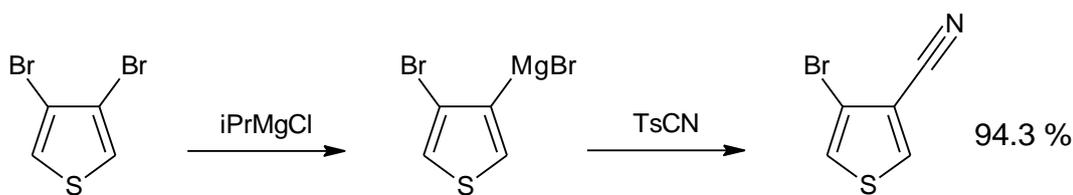
Figure 44. Cyanation using tosyl cyanide

Engstrom *et al.* (2009) reported another method where a carboxylic acid group is converted into a carbonitrile group (cf. figure 45). This method should also result in better yields but requires another starting material and could therefore not be tested.
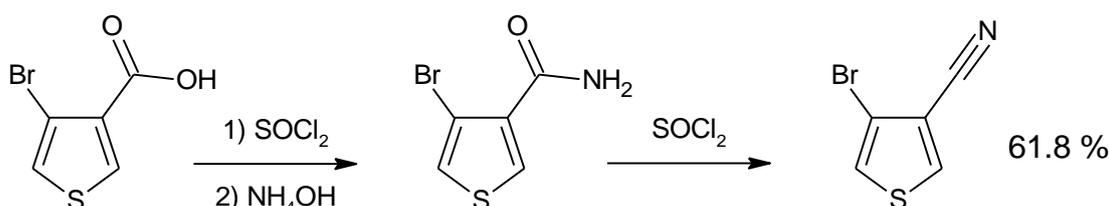
Figure 45. Synthesis used by Engstrom *et al.* (2009)

4.2 Polymerization

Vials with the synthesized polymers in solid state and in chloroform solution are shown in figure 46 and figure 47 respectively. Most notable is the difference in color between PFO #1 (yellow) and PFO #2 (green) which have the same composition. The differences are therefore believed to be an effect of different conjugated lengths. PFO #1 dissolved much faster and to a larger extend than PFO #2 indicating differences in their molecular weights as well.

Figure 46. Synthesized polymers in solid state. From the left: PFO #1, PFO #2, P8BT and P8FDNT

Figure 47. 25 µg/ml solutions in chloroform. From the left: PFO #1, PFO #2, P8BT and P8FDNT

The PFO #1 and #2 polymers were expected to have a large band gap due to their homopolymer structure and as seen in figure 47 there is no strong absorption of visible light but instead a slight bluish green fluorescence indicating large band gaps. P8BT and P8FDNT showed a much better absorption of visible light producing fluorescing yellow and deep orange solutions respectively.

4.3 Polymer characterization

4.3.1 Gel Permeation Chromatography (GPC)

The molecular weights of the polymers and the polydispersities were estimated with gel permeation chromatography using polystyrene standards. The retention times for the standards are listed in table 4 and plotted in figure 48.

Table 4. Molecular weights supplied by the manufacture versus retention times for polystyrene standards

M_p [g/mole]*	778,000	462,000	188,000	43,700	9,730	2,950
$\bar{M}_w$ [g/mole]	770,000	451,000	188,000	42,900	9,580	2,980
$\bar{M}_n$ [g/mole]	738,000	438,000	182,000	41,800	9,320	2,790
Retention time [min]	6.497	6.871	7.582	9.294	11.174	11.942

*M_p = Molecular weight at maximum peak intensity

$$y = 3E+08e^{-0,963x}$$
$$R^2 = 0,9926$$
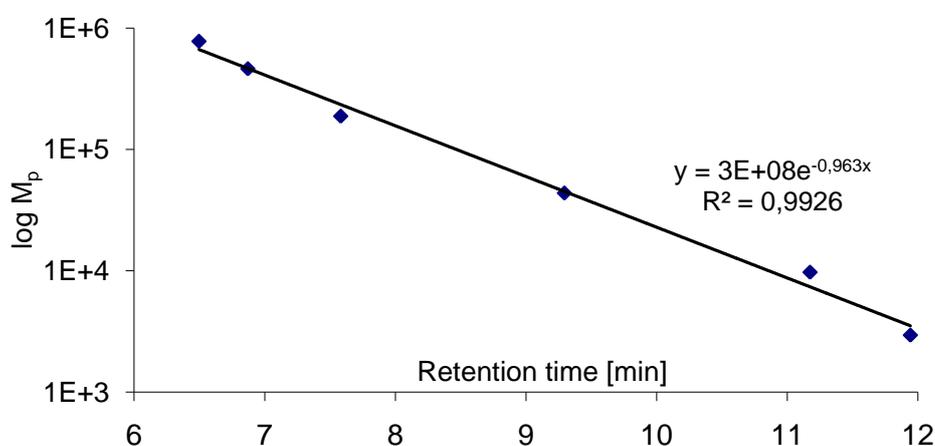
Figure 48. Molecular weight (M_p) of polystyrene standard versus retention times

The plot of the molecular weights as function of the retention times yields a straight line when plotted with an exponential y-axis. The outermost calibration values deviate slightly from the line indicating that they might be on the edge of the columns working range. The peak molecular weights of synthesized polymers were in the small end of this range (cf. table 5). This is problematic when the number and weight average molecular weights are calculated since the width of the peaks makes them extend further out of range. The validity of the results is therefore questionable and should be tested with a column designed for lower molecular weights.

Table 5. Retention times, rounded molecular weights and polydispersities of the synthesized polymers

	PFO #1	PFO #2	P8BT	P8FDNT
Retention time [min]	11.385	10.943	11.722	12.202
M_p [g/mole]	5,200	8,000	3,800	2,300
$\bar{M}_n$ [g/mole]	6,500	10,300	4,400	2,600
$\bar{M}_w$ [g/mole]	11,000	22,200	7,100	3,500
PDI	1.7	2.2	1.6	1.3

The small molecular weights are believed to be a result of the slightly impure materials that were purchased. The purity of the 5,5''-dibromo-3',4'-dinitroterthiophene (**9**) was not determined but was estimated to be the purest of the compounds used for polymerization based on the fact that it had been recrystallized very thoroughly and NMR did not show any traces of starting material. Even so the polymerization where it was used, the one of P8FDNT, yielded the shortest polymer. 5,5''-dibromo-3',4'-dinitroterthiophene was observed to have very low solubilities in common solvents, among them THF which was used for the polymerization. The low solubility might have resulted in 5,5''-dibromo-3',4'-dinitroterthiophene being a limiting factor.

4.3.2   Ultraviolet/visible light spectroscopy (UV/vis)

The optical properties of the synthesized polymers were measured with UV/vis spectroscopy. This was done for both chloroform solutions and for spin casted films. Films are more representative for the absorption of the active layer in the completed solar cell compared to solutions due to slight differences in absorption, [8][70] but solutions are better at comparing the different polymers absorption coefficient due to better concentration control.

Chloroform solutions

All of the chloroform solutions had concentrations of 25 µg/ml. The transmission spectra of the solutions are plotted in figure 49 below. The two PFO polymers produced nearly transparent solutions which also is manifested in the measured spectra. They have equal absorption spectra with an absorption most pronounced between 330 and 400 nm but with a slight absorption up to 425 nm. This is mostly outside the visual range.
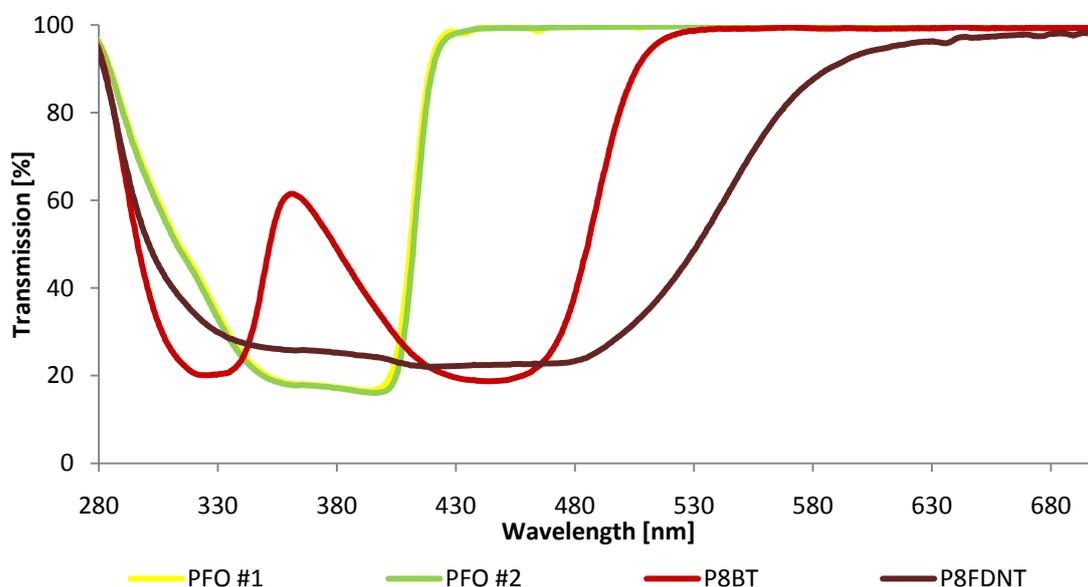
Figure 49. Absorption spectra of polymers in chloroform solutions

The spectrum for P8BT shows absorption in two separate domains, one at 325-340 nm and one at 400-480 nm. This separation into two different domains is an often observed effect caused by the donor-acceptor copolymer structure.[7] Another effect of the donor-acceptor copolymer structure is the narrowing of the band gap, which is observed by the absorption of longer wavelengths.

The spectrum of P8FDNT shows good absorption from 310 to 510 nm and absorption extending all the way up to 625 nm which is a relatively broad range compared to the other polymers. The low molecular weight of 2300 g/mole equal to only 3 repeating units indicates that much better optical properties could be expected if a proper conjugated length could be achieved. Unlike P8BT, P8FDNT does not have two separate absorption domains but one broad. This is believed to be an effect of the more complicated donor-donor-acceptor-donor structure of the P8FDNT rather than the donor-acceptor structure of the P8BT.

Films spin casted from 1,2-dichlorobenzene

The transmission spectra of the spin casted films are plotted in figure 50. Films were casted with quickly prepared solutions with unknown concentrations which is why the relative transmissions cannot be compared. Absorptions of films are often observed to red shift compared to solutions [8][70] and this is also observed in this case although small, in the order of 5-20 nm.
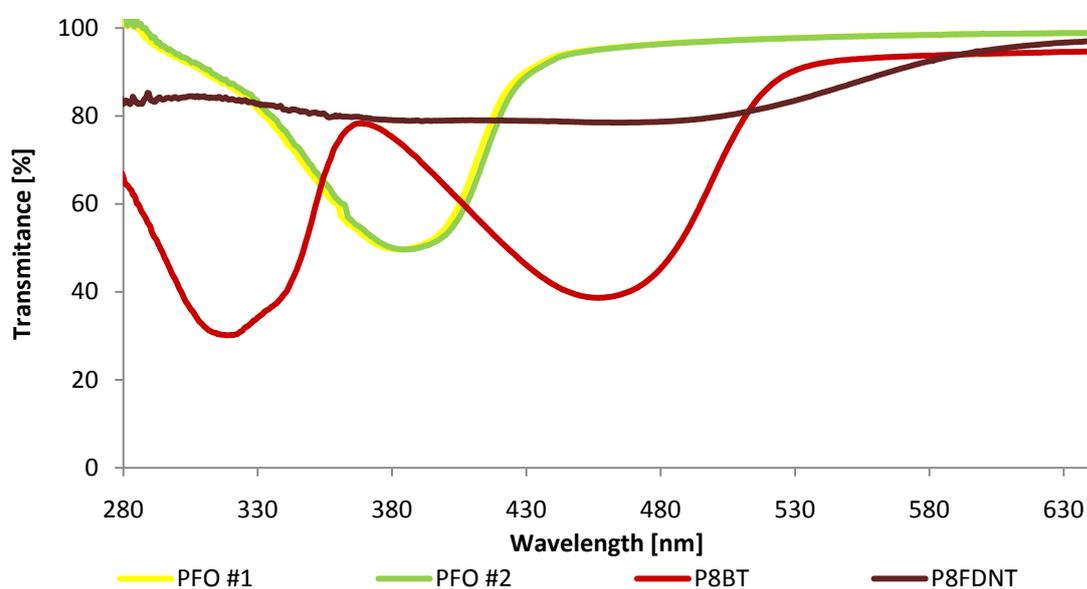
Figure 50. Absorption spectra of spin casted polymer films

The size of the polymers band gaps can be estimated from the visual performance. Cyclic voltammetry should be used if the size of the band gap has to be more precisely determined. Cyclic voltammetry also yields information on the HOMO and LUMO. By calculating the band gap using the longest wavelength with a significant absorption for each polymer one obtains the band gaps listed in table 6.

Table 6. Band gaps estimated from spin casted films

Polymer	PFO #1	PFO #2	P8BT	P8FDNT
Band gap [eV]	2.72	2.72	2.32	2.02
Reported		2.9 *	2.4 [+]	-

* Hino et al., 2006 (cyclic voltammetry)   [+] Kietzke et al., 2004 (cyclic voltammetry)

4.4 Solar cell manufacturing

Two solar cells of each of the solutions listed in table 3, page 40 were produced.

As seen in figure 51 and figure 52 problems with poor film forming abilities were encountered. In a few cases where uniform films were obtained (cf. figure 53 and figure 54) the absorptions were low, indicating the formation of thin films. These problems are believed to be an effect of the very low molecular weights, hence the short polymer chains do not entangle into each other efficiently causing crystallization.
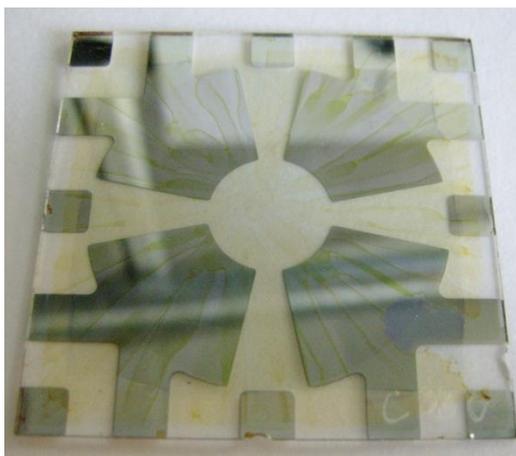
Figure 51. Solar cell produced with P8BT:PCBM (1:1)
Poor active layer film
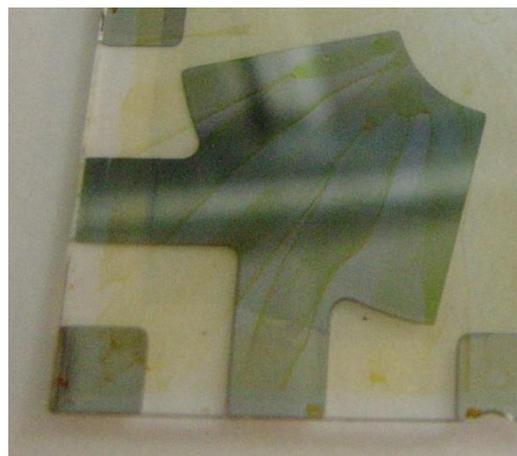
Figure 52. Zoom of the 3th quadrant form figure 51
Poor active layer film
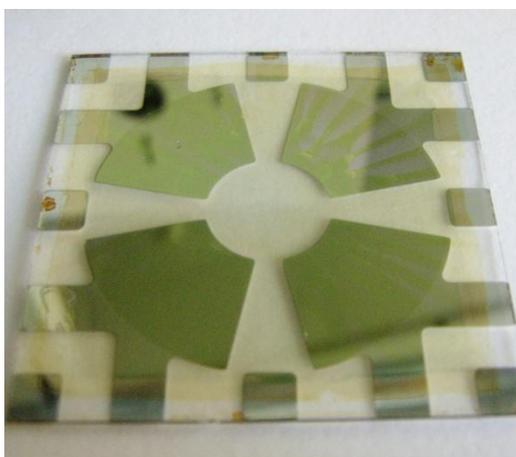
Figure 53. Solar cell produced with P8BT:PCBM (1:1)
Good active layer film
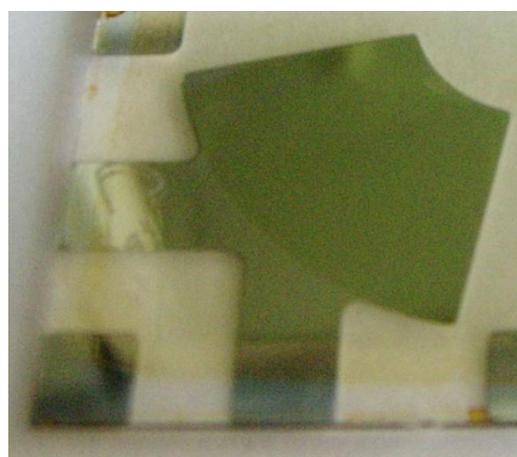
Figure 54. Zoom of the 3th quadrant form figure 53
Good active layer film

4.5 Solar cell characterization

The manufactured solar was characterized with current-voltage (I-V) curves. From the curves the open circuit voltages, the short circuit currents and the fill factors were determined. Along with the intensity of the light source these three values were used to calculate the power conversion efficiencies. The results from the three different polymer:PCBM blends are plotted in figure 55.
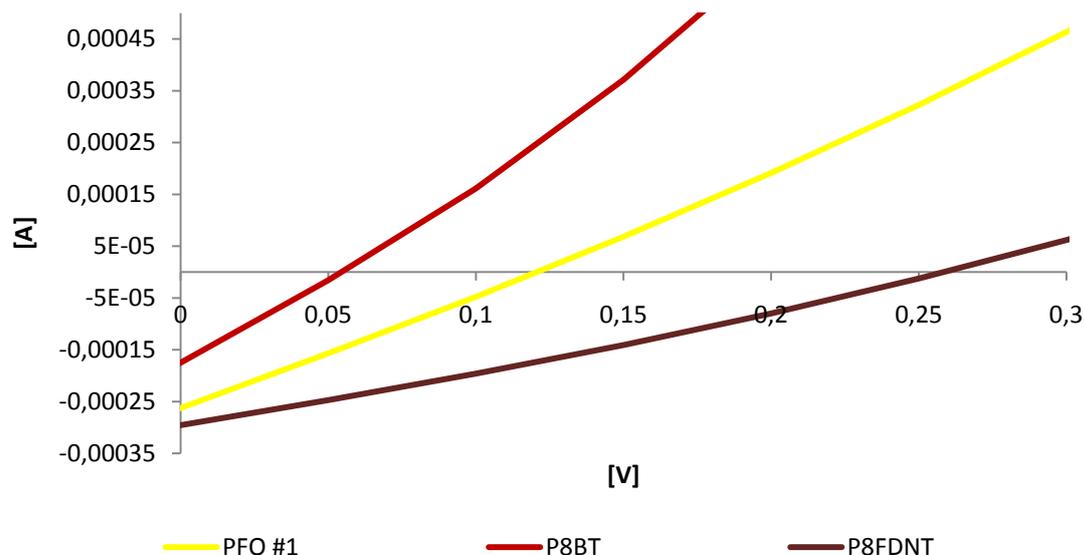
Figure 55. I-V curves for the three polymer:PCBM blends

Of the three blends, P8FDNT yielded the highest power conversion efficiency of 0.011 %. I-V data for all blends are listed in table 7.

Table 7. Data obtained from I-V measurements

Active layer	PCE (%)	V_{oc} (V)	I_{sc}(mA/cm^2)	FF (%)	MaxPow (mW)
PFO #1 : PCBM (1:1)	**0.004**	0.121	-0.131	25.66	0.008
P8BT : PCBM (1:1)	**0.001**	0.054	-0.087	25.89	0.002
P8FDNT : PCBM (1:1)	**0.011**	0.258	-0.148	27.94	0.021

All of the manufactured solar cells yielded very low efficiencies. The poor film forming abilities mainly due to the small conjugated lengths are believed to be a key contributor in the poor performance but also the large band gaps and lack of LUMO-LUMO offset optimization are contributors.

LUMO of PFO, P8BT and PCBM has been reported to be -3.1 eV, -3.2 eV and -4.3 eV versus vacuum respectively.[26][36][52] The LUMO offsets for PFO:PCBM and P8BT:PCBM blends are therefore 1.2 and 1.1 eV respectively, much larger than the optimal value of 0.3-0.5 eV. Without cyclic voltammetry measurements no LUMO value for P8FDNT could be obtained and the LUMO offset is therefore unknown.

5 Conclusion

Three different conductive polymers were synthesized, characterized and tested in polymer solar cells using [6,6]-phenyl-C_{61}-butyric acid methyl ester as an electron acceptor. A maximum power conversion efficiency of 0.011 % was achieved using a novel copolymer obtained by Suzuki coupling of 9,9-dioctylfluorene-2,7-diboronic acid bis(1,3-propanediol) ester and 5,5''-dibromo-3',4'-dinitroterthiphene. Low molecular weights were a general problem in all of the performed polymerizations resulting in poor film forming abilities and affecting the solar cell performance.

The synthesis of a low band gap electron donating monomer was successfully attempted but could not be isolated due to purification difficulties. Another synthesis strategy was attempted but this strategy resulted in problems with dehalogenation. The synthesis of an electron accepting monomer was also attempted but could not be finalized due to an inactive nickel catalyst.

The synthesis of block copolymers was attempted using GRIM polymerization, but failed due to an inactive nickel catalyst.

6 References

1. ASTM. 2003. *Reference Solar Spectral Irradiance: Air Mass 1.5*. [online]. Available form World Wide Web: <http://rredc.nrel.gov/solar/spectra/am1.5/ASTMG173/ASTMG173.xls>

2. Baumann, T., Vogt, H. & Bräse, S. 2007. The Proline-Catalyzed Asymmetric Amination of Branched Aldehydes. *European Journal of Organic Chemistry*, p.266–282.

3. Bayardon, J. & Sinou, D. 2005. Synthesis of an Enantiopure Fluorous 1,2-Diphenyl-1,2-diaminoethane. *Synthesis*, 3, p.425–428.

4. Bellamy, F. D. & Ou, K. 1984. Selective Reduction of Aromatic Nitro Compounds With Stannous Chloride in Non Acidic and Non Aqueous Medium. *Tetrahedron Letters*, 25, pp.839-842.

5. Bockstaller, M. R. & Thomas, E. L. 2002. *ELThomas*. [online]. Available form World Wide Web: <http://web.mit.edu/tinytech/Nanostructures/Spring2003/ELThomas/EncyclopediaMarcelDekker2002.pdf>

6. Brabec, C. J., Winder, C., Sariciftci, S. N., Hummelen, J. C., Dhanabalan, A., van Hal, P. A. & Janssen, R. A. J. 2002. A Low-Band Gap Semiconducting Polymer for Photovoltaic Devices and Infrared Emitting Diodes. *Advanced Functional Materials*, 12, pp.709-712.

7. Bundgaard, E. 2007. *Low Band Gap Polymers For Organic Photovoltaics*. Risø National Laboratory and Roskilde University Centre.

8. Bundgaard, E. & Krebs, F. C. 2007. Low Band Gap Polymers For Organic Photovoltaics. *Soler Energy Materials & Solar Cells*, 91, pp.954-985.

9. Burger, C., Ruland, W. & Semenov, A. N. 1990. Polydispersity effects on the microphase-separation transition in block copolymers. *Macromolecules*, 23, pp.3339-3346.

10. Chen, X. L. & Jenekhe, S. A. 1997. Bipolar Conducting Polymers: Blends of p-Type Polypyrrole and an n-Type Ladder Polymer. *Macromolecules*, 30, pp.1728-1733.

11. Chochos, C. L., Economopoulos, S. P., Deimede, V., Gregoriou, V. G., Lloyd, M. T., Malliaras, G. G. & Kallitsis, J. K. 2007. Synthesis of a Soluble n-Type Cyano Substituted Polythiophene Derivative: A Potential Electron Acceptor in Polymeric Solar Cells. *Journal of Physical Chemistry C*, 111, pp.10732-10740.

12. Coakley, K. M. & McGehee, M. D. 2004. Conjugated Polymer Photovoltaic Cells. *Chemistry of Materials*, 16, pp.4533-4542.

13. Corey, E. J., Lee, D.-H. & Sarshar, S. 1995. Convenient Routes to Symmetrical Benzils and Chiral 1,2-Diaryl-1,2-diaminoethanes, Useful Controllers and Probes for Enantioselective Synthesis. *Tetrahedron: Asymmetry*, 6, pp.3-6.

14. Dennler, G. & Sariciftci, S. N. 2005. Flexible Conjugated Polymer-base Plastic Solar Cells: From Basics to Applications. *Proceedings of the IEEE*, 93, pp.1429-1439.

15. Energy Information Administration. 2006. *International Energy Outlook 2006*. report # DOE/EIA-0484.

16. Engstrom, K. M., Baize, A. L., Frenczyk, T. S., Kallemeyn, J. M., Mulhern, M. M., Rickert, R. C. & Wagaw, S. 2009. Improved Synthesis of 3-Substituted-4-amino-[3,2-c]-thienopyridines. *The Journal of Organic Chemistry*, 74, pp.3849-3855.

17. Esteves, P. M., Carneiro, J. W. d. M., Cardoso, S. P., Barbosa, A. G. H., Laali, K. K., Rasul, G., Prakash, G. K. S. & Olah, G. A. 2003. Unified Mechanistic Concept of Electrophilic Aromatic Nitration: Convergence of Computational Results and Experimental Data. *Journal of the American Chemical Society*, 125, p.4836–4849.

18. Gronowitz, S. 1959. New Syntheses of 3-bromothiophene and 3,4-dibromothiophene. *Acta Chemica Scandinavica*, 13, pp.1045-1046.

19. Günes, S., Neugebauer, H. & Sariciftci, S. N. 2007. Conjugated Polymer-Based Organic Solar Cells. *Chemical Reviews*, 107, pp.1324-1338.

20. Hadipour, A., de Boer, B. & Blom, P. W. M. 2007. Solution-processed organic tandem solar cells with embedded optical spacers. *Journal of Applied Physics*, 102, p.074506.

21. Halls, J. J. M., Cornil, J., dos Santos, D. A., Silbey, R., Hwang, D. H., Holmes, A. B., Brédas, J. L. & Friend, R. H. 1999. Charge- and energy-transfer processes at polymer/polymer interfaces: A joint experimental and theoretical study. *Physical Review B*, 60, pp.5721-5727.

22. Harris, D. C. 2003. *Quantitative Chemical Analysis 6th Edition*. W. H. Freeman and Company.

23. Haugeneder, A., Neges, M. & Kallinger, C. *et al.*. 1999. Exciton diffusion and dissociation in conjugated polymer/fullerene blends and heterostructures. *Physical Review B*, 59, pp.15346-15351.

24. Hayes, A. W. 2007. *Principles and methods of toxicology*. ISBN 084933778X: CRC Press.

25. Hermann, W. & Simon, A. J. 2007. *Global Climate and Energy Project*. [online]. [Accessed 9th of June 2009]. Available form World Wide Web: <http://gcep.stanford.edu/pdfs/GCEP_Exergy_Poster_web.pdf>

26. Hino, Y., Kajii, H. & Ohmori, Y. 2006. Transient characteristics of polyfluorene-based polymer light-emitting diodes and their application for color tunable devices. *Thin Solid Films*, 499, pp.359-363.

27. Hoffmann, K. J. & Carlsen, P. H. J. 1999. Study of an Efficient and Selective Bromination Reaction of Substituted Thiophenes. *Synthetic Communications*, 29, pp.1607-1610.

28. Hoppe, H. & Sariciftci, N. S. 2004. Organic solar cells: An overview. *Journal of Materials Research*, 19, pp.1924-1945.

29. Hung, L. S., Tang, C. W. & Mason, M. G. 1997. Enhanced electron injection in organic electroluminescence devices using an Al/LiF electrode. *Applied Physics Letters*, 70, pp.152-154.

30. Huynh, W. U., Dittmer, J. J. & Alivisatos, A. P. 2002. Hybrid Nanorod-Polymer Solar Cells. *Science*, 295, pp.2425-2428.

31. International Energy Agency. 2007. *Renewables in Global Energy Supply - An IEA Fact Sheet*.

32. Iovu, M. C., Sheina, E. E. & Richard, M. D. 2005. Grignard Metathesis (GRIM) Method for the Synthesis of Regioregular Poly(3-alkylthiophenes) with Well-Defined Molecular Weights. *Polymer Preprints*, 46, pp.660-661.

33. Janssen, R. A. J. 2006. *Oral Presentations*. [online]. [Accessed 9th of June 2009]. Available form World Wide Web: <http://www-molycell.cea.fr/home/liblocal/docs/Oral presentations ECHOS 06/28-PL1 René Janssen.pdf>

34. Katrizky, A. R. & Taylor, R. 1990. *Electrophilic substitution of heterocycles: quantitative aspects*. ISBN 0120206471: Academic Press.

35. Kiebooms, R., Monon, R. & Lee, K. 2001. Chapter 1: Synthesis, Electrical, and optical properties of conjugated polymers. *In*: H. S. NALWA, (ed). *Handbook of Advanced Electronic and Photonic Materials and Devices*, Academic Press, pp.1-86.

36. Kietzke, T., Neher, D., Kumke, M., Montenegro, R., Landfaster, K. & Scherf, U. 2004. A Nanoparticle Approach To Control the Phase Separation in Polyfluorene Photovoltaic Devices. *Macromolecules*, 37, pp.4882-4890.

37. Koelsch, C. F. & Whitney, A. G. 1941. The Rsoenmund-von Braun Nitrile Synthesis. *Contribution from the School of Chemistry of the University of Minnesota*, pp.795-803.

38. Kroon, R., Lenes, M., Hummelen, J. C., Blom, P. W. M. & de Boer, B. 2008. Small Band Gap Polymers for Organic Solar Cells (Polymer Material Development in the Last 5 Years). *Polymer Reviews*, 48, pp.531-582.

39. McMurry, J. 2003. *Fundamentals of Organic Chemistry 5th Edition*. Thomson. Brooks/Cole.

40. Mihailetchi, V. D., Blom, P. W. M., Hummelen, J. C. & Rispens, M. T. 2003. Cathode dependence of the open-circuit voltage of polymer:fullerene bulk heterojunction solar cells. *Journal of Applied Physics*, 94, pp.6849-6854.

41. Mozingo, R., Harris, S. A., Wolf, D. E., Hoffhine Jr., C. E., Easton, N. R. & Folkers, K. 1945. Hydrogenation of Compounds Containing Divalent Sulfur. *Journal of the American Chemical Society*, 12 67, pp.2092-2095.

42. Olson, D. C., Piris, J., Collins, R. T., Shaheen, S. E. & Ginley, D. S. 2006. Hybrid photovoltaic devices of polymer and ZnO nanofibercomposites. *Thin Solid Films*, 496, pp.26-29.

43. Organic Chemistry Portal. a. *Acyloin Condensation*. [online]. [Accessed 9th of June 2009]. Available form World Wide Web: <http://www.organic-chemistry.org/namedreactions/acyloin-condensation.shtm>

44. Organic Chemistry Portal. b. *Rosenmund-von Braun Reaction*. [online]. [Accessed 9th of June 2009]. Available form World Wide Web: <http://www.organic-chemistry.org/namedreactions/rosenmund-von-braun-reaction.shtm>

45. Organic Chemistry Portal. c. *Suzuki Coupling*. [online]. [Accessed 9th of June 2009]. Available form World Wide Web: <http://www.organic-chemistry.org/namedreactions/suzuki-coupling.shtm>

46. Petersen, M. H., Hagemann, O., Nielsen, K. T., Jørgensen, M. & Krebs, F. C. 2007. Low band gap poly-thienopyrazines for solar cells—Introducing the 11-thia-9,13-diaza-cyclopenta[b]triphenylenes. *Solar Energy Materials & Solar Cells*, 91, pp.996-1009.

47. Pine, D. J. 2007. *Department of Physics and Center for Soft Matter Research*. [online]. [Accessed 9th of June 2009]. Available form World Wide Web: <http://physics.nyu.edu/pine/research/nanocopoly.html>

48. Radano, C. P., Janssen, R. A. J. & Meijer, E. W. 2004. Alternating Donor-Acceptor Block Copolymers. *Polymeric Materials: Science & Engineering*, 91, pp.740-741.

49. Renewable Energy Policy Network for the 21st Century. 2006. *Renewables - Global Status Report - 2006 Update*.

50. Roncali, J. 1997. Synthetic Principles for Bandgap Control in Linear -Conjugated Systems. *Chemical Rewievs*, 97, pp.173-205.

51. Rühlmann, K. 1971. Die Umsetzung von Carbonsäureestern mit Natrium in Gegenwart von Trimethylchlorsilan. *Synthesis*, pp.236-253.

52. Scharber, M. C., Mühlbacher, D., Koppe, M., Denk, P., Waldauf, C., Heeger, A. J. & Brabec, C. J. 2006. *Advanced Materials*, 18, pp.789-794.

53. Schlatmann, A. R., Wilms Floet, D., Hilberer, A., Garten, F. & Smulders, P. J. M. 1996. Indium contamination from the indium-tin-oxide electrode in polymer light-emitting diodes. *Applied Physics Letters*, 69, pp.1764-1766.

54. Spanggaard, H. & Krebs, F. C. 2004. A Brief history of the development of organic and polymeric photovoltaics. *Solar Energy Materials & Solar Cells*, 83, pp.125-146.

55. Sun, S.-S. 2003. Design of a block copolymer solar cell. *Solar Energy Materials & Solar Cells*, 79, pp.257-264.

56. Sun, S.-S., Fan, Z., Wang, Y., Winston, K. & Bonner, C. E. 2005. Morphological effects to carrier mobility in a RO-PPV/SF-PPV donor/acceptor binary thin film opto-electronic device. *Materials Science and Engineering B*, 116, pp.279-282.

57. Tamao, K., Sumitani, K. & Kiso, Y. *et al.*. 1976. Nickel-Phosphine Complex-Catalyzed Grignard Coupling. I. Cross-Coupling of Akyl, Aryl and Alkenyl Grignard Reagents with Aryl and Alkenyl Halides: General Scope and Limitation. *Bulletin of the Chemical Society of Japan*, 49, pp.1958-1969.

58. Tang, C. W. 1986. Two-layer organic photovoltaic cell. *Applied Physics Letters*, 48, p.183.

59. Tanner, D. D., Ruo, T. C., Takiguchi, H., Guillanume, A., Reed, D. W., Setiloane, B. P., Tan, S. L. & Meintzer, C. P. 1983. On the Mechanism of N-Bromosuccinimide Brominations. Bromination of Cyclohexane and Cyclopentane with N-Bromosuccinimide. *Journal of Organic Chemistry*, 48, pp.2743-2747.

60. Tao, M. 2008. Inorganic Photovoltaic Solar Cells: Silicon and Beyond. *The Electrochemical Society Interface*, Winter, pp.30-35.

61. Tollis, S., Narducci, V., Cianfriglia, P., Sterzo, C. L. & Viola, E. 1998. Full Picture of the Catalytic Cycle Underlying Palladium-Catalyzed Metal-Carbon Bond Formation. *Organometallics*, 17, pp.2388-2390.

62. van de Wetering, K. I. 2007. *Donor-Acceptor Block Copolymers: Synthesis and Properties*. ISBN: 978-90-36729-43-7.

63. van Duren, J. K. J., Yang, X., Loos, J., Bulle-Lieuwma, C. W. T., Sieval, A. B., Hummelen, J. C. & Janssen, R. A. J. 2004. Relating the Morphology of Poly(p-phenylene vinylene)/Methanofullerene Blends to Solar-Cell Performance. *Advanced Functional Materials*, 14, pp.425-434.

64. van Mullekom, H. A. M., Vekemans, J. A. J. M., Havinga, E. E. & Meijer, E. W. 2001. Developments in the chemistry and band gap engineering of donor±acceptor substituted conjugated polymers. *Materials Science and Engineering. R-Reports: A review Journal*, 32, pp.1-40.

65. Wagner, R., Donner, P. L., Kempf, D. J., Maring, C. J., Stoll, V. S., Ku, Y.-Y. & Pu, Y.-M. 2006. *ANTI-INFECTIVE AGENTS - Patent*. [online]. [Accessed 9th of June 2009]. Available form World Wide Web: <http://www.faqs.org/patents/app/20080214528>

66. Wen, L. & Rasmussen, S. C. 2007. Synthesis and structural characterization of 2,5-dihalo-3,4-dinitrothiophenes. *Journal of Chemical Crystallography*, 37, pp.387-398.

67. Western, E. C. 2004. *The University of Alabama*. [online]. Available form World Wide Web: <http://www.bama.ua.edu/~chem/seminars/student_seminars/fall04/papers-f04/western-sem.pdf>

68. Wienk, M. M., Turbiez, M. G. R., Struijk, M. P., Fonrodona, M. & Janssen, R. A. J. 2006. Low-band gap poly(di-2-thienylthienopyrazine):fullerene solar cells. *Applied Physics Letters*, 88, p.153511.

69. Wikipedia. 2009. *Alkylimino-de-oxo-bisubstitution*. [online]. [Accessed 9th of June 2009]. Available form World Wide Web: <http://en.wikipedia.org/wiki/Alkylimino-de-oxo-bisubstitution>

70. Zhang, C., Choi, S., Haliburton, J., Cleveland, T., Li, R., Sun, S.-S., Ledbetter, A. & Bonner, C. E. 2006. Design, Synthesis, and Characterization of a -Donor-Bridge-Acceptor-Bridge-Type Block Copolymer via Alkoxy- and Sulfone- Derivatized Poly(phenylenevinylenes). *Macromolecules*, 39, pp.4317-4326.

Appendix A

Chemicals

Synthesis of 2,5-dibromo-3,4-dinitrothiophene (1)
- 2,5-dibromothiophene 95%, Aldrich, Lot.: S67793-079
- Sulfuric acid 95-97%, Fluka, Lot.: 70580
- Sulfuric acid fuming (20 % SO3), Sigma-Aldrich, Lot.: 82070
- Nitric acid 68-70% ACS, Acros Organics, Lot.: A0235818

Synthesis of 2-(tributylstannyl)thiophene (2)
- 2-bromothiophene 98%, Aldrich, Lot.: 0702813J-338
- n-Butyllithium 1.6 M in hexanes, Aldrich, Lot.: S45934-507
- Tributyltin chloride 96%, Aldrich, Lot.: S43879-118

Synthesis of 3',4'-dinitro-[2,2';5',2'']-terthiophene (3)
- Tetrakis(triphenylphosphine)palladium(0), synthesized by Risø National Laboratory

Synthesis of [2,2';5',2'']-terthiophene-3',4'-diamine dihydrochloride (4)
- Stannous chloride 98 %, Aldrich, Lot.: U07675

Synthesis of methyl 3,5-bis(2-ethylhexyloxy)benzoate (5)
- Potassium Carbonate >99 % A.C.S reagent, Aldrich, Lot.: 013K0073
- Methyl 3,5-dihydroxybenzoate 97 %, Aldrich, Lot.: S38186-258
- 2-ethylhexyl bromide 95 %, Acros Organics, Lot.: A018588501

Synthesis of 1,2-bis(3,5-bis(2-ethylhexyloxy))ethane-1,2-dione (6)
- Naphthalene >98.0 % purum, Fluka Analytical, Lot.: 1316828
- Lithium rods >99 %, Merck, Lot.: 7243457
- Trimethylsilyl chloride >97 %, Aldrich, Lot.: 05429PH-358
- Acetic acid 99-100 % technical grade, AppliChem, Lot.: E2748
- Copper acetate monohydrate 99%, Merck, Lot.: 6331528
- Ammonium nitrate 99.5 %, JT Baker, 0612401028

Synthesis of 2,3-bis(3,5-bis(2-ethylhexyloxy)phenyl)-5,7-bis(thiophene-2-yl)thieno[3,4-b]pyrazine (7)
- Triethylamine >98.0 % Baker grade, J.T. Baker, Lot.: 10076

Synthesis of 2,3-bis(3,5-bis(2-ethylhexyloxy)phenyl)-5,7-bis(5-bromothiophen-2-yl)thieno[3,4-b]pyrazine (8)
- N-bromosuccinimide 99%, Sigma-Aldrich, Lot.: S67255-488

Synthesis of 5,5''-dibromo-3',4'-dinitroterthiophene (9)
- N-bromosuccinimide 99%, Sigma-Aldrich, Lot.: S67255-488

Synthesis of 5,5''-dibromoterthiophene-3',4'-diamine dihydrochloride (10)
- Stannous chloride 98 %, Aldrich, Lot.: U07675
- Stannous chloride dehydrate 98-101%, Merck, Lot.: B684714 532
- Magnesium powder 99%, Riedel-de Haën, Lot.: 30510
- Iron powder -325 mesh 97%, Aldrich, Lot.: S660432-478
- Hydrazine monohydrate 98%, Aldrich, S07996-453

- Formic acid 85%, Bie & Berntsen, Lot.: 6157110
- Zinc dust <10 µm >98%, Aldrich, Lot.: 10418AJ-478

Synthesis of tetrabromothiophene (11)
- Bromine >99.8% p.a., Acros Organics, Lot.: A014746001
- Thiophene >99 %, Aldrich, Lot.: S53458-228

Synthesis of 3,4-dibromothiophene (12)
- Zinc dust <10 µm >98%, Aldrich, Lot.: 10418AJ-478
- Acetic acid 99-100 % technical grade, AppliChem, Lot.: E2748

Synthesis of 4-bromothiophene-3-carbonitrile (13)
- Copper(I)cyanide >99.0%, Fluka, Lot.: 1329087

Synthesis of 4-hexylthiophene-3-carbonitrile (14)
- [1,3-Bis(diphenylphosphino)propane]dichloronickel(II), Aldrich
- Hexyl bromide 99%, Acros Organics, Lot.: A018289801
- Magnesium turnings >99%, Merck, Lot.: S22278 725

GRIM polymerization 1 – homopolymer (P3HT)
- 2,5-dibromo-3-hexylthiophene 97%, Aldrich, Lot.: 16298MJ
- Methylmagnesium bromide 3.0M in Et_2O, Aldrich, Lot.: 04520BH
- [1,3-Bis(diphenylphosphino)propane]dichloronickel(II), Aldrich

GRIM polymerization 2 – homopolymer (PFO)
- 9,9-dioctyl-2,7-dibromofluorene 96 %, Aldrich, Lot.: 13722DB
- Methylmagnesium bromide 3.0M in Et_2O, Aldrich, Lot.: 04520BH
- [1,3-Bis(diphenylphosphino)propane]dichloronickel(II), Aldrich

Suzuki polymerization 1 & 2 – Homopolymer (PFO) #1 & #2
- 9,9-dioctyl-2,7-dibromofluorene 96 %, Aldrich, Lot.: 13722DB
- 9,9-dioctylfluorene-2,7-bis(trimethyleneborate) 97 %, Aldrich, Lot.: 06510CE
- Tetrakis(triphenylphosphine)palladium(0), synthesized by Risø National Laboratory
- Potassium Carbonate >99 % A.C.S reagent, Aldrich, Lot.: 013K0073

Suzuki polymerization 3 – Alternating copolymer (P8BT)
- 4,7-dibromobenzo[c][1,2,5]thiadiazole 95%, Aldrich, Lot.: 67196MJ
- 9,9-dioctylfluorene-2,7-bis(trimethyleneborate) 97 %, Aldrich, Lot.: 06510CE
- Tetrakis(triphenylphosphine)palladium(0), synthesized by Risø National Laboratory
- Potassium Carbonate >99 % A.C.S reagent, Aldrich, Lot.: 013K0073

Suzuki polymerization 4 – Alternating copolymer (P8FDNT)
- 9,9-dioctylfluorene-2,7-bis(trimethyleneborate) 97 %, Aldrich, Lot.: 06510CE
- Tetrakis(triphenylphosphine)palladium(0), synthesized by Risø National Laboratory
- Potassium Carbonate >99 % A.C.S reagent, Aldrich, Lot.: 013K0073

NMR solvents
- Chloroform-d_1 99.8 %, Deutero GmbH, Lot.: B9935
- Dimethylsulfoxide-d_6 99.9 %, Aldrich, Lot.: 01024EH
- Pyridine- d_5 99.5 %, Cambridge Isotope Laboratories Inc, Lot.: BA-312

Appendix B

Attempts to obtain 5,5''-dibromoterthiophene-3',4'-diamine

Sn1

5,5''-dibromo-3',4'-dinitroterthiophene (**9**) (0.10 g, 0.2 mmol) and stannous chloride dihydrate (0.048 g, 0.2 mmol) were dissolved in a mixture of absolute ethanol (2 ml), THF (0.5 ml) and conc. hydrochloric acid (0.5 ml) under a nitrogen atmosphere. The mixture was stirred for 28 hours at room temperature. The reaction was followed by TLC (THF/Heptane 2:3 on silica). The solvents were removed and the pH was adjusted to above 10 with sodium hydroxide pellets. The solution was continuously extracted with ethyl acetate. The ethyl acetate was evaporated to yield a dark solid. ^{1}H NMR on a CDCl$_3$-solution of the solid did not yield any specific peaks.

Sn2

5,5''-dibromo-3',4'-dinitroterthiophene (**9**) (11.00 g, 22.14 mmol) and stannous chloride dihydrate (30.0 g, 132.8 mmol) were dissolved in a mixture of absolute ethanol (200 ml), NMP (350 ml) and conc. hydrochloric acid (100 ml) under a nitrogen atmosphere. The mixture was stirred for 95 hours at room temperature. The solution was poured into water (5 L) and the pH of the mixture was adjusted to ca. 9 with sodium hydroxide solution. Black sticky lumps of crude product were collected by filtration. The lumps along with the filter paper were placed in a soxhlet apparatus and extracted with ethyl acetate (200 ml) to yield a dark brown solution. Conc. hydrochloric acid (30 ml) was added and the solution was dried by rotary evaporation to yield a gray solid. ^{1}H NMR on a CDCl$_3$-solution of the solid did not yield any specific peaks.

Sn3

5,5''-dibromo-3',4'-dinitroterthiophene (**9**) (0.50 g, 1.0 mmol) and stannous chloride dihydrate (1.42 g, 6.3 mmol) were suspended in a mixture of absolute ethanol (10 ml), NMP (20 ml) and conc. hydrochloric acid (5 ml) under a nitrogen atmosphere. The mixture was stirred for 70 hours at room temperature. The solution was poured into ice water (200 ml), pH adjusted to ca. 9 with NaOH solution and filtered to collect a dark solid. The solid was dissolved in chloroform (200 ml) and conc. hydrochloric acid (10 ml) was added to precipitate a dark green solid which was collected by filtration and washed with hexane. ^{1}H NMR on a D$_2$O-solution of the solid did not yield any specific peaks.

Sn4

5,5''-dibromo-3',4'-dinitroterthiophene (**9**) (9.92 g, 20.00 mmol) and stannous chloride dihydrate (27.08 g, 120.00 mmol) were suspended in a mixture of absolute ethanol (200 ml), dry THF (150 ml) and conc. hydrochloric acid (75 ml) under a nitrogen atmosphere. The mixture was stirred for 28 hours at room temperature. The organic solvents were evaporated and sodium hydroxide was added until the pH was well above 9. The mixture was continuous extracted with ethyl acetate until the ethyl acetate phase became clear. Conc. hydrochloric acid (150 ml) was then

added to the extract and the solvent was removed in vacuum. The resultant green suspension was filtered and a brown solid collected and washed with heptane and dried in vacuum at room temperature. Yield: 0.04 g

^{1}H NMR (CDCl$_3$) showed two very week peaks with equal integrals at 6.84 (d) and 7.04 (d) ppm which is believed to be the reduced compound, and two stronger peaks at 7.16 (d) and 7.31 (d) ppm corresponding to 5,5''-dibromo-3',4'-dinitroterthiophene.

Sn5

5,5''-dibromo-3',4'-dinitroterthiophene (**9**) (0.496 g, 1.00 mmol) and stannous chloride (1.138 g, 6.00 mmol) were suspended in a mixture of absolute ethanol (8 ml), dry THF (8 ml) and conc. hydrochloric acid (4 ml) under a nitrogen atmosphere. The mixture was heated to 35 °C and stirred for 22 hours. The solvents were evaporated and sodium hydroxide solution (10 M) was added until a pH of ca. 10. The mixture was continuous extracted with ethyl acetate for 2 hours. The obtained extract was concentrated in vacuum and conc. hydrochloric acid (20 ml) was added. Green precipitate was collected by evaporation. ^{1}H NMR on a D$_2$O-solution of the solid did not yield any specific peaks.

Sn6

5,5''-dibromo-3',4'-dinitroterthiophene (**9**) (0.251 g, 0.506 mmol) and stannous chloride (0.576 g, 3.04 mmol) were dissolved in a mixture of absolute ethanol (3.0 ml), dry THF (2.0 ml) and conc. hydrochloric acid (1.5 ml). The initial light orange color of the solution quickly turned darker. The reaction was stirred for 20 hours at room temperature. A dark solid (ca. 2 g) was obtained by rotary evaporation. This was suspended in ethanol and filtered. The ethanol extract was dried by rotary evaporation yielding a black solid. ^{1}H NMR on D$_2$O and CDCl$_3$-solutions of the solid did not yield any specific peaks.

Sn7

5,5''-dibromo-3',4'-dinitroterthiophene (**9**) (0.10 g, 0.20 mmol) was dissolved in dry THF (2.0 ml), ethanol (2.0 ml) and conc. hydrochloric acid (1.0 ml). Stannous chloride (0.23 g, 1.21 mmol) was added and the reaction was stirred at room temperature for 95 hours. The organic solvents were evaporated and concentrated NaOH was added until pH was above 10. Precipitated solid was collected by filtration and then dissolved in ethyl acetate (25 ml) before adding conc. hydrochloric acid (15 ml) and filtering of the dark brown solid. ^{1}H NMR on D$_2$O and CDCl$_3$-solutions of the solid did not yield any specific peaks.

Sn8

5,5''-dibromo-3',4'-dinitroterthiophene (**9**) (6.00 g, 12.1 mmol) and stannous chloride dihydrate (54.57 g, 241.9 mmol) were suspended in a mixture of absolute ethanol (250 ml), dry THF (150 ml) and conc. hydrochloric acid (150 ml) under a nitrogen atmosphere. The mixture was stirred

for 40 hours at room temperature. The mixture was filtered to remove a beige residue resulting in a yellow solution. The solvent was evaporated from the yellow solution to yield a light brown solid (14.6 g).

^{1}H NMR (CDCl$_3$) showed two peaks with equal integrals at 6.84 (d) and 7.04 (d) ppm.

Fe1

5,5''-dibromo-3',4'-dinitroterthiophene (**9**) (0.10 g, 0.2 mmol) and reduced iron (0.350 g, 6.3 mmol) were suspended in a mixture of absolute ethanol (1 ml), THF (1 ml) and conc. hydrochloric acid (0.25 ml) under a nitrogen atmosphere. The mixture was stirred for 0.5 hour at room temperature. A greenish yellow precipitate with excess iron (2.1 g) was collected. TLC (THF/Heptane 2:3 on silica) confirmed the reduction but the large amount of precipitate collected indicated that it was highly contaminated, presumably with ferrous chloride tetrahydrate. The small amount made purification experiment difficult.

Fe2

5,5''-dibromo-3',4'-dinitroterthiophene (**9**) (8.00 g, 16.1 mmol) and reduced iron dust (-325 mesh, 17.92 g, 322.0 mmol) were suspended in a mixture of absolute ethanol (100 ml) and THF (100 ml) under a nitrogen atmosphere. Conc. hydrochloric acid (100 ml) was added in portions over a period of 1.5 hours due to the highly exothermic nature of the reaction. The mixture was stirred for an additional 8 hours at room temperature. The mixture was filtered to remove excess iron along with a light green solid, presumably ferrous chloride tetrahydrate. Conc. hydrochloric acid (5 ml) was added to the resultant reddish-brown solution and the solvent was removed to give a dark green solid (27.9 g). The solid was dissolved in water and sodium hydroxide was added in order to raise the pH but this yielded a thick yellow paste from which nothing could be extracted with ethyl acetate or diethyl ether.

Fe3

5,5''-dibromo-3',4'-dinitroterthiophene (**9**) (2.01 g, 4.0 mmol) and reduced iron (3.00 g, 53.7 mmol) were suspended in a mixture of absolute ethanol (20 ml), THF (20 ml) and conc. hydrochloric acid (3 ml) under a nitrogen atmosphere. The mixture was stirred for 2.5 hours at room temperature. The mixture was filtered to remove a light green solid which was washed with ethanol. Conc. hydrochloric acid (5 ml) was added to the resultant reddish-brown solution and the solvent was removed to give a dark green solid. The solid was dissolved in water and extracted with chloroform but no product pure product was obtained.

Zn1

5,5''-dibromo-3',4'-dinitroterthiophene (**9**) (0.20 g, 0.4 mmol), ammonium formate (1.50 g, 23.8 mmol) and zinc dust (0.15 g, 2.3 mmol) (zinc dust was activated by treatment with 0.1 M hydrochloric acid for 5 minuts, filtering and washing with dry diethyl ether before use) were

suspended in a mixture 15 ml THF and 45 ml methanol and heated to 40 °C for 2 hours. According to TLC (THF/Heptane 2:3 on silica) no reduction was obtained.

Zn2

5,5''-dibromo-3',4'-dinitroterthiophene (**9**) (0.10 g, 0.2 mmol), ammonium formate (0.50 g, 7.9 mmol) and zinc dust (0.016 g, 0.24 mmol) (zinc dust was activated as in Zn1) were suspended in methanol (5 ml) at stirred for one hours. According to TLC (THF/Heptane 2:3 on silica) no reduction was obtained.

Zn3

Hydrazinium monoformate was prepared by slowly neutralizing equal moles of hydrazine hydrate and 85 % formic acid in an ice water bath, while stirring and protected by nitrogen. 5,5''-dibromo-3',4'-dinitroterthiophene (**9**) (1.0 g, 2.0 mmol) and zinc dust (0.26 g, 4.0 mmol) (zinc dust was activated as in Zn1) were suspended in methanol (20 ml) under nitrogen. Hydrazinium monoformate (2 ml) was added and the reaction was stirred for 1 hour. According to TLC (THF/Heptane 2:3 on silica) no reduction was obtained.

Zn4

Hydrazinium monoformate was prepared as in Zn3. 5,5''-dibromo-3',4'-dinitroterthiophene (**9**) (1.0 g, 2.0 mmol) and zinc dust (0.26 g, 4.0 mmol) (zinc dust was activated as in Zn1) were suspended in a mixture of methanol (10 ml) and THF (10 ml) under nitrogen. Hydrazinium monoformate (2 ml) was added and the reaction was stirred for 1 hour. According to TLC (THF/Heptane 2:3 on silica) no reduction was obtained.

Appendix C

NMR spectra were calibrated using the solvent peak (cf. table 8) and where possible the TMS peak. Signals caused by residual water is also listed in table 8.

Table 8. NMR signals from solvents and water.

Solvent	^{1}H signal(s) [ppm]	^{13}C signal(s) [ppm]	Water signal [ppm]
CDCl$_3$	7.27	77.2	1.6
DMSO-d$_6$	2.50	-	3.3
Pyridine-d$_5$	8.74 , 7.58 , 7.22	150.3 , 135.9 , 123.9	4.9

The performed NMR measurements are listed in table 9.

Table 9. Performed NMR measurements

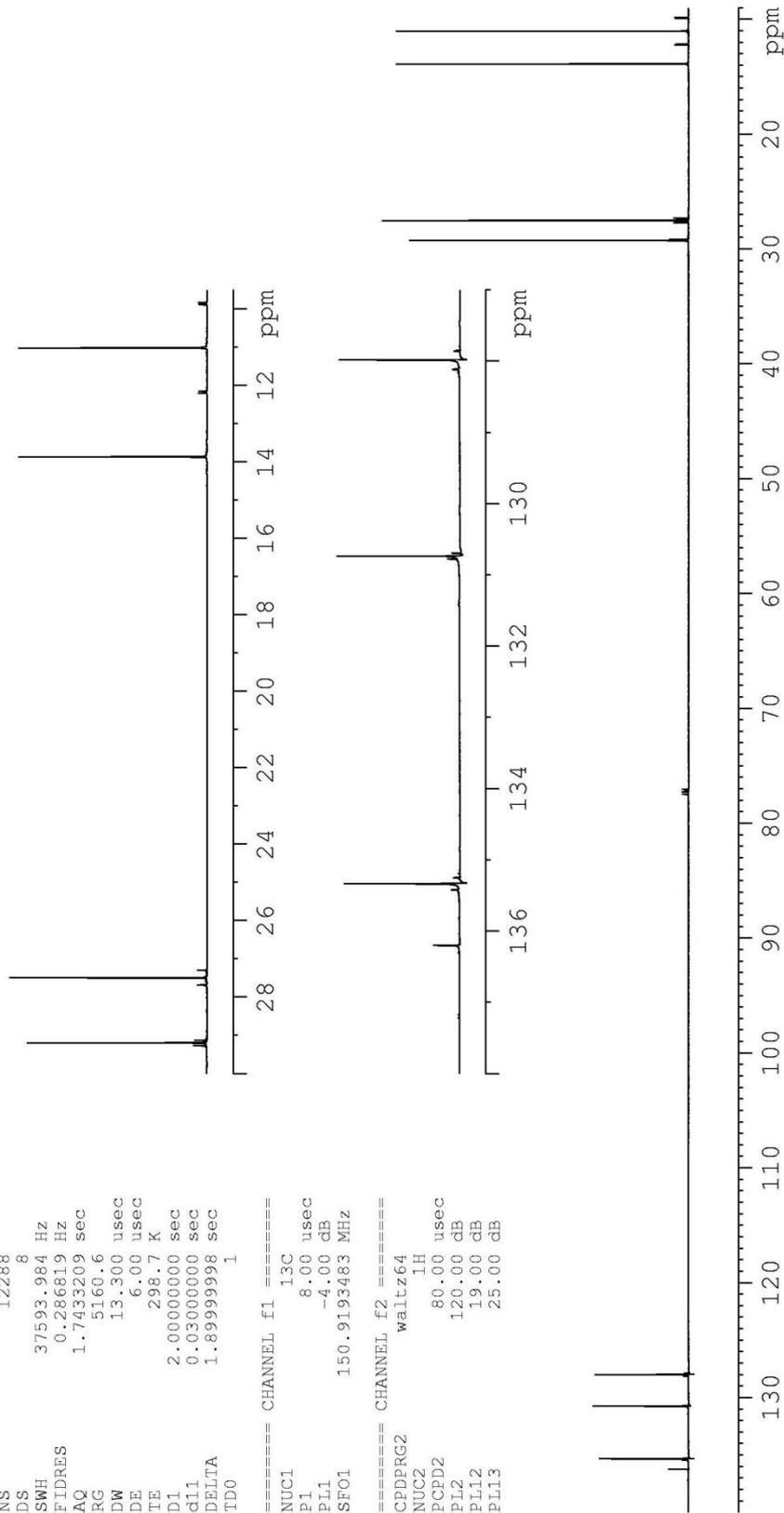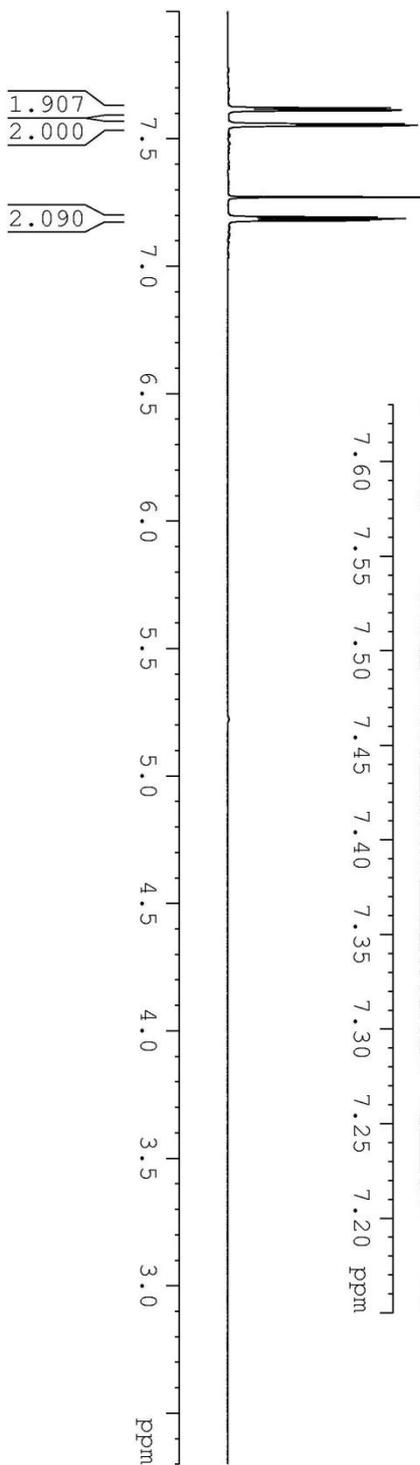| Compound	Nucleus
2-(tributylstannyl)thiophene	^{1}H ^{13}C
3',4'-dinitroterthiophene	^{1}H ^{13}C
Terthiophene-3',4'-diamine dihydrochloride	^{1}H
Methyl 3,5-bis(2-ethylhexyloxy)benzoate	^{1}H
1,2-bis(3,5-bis(2-ethylhexyloxy)phenyl)ethane-1,2-dione	^{1}H ^{13}C ^{13}C, DEPT 90 ^{13}C, DEPT135
2,3-bis(3,5-bis(2-ethylhexyloxy)phenyl)-5,7-bis(thiophene-2-yl)thieno-[3,4-b]pyrazine	^{1}H
5,5''-dibromo-3',4'-dinitroterthiophene	^{1}H ^{13}C

Current Data Parameters
NAME   Lasse
EXPNO   42
PROCNO   1

F2 - Acquisition Parameters
Date_   20090309
Time   8.01
INSTRUM   drx600
PROBHD   5 mm TXI 1H-13
PULPROG   zg
TD   32768
SOLVENT   CDCl3
NS   2
DS   8
SWH   8389.262 Hz
FIDRES   0.256020 Hz
AQ   1.9530824 sec
RG   2.8
DW   59.600 usec
DE   6.00 usec
TE   298.7 K
D1   3.0000000 sec
TD0   1

======== CHANNEL f1 ========
NUC1   1H
P1   6.00 usec
PL1   -2.00 dB
SFO1   600.1327080 MHz

F2 - Processing parameters
SI   65536
SF   600.1300112 MHz
WDW   no
SSB   0
LB   0.00 Hz
GB   0
PC   1.40

64
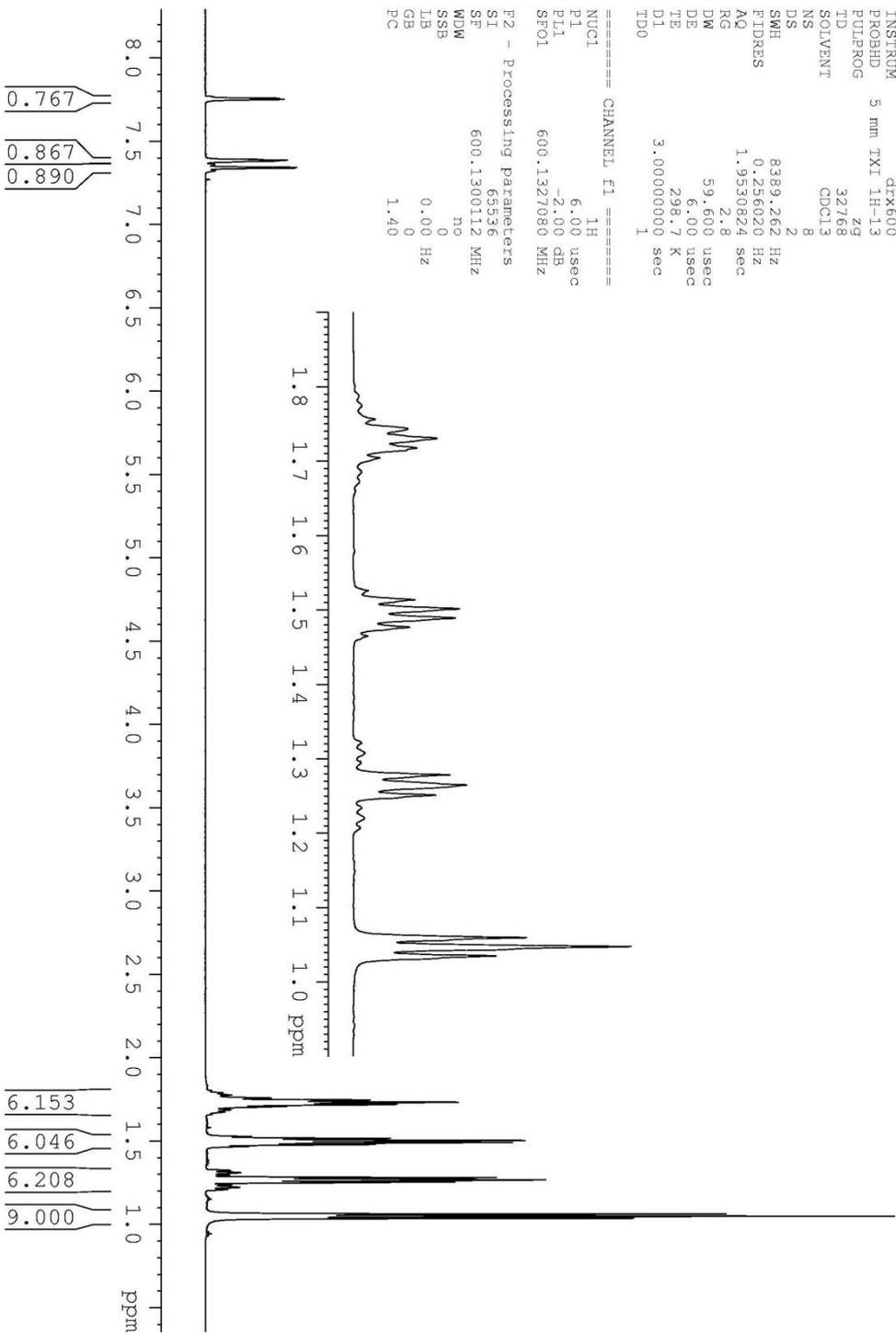
2-(tributylstannyl)thiophene in CDCl3

Current Data Parameters
NAME   Lasse
EXPNO   41
PROCNO   1

F2 - Acquisition Parameters
Date_   20090308
Time   13.38
INSTRUM   drx600
PROBHD 5 mm TXI 1H-13
PULPROG   zgpg
TD   131072
SOLVENT   CDCl3
NS   12288
DS   8
SWH   37593.984 Hz
FIDRES   0.286819 Hz
AQ   1.7433209 sec
RG   5160.6
DW   13.300 usec
DE   6.00 usec
TE   298.7 K
D1   2.00000000 sec
d11   0.03000000 sec
DELTA   1.89999998 sec
TD0   1

======== CHANNEL f1 ========
NUC1   13C
P1   8.00 usec
PL1   -4.00 dB
SFO1   150.9193483 MHz

======== CHANNEL f2 ========
CPDPRG2   waltz64
NUC2   1H
PCPD2   80.00 usec
PL2   120.00 dB
PL12   19.00 dB
PL13   25.00 dB

ppm

12 14 16 18 20 22 24 26 28 ppm

130 132 134 136 ppm

130 120 110 100 90 80 70 60 50 40 30 20 ppm

3',4'-dinitroterthiophene in CDCl3

1.907
2.000
2.090

7.5   7.0   6.5   6.0   5.5   5.0   4.5   4.0   3.5   3.0   ppm

7.60 7.55 7.50 7.45 7.40 7.35 7.30 7.25 7.20 ppm

Terthiophene-3',4'-diamine in DMSO-d6

Current Data Parameters
NAME   Lasse_Risoe
EXPNO   14
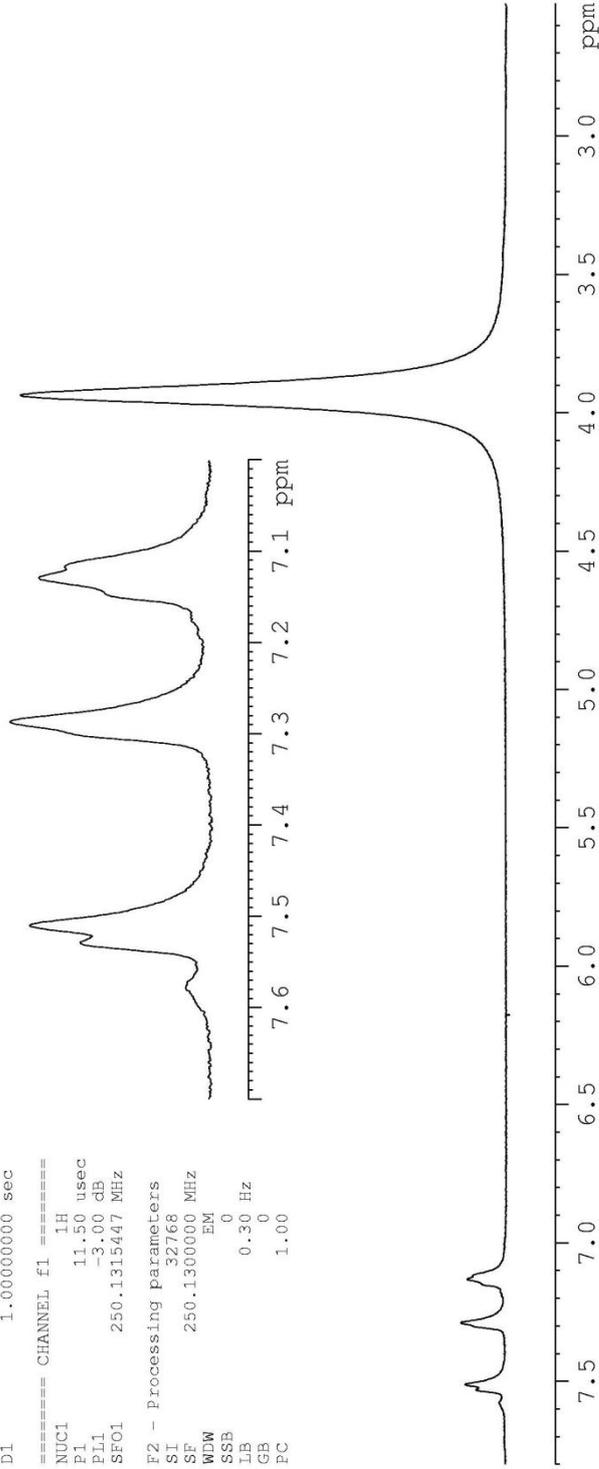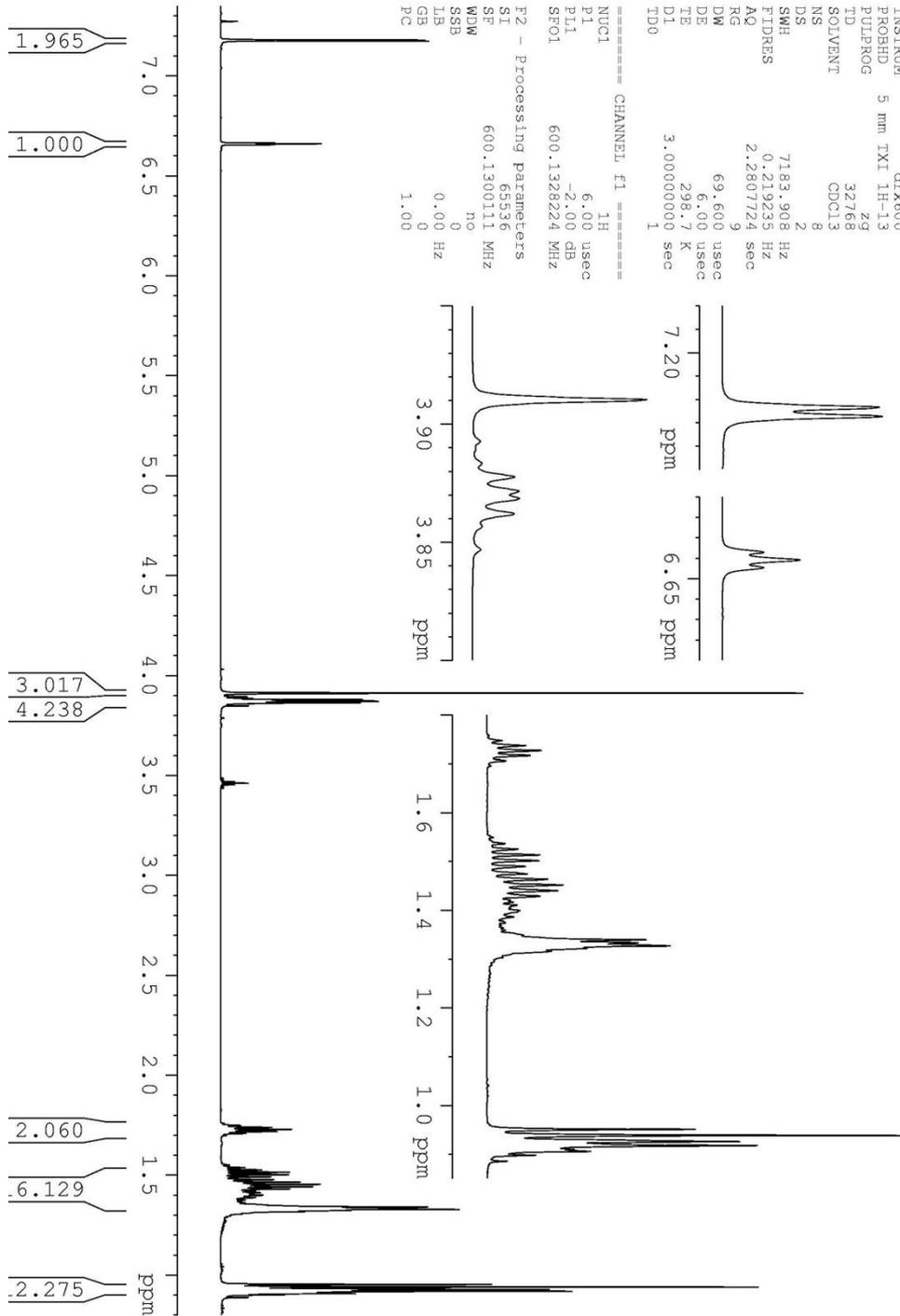PROCNO   1

F2 - Acquisition Parameters
Date_   20081113
Time   13.55
INSTRUM   dpx250
PROBHD   5 mm Multinucl
PULPROG   zg30
TD   34160
SOLVENT   DMSO
NS   16
DS   2
SWH   5175.983 Hz
FIDRES   0.151522 Hz
AQ   3.2999060 sec
RG   724.1
DW   96.600 usec
DE   6.00 usec
TE   300.0 K
D1   1.00000000 sec

======== CHANNEL f1 ========
NUC1   1H
P1   11.50 usec
PL1   -3.00 dB
SFO1   250.1315447 MHz

F2 - Processing parameters
SI   32768
SF   250.1300000 MHz
WDW   EM
SSB   0
LB   0.30 Hz
GB   0
PC   1.00

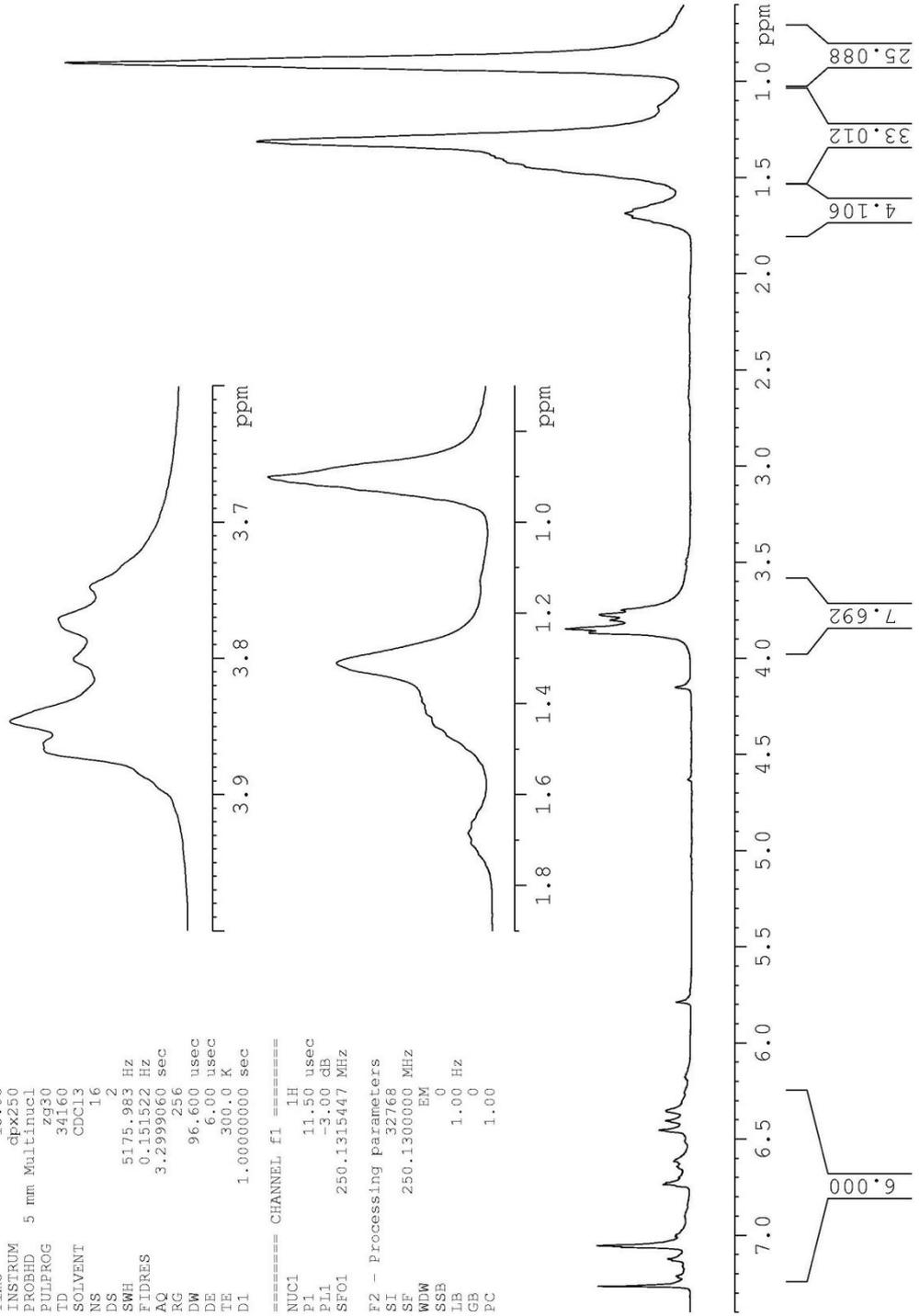Methyl 3,5-bis(2-ethylhexyloxy)benzoate in CDCl3

1,2-bis(3,5-bis(2-ethylhexyloxy)phenyl)ethane-1,2-dione in CDCl3

Current Data Parameters
NAME   Lasse_Risoe
EXPNO   2
PROCNO   1

F2 - Acquisition Parameters
Date_   20081106
Time   15.08
INSTRUM   dpx250
PROBHD   5 mm Multinucl
PULPROG   zg30
TD   34160
SOLVENT   CDCl3
NS   16
DS   2
SWH   5175.983 Hz
FIDRES   0.151522 Hz
AQ   3.2999060 sec
RG   256
DW   96.600 usec
DE   6.00 usec
TE   300.0 K
D1   1.00000000 sec

======= CHANNEL f1 =======
NUC1   1H
P1   11.50 usec
PL1   -3.00 dB
SFO1   250.1315447 MHz

F2 - Processing parameters
SI   32768
SF   250.1300000 MHz
WDW   EM
SSB   0
LB   1.00 Hz
GB   0
PC   1.00

25.088
33.012
4.106
7.692
6.000

1,2-bis(3,5-bis(2-ethylhexyloxy)phenyl)ethane-1,2-dione in CDCl3

70

1,2-bis(3,5-bis(2-ethylhexyloxy)phenyl)ethane-1,2-dione in CDCl13
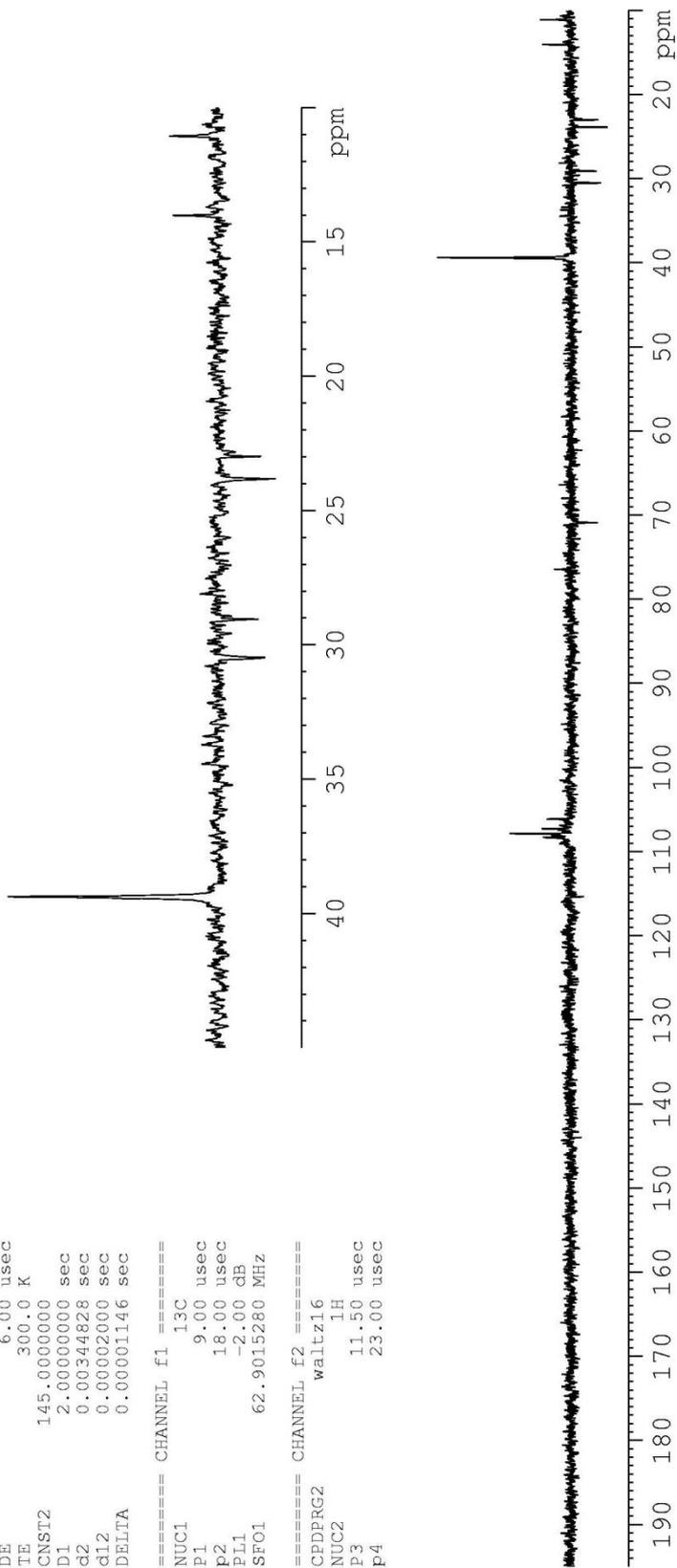
DEPT90

Current Data Parameters
NAME   Lasse_Risoe
EXPNO   7
PROCNO   1

F2 - Acquisition Parameters
Date_   20081110
Time   11.18
INSTRUM   dpx250
PROBHD   5 mm Multinucl
PULPROG   dept90
TD   65536
SOLVENT   CDCl3
NS   256
DS   4
SWH   15060.241 Hz
FIDRES   0.229801 Hz
AQ   2.1758451 sec
RG   11585.2
DW   33.200 usec
DE   6.00 usec
TE   300.0 K
CNST2   145.0000000
D1   2.00000000 sec
d2   0.00344828 sec
d12   0.00002000 sec
DELTA   0.00001146 sec

======== CHANNEL f1 ========
NUC1   13C
P1   9.00 usec
p2   18.00 usec
PL1   -2.00 dB
SFO1   62.9015280 MHz

======== CHANNEL f2 ========
CPDPRG2   waltz16
NUC2   1H
P3   11.50 usec
p4   23.00 usec

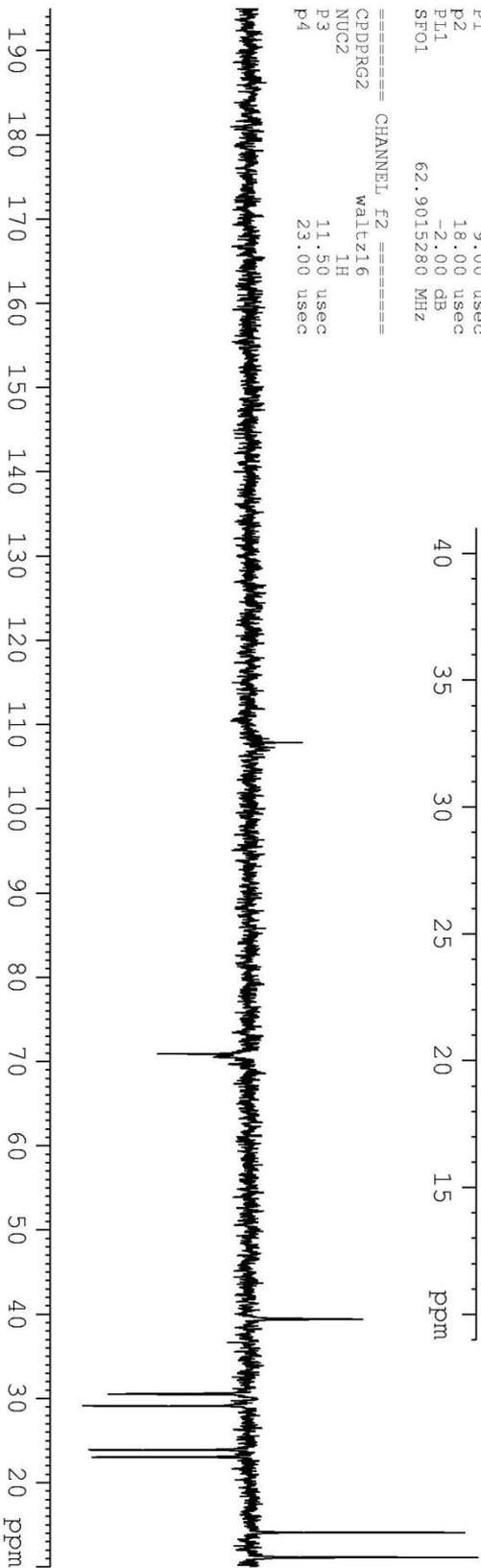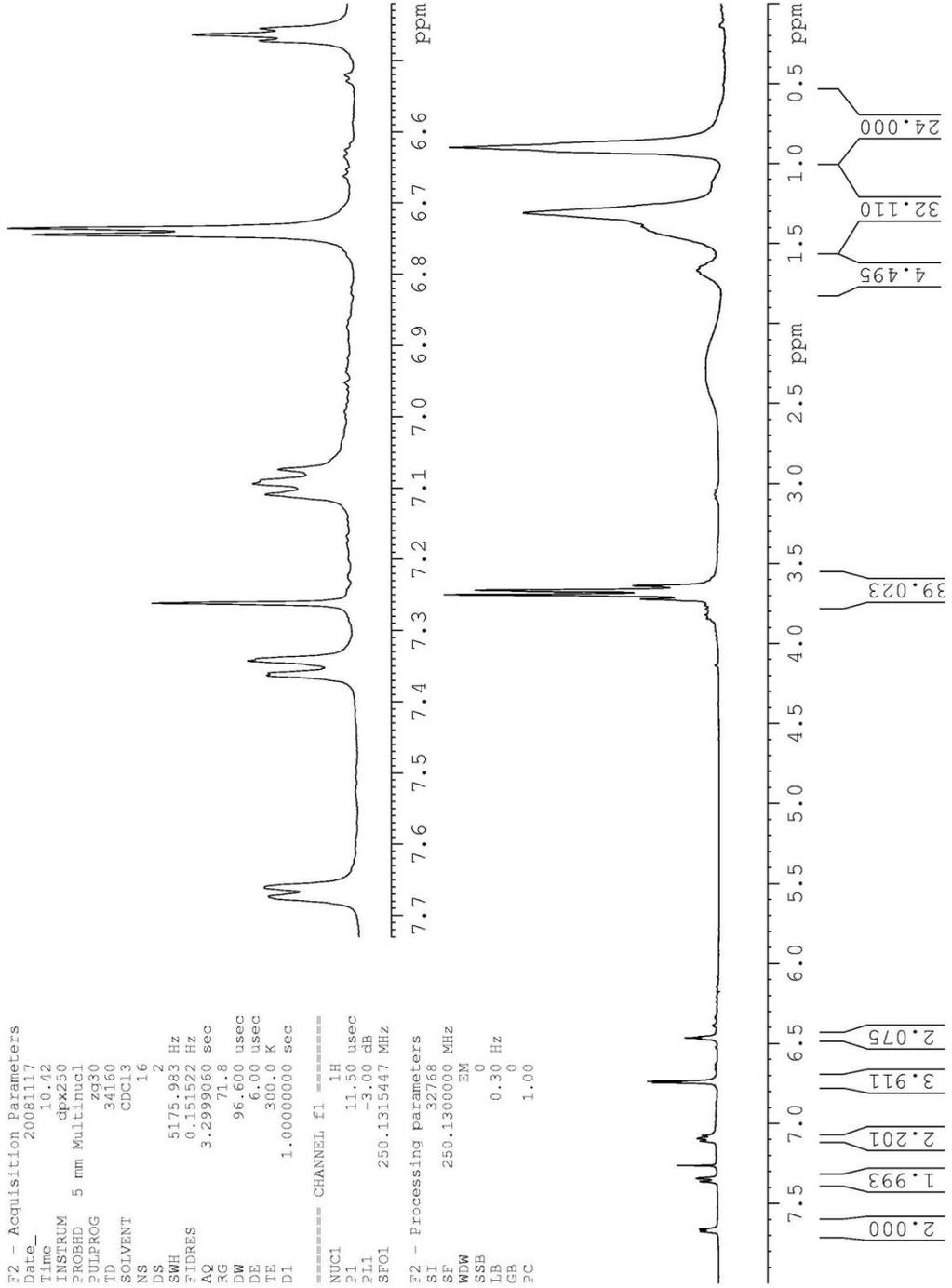1,2-bis(3,5-bis(2-ethylhexyloxy)phenyl)ethane-1,2-dione in CDCl3

DEPT135

2,3-bis(3,5-bis(2-ethylhexyloxy)phenyl)-5,7-di(thiophene-2-yl)-[3,4-b]pyrazine in CDC

Current Data Parameters
NAME   Lasse_Risoe
EXPNO   18
PROCNO   1

F2 - Acquisition Parameters
Date_   20081117
Time   10.42
INSTRUM   dpx250
PROBHD   5 mm Multinucl
PULPROG   zg30
TD   34160
SOLVENT   CDCl3
NS   16
DS   2
SWH   5175.983 Hz
FIDRES   0.151522 Hz
AQ   3.2999060 sec
RG   71.8
DW   96.600 usec
DE   6.00 usec
TE   300.0 K
D1   1.00000000 sec

======= CHANNEL f1 =======
NUC1   1H
P1   11.50 usec
PL1   -3.00 dB
SFO1   250.1315447 MHz

F2 - Processing parameters
SI   32768
SF   250.1300000 MHz
WDW   EM
SSB   0
LB   0.30 Hz
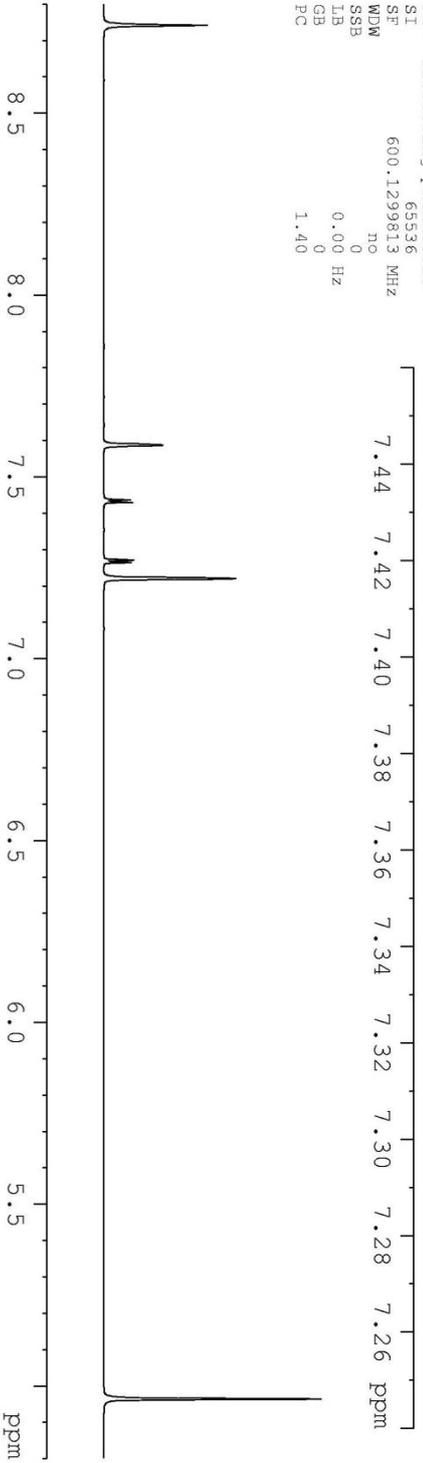GB   0
PC   1.00

5,5''-dibromo-3',4'-dinitroterthiophene in Pyridine-d5

5,5''-dibromo-3',4'-dinitroterthiophene in Pyridine-d5

Current Data Parameters
NAME   Lasse
EXPNO   39
PROCNO   1

F2 - Acquisition Parameters
Date_   20090308
Time   7.40
INSTRUM   drx600
PROBHD 5 mm TXI 1H-13
PULPROG   zgpg
TD   131072
SOLVENT   Pyr
NS   12288
DS   8
SWH   37593.984 Hz
FIDRES   0.286819 Hz
AQ   1.7433209 sec
RG   2896.3
DW   13.300 usec
DE   6.00 usec
TE   298.7 K
D1   2.00000000 sec
d11   0.03000000 sec
DELTA   1.89999998 sec
TD0   1

======== CHANNEL f1 ========
NUC1   13C
P1   8.00 usec
PL1   -4.00 dB
SFO1   150.9193483 MHz

======== CHANNEL f2 ========
CPDPRG2   waltz64
NUC2   1H
PCPD2   80.00 usec
PL2   120.00 dB
PL12   19.00 dB
PL13   25.00 dB